Master Thesis in Geographical Information Science nr 210

# GIS-based Multi-Criteria Decision Analysis (MCDA) framework for Flood Risk Assessment in the Thermi Basin

**Polyxeni Karapanagiotidou**

2026
Department of
Physical Geography and Ecosystem Science
Centre for Geographical Information Systems
Lund University
Sölvegatan 12
S-223 62 Lund
Sweden

Polyxeni Karapanagiotidou (2026). GIS-based Multi-Criteria Decision Analysis (MCDA) framework for Flood Risk Assessment in the Thermi Basin

Master degree thesis, 30/ credits in Master in Geographical Information Science
Department of Physical Geography and Ecosystem Science, Lund University

**Disclaimer**
This document describes work undertaken as part of a program of study at the University of Lund. All views and opinions expressed herein remain the sole responsibility of the author, and do not necessarily represent those of the institute.

# GIS-based Multi-Criteria Decision Analysis (MCDA) framework for Flood Risk Assessment in the Thermi Basin

---

Polyxeni Karapanagiotidou
Master thesis, 30 credits, in Geographical Information Sciences

Supervisor 1
Ali Mansourian,
Lund University

Examiner 1 Andreas Persson,
Lund University
Examiner 2 Rachid Oucheikh,
Lund University

**Acknowledgements**

Firstly, I would like to express my gratitude to my supervisor, Ali Mansourian, for his continuous guidance throughout my thesis and for his insightful observations. I am also thankful to the participants for their time and willingness to contribute to the questionnaire survey of this study. Finally, I would like to thank my family and friends for their encouragement throughout the whole process.

**Abstract**

Flooding is one of the most frequent and catastrophic natural hazards with significant socioeconomic and environmental consequences. The increasing frequency and intensity of extreme precipitation events due to climate change combined with other underlying factors such as unplanned urbanization, environmental degradation, poverty, social inequalities and weak governance have changed flood risk patterns. The complex nature of flood risk highlights the need for a better understanding of its conceptual context and comprehensive flood risk assessments that beyond hazard, assess exposure, vulnerability and capacity factors. To address this necessity, the study develops a GIS-based Multi-Criteria Decision Analysis (MCDA) framework that considers diverse parameters to assess and map flood risk. The framework is applied to the Thermi Basin in northern Greece which is characterised by diverse land use/ land cover, complex hydrography, varied topography and seasonal precipitation events of ranging intensity. In this context, seventeen parameters representing flood risk components (hazard, exposure and vulnerability/ capacity) are selected. These parameters are then weighted using Analytic Hierarchy Process (AHP) through local experts and stakeholder's participation and a Weighted Overlay Analysis is applied in GIS to create the flood risk map. The flood risk map visualizes the spatial distribution of flood risk ranging from low to high. The results indicate that 8,26% (503ha) of the study area is classified as low flood risk, 83,94% (5114ha) as moderate flood risk and 7,80% (476ha) as high flood risk. An impact analysis is also applied to evaluate potential impacts on the environment, infrastructure and population while the results are validated using official Areas of Potential Significant Flood Risk (APSFR) and flood-prone locations. Finally, the framework proposes some indicative strategies for each flood risk zone that local authorities and flood risk management stakeholders can further develop to support their mitigation efforts within a sustainable decision-making context.

**Keywords:** Geography, Geographical Information Systems (GIS), Physical Geography, Flood Risk Assessment, GIS-based MCDA, AHP

## Table of Contents

## List of Tables

## List of Figures

**Acronyms**

| | |
|---|---|
| ASTER | Advanced Spaceborne Thermal Emission and Reflection Radiometer |
| AHP | Analytic Hierarchy Process |
| ANP | Analytic Network Process |
| AUC | Area Under the Curve |
| APSFR | Areas of Potential Significant Flood Risk |
| ANNs | Artificial Neural Networks |
| CHRS | Center for Hydrometeorology and Remote Sensing |
| CI | Consistency Index |
| CR | Consistency Ratio |
| DEA | Data Envelopment Analysis |
| DEM | Digital Elevation Model |
| DSWM | Digital Soil Map of the World |
| ELECTRE | Elimination and Choice Translating Reality |
| EM-DAT | Emergency Events Database |
| FAO | Food and Agriculture Organization |
| FR | Frequency Ratio |
| FAHP | Fuzzy Analytic Hierarchy Process |
| GIS | Geographic Information Systems |
| GP | Goal Programming |
| ELSTAT | Hellenic Statistical Authority |
| IPCC | Intergovernmental Panel on Climate Change |
| LULC | Land Use and Land Cover |
| MAUT | Multi-Attribute Utility Theory |
| MCDA | Multi-Criteria Decision Analysis |
| NDVI | Normalized Difference Vegetation Index |
| OSM | OpenStreetMap |
| PCM | Pairwise Comparison Matrix |
| PERSIANN-CCS | Precipitation Estimation from Remotely Sensed Information using Artificial Neural Network Cloud Classification System |
| PROMETHEE | Preference Ranking Organization Method for Enrichment of Evaluations |
| PAR | Pressure And Release |
| RI | Random Index |
| ROC | Receiver Operating Characteristic |
| SMART | Simple Multi-Attribute Rating Technique |
| SURE | Simulated Uncertainty Range Evaluations |
| TOPSIS | Technique for Order Preferences by Similarity to Ideal Solutions |
| TWI | Topographic Wetness Index |
| USGS | U.S. Geological Survey |
| UNDRR | United Nations Office for Disaster Risk Reduction |
| WPM | Weighted Product Model |
| WSM | Weighted Sum Model |

## 1. Introduction

The frequency and intensity of catastrophic events have increased in recent years, causing major socioeconomic and environmental impacts. The complex and systemic nature of disaster risk is exacerbated by underlying factors such as poverty, social inequalities, climate change, environmental degradation, unplanned urbanization and weak governance, creating a feedback loop in which disaster risks and their impacts reinforce each other (UNDRR, 2020).

Disaster risk results from and increase social and spatial inequalities. Vulnerability is differently distributed with some population groups more affected due to their living environments, socio-spatial inequalities and limited participation in decision-making processes. Climate change increases the frequency and intensity of extreme weather events, which in turn generate new or intensify existing risks. Environmental degradation reduces ecosystems and ecosystems' services undermining the capacity of communities to prevent, adapt to, recover from and mitigate disasters. Unplanned urbanization often leads to informal settlements in high-risk areas, increasing exposure while contributing to resource depletion, increased energy consumption and unequal access to goods. While weak institutional frameworks, inadequate coordination and insufficient enforcement of laws further exacerbate vulnerabilities (UNDRR, 2020).

Flooding is one of the most frequent and catastrophic natural hazards with significant socioeconomic and environmental consequences. According to Intergovernmental Panel on Climate Change (IPCC), climate change has led to an increase in extreme precipitation events from 1950 to 2018 in Europe, showing spatial and seasonal variations. Central Europe has experienced increased precipitation while Mediterranean region has experienced mixed trends with increases in Eastern Mediterranean and decreases in Western Mediterranean (Seneviratne et al., 2021). According to the published data of Emergency Events Database (EM-DAT), between 2000 and 2025, Europe experienced 490 flood events (including coastal, flash, general and riverine floods) resulting in 2538 deaths, 9037 injuries and affecting more than 10 million people. These events displaced 157789 individuals and led to significant economic losses. In particular, the total damage (adjusted for inflation) reached $235,24 billion, damage amounted to $55,49 billion (adjusted) and reconstruction costs were estimated at $3,35 billion (adjusted) (EM-DAT,n.d.).

Disasters pose an escalating threat to future development, with the potential to reverse the progress societies have made so far. Current development patterns can increase exposure to hazards while disaster impacts, in turn, increase social and economic inequalities and undermine future development, reinforcing the feedback loop of exposure and vulnerability (UNDRR, 2020). As disaster risk faces three critical negative spirals -excessive losses due to inappropriate disaster risk reduction, low insurance coverage shifting financial pressure of risk to central governments and expensive emergency relief efforts that fail to address long term recovery or underlying vulnerabilities (UNDRR, 2025)- traditional approaches need to be reviewed. Understanding the conceptual context of flood risks, learning from past experiences and aligning efforts with the unique characteristics of the study areas are important.

The complex nature of flood risk highlights the need for comprehensive assessments that beyond hazard consider exposure, vulnerability and capacity. Multi-Criteria Decision Analysis (MCDA) combined with Geographic Information Systems (GIS) provides an effective methodological framework for flood risk assessment (Theochari et al., 2021).This structured framework enables the combination of spatial and non-spatial parameters to identify and map flood risk areas at different spatial scales (Gupta & Dixit, 2022; Theochari et al., 2021).

Despite these capabilities, most studies mainly focus on hazards or partially consider other components of flood risk. As a result, important parameters are often underestimated, raising concerns about the comprehensive representation of flood risk. In the wider area of Thermi, no study has been identified through literature review that comprehensively assesses all components of flood risk. In parallel, land use and land cover changes associated with rapid urban expansion observed in the wider area along with its socioeconomic and environmental characteristics, are likely to modify current flood risk patterns. Moreover, these pressures are expected to intensify under climate change scenarios that predict more frequent and intense precipitation events. In this context and given the complex nature of flood risk, a better understanding of its conceptual context and holistic approaches that beyond hazard consider exposure, vulnerability and capacity parameters are required.

To address this gap, the study aims to develop a GIS-based MCDA framework to identify and map flood risk within Thermi Basin. The framework integrates hazard with exposure, vulnerability and capacity parameters, weighting them using the Analytic Hierarchy Process (AHP) based on expert judgments and aggregating them through Weighted Overlay Analysis in GIS to create a flood risk map. Then, it applies an impact analysis on the environment, infrastructure and population and validates the results against official Areas of Potential Significant Flood Risk (APSFR) and eighteen documented flood-prone locations. Finally, the study proposes some indicative strategies for each flood risk zone that decision-makers can further develop to support their mitigation efforts.

The specific objectives of the study are to:

- Identify and select appropriate flood hazard, exposure and vulnerability/ capacity parameters based on literature review.
- Assign weights to the selected parameters using MCDA-AHP method through expert judgements.
- Integrate, standardize and analyze data in GIS to assess and map flood risk.
- Assess potential impacts on the environment, infrastructure and population.
- Validate the results using official Areas of Potential Significant Flood Risk (APSFR) and flood-prone locations.
- Propose indicative strategies for each flood risk zone.

Therefore, the study is centered on the following research questions:

- What are the main hazard, exposure and vulnerability/ capacity parameters that influence flood risk in the study area and what weights should be assigned to reflect their relative significance?
- What is the spatial distribution of flood risk across the study area based on the analysis of relevant datasets in GIS?
- What are the potential impacts on the environment, infrastructure and population across different flood risk levels and what indicative strategies can be proposed for each flood risk zone?

## 2. Background

### 2.1. GIS-based MCDA

Decision-making often requires simultaneous consideration of multiple parameters under conditions of complexity, uncertainty and different interests (Abdullah et al., 2021). To address these challenges, Multi-Criteria Decision Analysis (MCDA) provides a systematic and transparent framework for assessing different options that could lead to decisions (Abdullah et al., 2021; Dell' Ovo et al., 2020).

MCDA typically consists of several stages including defining the decision context, identifying objectives and parameters, identifying and evaluating alternatives, assigning weights to parameters, aggregating results, visualizing results and conducting sensitivity analysis (Dell' Ovo et al., 2020). Among these, problem structuring, parameters selection, weighting and aggregation are particularly important as they influence the problem-solving process (Dell' Ovo et al., 2020).

Effective problem structuring requires a clear understanding and organization of the decision problem as it influences the analysis and determines the problem-solving orientation (Guitouni & Martel, 1998). Stakeholder analysis is also important, as it involves the proper identification of stakeholders and understanding of their roles and responsibilities to capitalize their knowledge and expertise in the decision-making process (Dell' Ovo et al., 2020).

Parameters selection is a critical stage in MCDA as it significantly influences decision-making (Abdullah et al., 2021). Parameters define and structure the decision problem (Dell' Ovo et al., 2020) and their quantity and quality vary depending on the problem type (Abdullah et al., 2021). According to Dell' Ovo et al. (2020) parameters should be systemic, consistent, independent, comparable and measurable and can be identified through value-based approaches, stakeholders' participation or literature review.

Weighting parameters refers to the process of representing the preferences of stakeholders involved by assigning relative importance to each of them. Several methods have been developed to support the weighting process differing in methodology and levels of involvement of stakeholders, leading to different results (Dell' Ovo et al., 2020). Common weighting methods in the context of water-related

disaster events include Analytical Hierarchy Process (AHP), Analytic Network Process (ANP), Multi-Attribute Utility Theory (MAUT) and Simple Multi-Attribute Rating Technique (SMART) (Abdullah et al., 2021). For example, AHP deconstructs complex decision problems into a hierarchical framework and applies pairwise comparisons to transform qualitative judgements into consistent and measurable weights representing the importance of parameters (Sun et al., 2013; Meesariganda & Ishizaka, 2016) while fuzzy AHP translates subjective judgements into linguistic variables represented as fuzzy intervals (Aruldoss et al., 2013; Ho & Ma, 2017). ANP models complex interdependencies and relationships among decision elements through network structures and super-matrix processes (Cheng & Li, 2005; Sánchez-Garrido et al., 2022). MAUT assigns utility scores and uses weighted sums to support decision-making under risk and conflicting objectives (Kahraman & Kaya, 2012; Mateo, 2012a; Khalafalla & Rueda-Benavides, 2024). SMART assigns weights on a 1-100 scale, normalizes attributes and aggregates the final attributes values to provide total ranking (Dwanoko et al., 2018; Dervishaj et al., 2017).

Aggregation considers the performance of alternatives and preferences of stakeholders to support optimization, sorting or ranking (Dell' Ovo et al., 2020) while aggregation methods can be divided into three categories: compensatory, partially compensatory and non-compensatory (Guitouni & Martel, 1998). Compensatory methods use value functions and analytical approaches to provide an efficient solution that balances performance of independent parameters (Guitouni & Martel, 1998; Dell' Ovo et al., 2020). Partially compensatory methods use pairwise comparisons to define outranking relations and evaluate compensation (Guitouni & Martel, 1998; Dell' Ovo et al., 2020) while non-compensatory methods use rules by transforming knowledge from observed data to classify alternatives and support decision-making (Dell' Ovo et al., 2020). Common aggregation methods in the context of water-related disaster events include Data Envelopment Analysis (DEA), Weighted Sum Model (WSM), Weighted Product Model (WPM), Goal Programming (GP), Technique for Order Preferences by Similarity to Ideal Solutions (TOPSIS), Simulated Uncertainty Range Evaluations (SURE), Elimination and Choice Translating Reality (ELECTRE) and Preference Ranking Organization Method for Enrichment of Evaluations (PROMETHEE) (Abdullah et al., 2021). For example, DEA evaluates the relative efficiency of decision-making units to compare several inputs and outputs through linear programming

(Amirteimoori et al., 2006; Abdullah et al., 2021). WSM aggregates uniform parameters by summing the weighted scores of different alternatives (Abdullah et al., 2021). WPM evaluates alternatives similarly to WSM, but uses multiplication, not addition (Abdullah et al., 2021). GP addresses multiple conflicting decision problems by minimizing deviations from predetermined goal values (Colapinto et al., 2015; Gütmen et al., 2024). TOPSIS ranks alternatives by calculating their relative proximity to an ideal solution and distance from a negative ideal solution using Euclidean distance (Balali et al., 2022; Abdullah et al., 2021). SURE manages uncertainty and preference overlaps by modeling alternatives with triangular distributions (Hodgett & Siraj, 2018; Abdullah et al., 2021). ELECTRE selects, sorts or ranks alternatives by constructing agreement, neutral and disagreement sets and matrices (Abdullah et al. 2021; Vahdani et al., 2010; Akram et al., 2022). PROMETHEE uses preference functions and comparisons of multiple conflicting parameters to rank alternatives across partial (PROMETHEE I), complete (PROMETHEE II) and advanced (PROMETHEE III-VI) ranking formats (Mateo, 2012b; Papathanasiou & Ploskas, 2018; Akram & Bibi, 2023)

The selection of the most appropriate MCDA method for each stage can differentiate and be guided by multiple factors including the number of the decision-makers, objectives and alternatives involved, potential constraints, risk tolerance, uncertainties, scales and units, data availability and general problem-solving orientation (Greene et al., 2011).

MCDA methods have been widely applied together with Geographical Information Systems (GIS) to address spatial problems (Greene et al., 2011; Dell' Ovo et al., 2020). GIS-based MCDA approaches provide more holistic and informed solutions increasing the reliability of the final decision by combining the capabilities of MCDA with GIS (Feizizadeh & Kienberger, 2017; Dell' Ovo et al., 2020). Such frameworks typically include procedures like collecting and standardizing parameters expressed as spatial data with uniform units, weighting parameters to represent their relative importance and aggregating them into a single index for the assessing alternatives (Feizizadeh & Kienberger, 2017; Dell' Ovo et al., 2020). Over time, various combinations of MCDA methods and GIS applications have been proposed (Greene et al., 2011). Among these, the AHP is one of the most widely used due to its capabilities and ease of integration with GIS (Feizizadeh & Kienberger, 2017). However, GIS-based MCDA methods have

also limitations related to uncertainties in model selection, system representation, parameters weighting, data quality and subjectivity of expert judgments (Feizizadeh & Kienberger, 2017).

## 2.2. Flood Risk Conceptualization and Assessment

### 2.2.1. Disaster Risk

The conceptualization of disaster risk has evolved significantly over the past decades; a transformation that is reflected in the official definitions adopted by the United Nations. The term was formally introduced in the United Nations Office for Disaster Risk Reduction (UNDRR) Terminology (2009) providing a more probabilistic definition to risk mainly focusing on the likelihood of hazards and their potential impacts (UNDRR, 2009). The definition also implied the importance of understanding the nature of hazards and the socioeconomic context in which risk is experienced.

A significant advancement was made with the revised definition proposed in 2017 by the UNDRR, as part of the implementation of the Sendai Framework for Disaster Risk Reduction (2015–2030) and its effort to establish a common terminology context. This definition introduced a more sophisticated dimension. Disaster risk is defined not only by its likelihood and its potential impacts but also as the continuous interaction among hazard, exposure, vulnerability and capacity (UNDRR, 2017). These components are considered as distinct and shaped by social, institutional, political and economic conditions that influence communities' perceptions and their capacity to manage risk (UNDRR, 2017). Consequently, disaster risk is perceived as a dynamic system in which multiple factors interact over time and when combined, disaster risk materializes.

According to UNDRR (2017), disaster risk is defined as:

*"The potential loss of life, injury, or destroyed or damaged assets which could occur to a system, society or a community in a specific period of time, determined probabilistically as a function of hazard, exposure, vulnerability and capacity."*

This relationship of disaster risk, as defined by hazard, exposure, vulnerability and capacity components, is often simplified and represented by the following formula.

*Disaster Risk = f(Hazard, Exposure, Vulnerability, Capacity)*

This equation implies that any change in one or more of these factors directly influences the level of the total disaster risk. Crichton (1999) also conceptualized this relationship using the "Risk Triangle", where hazard, exposure and vulnerability form the sides of a triangle and the area enclosed represents the overall risk. Modifying any triangle's side changes the total area or the overall disaster risk, highlighting the interdependent relationship among them. However, in this case, capacity is not clearly included in the model.

### 2.2.2. Flood Risk

Disaster risk increases in terms of intensity and frequency of hazard events due to human activities that contribute to climate change along with the poor decision-making in urban planning and inappropriate environmental management (UNDRR, 2024). The potential impacts on population, infrastructure and the environment are intensified when vulnerability and exposure levels are higher. To reduce disaster risk and promote sustainable development, it is crucial to adopt preventive strategies that reduce exposure and vulnerability and increase resilience. A crucial initial step in assessing flood risk is the understanding of its nature through the analysis of its components. This process involves not only identifying the direct triggers of hazard but also addressing its root causes shaped by historical, social, economic and political factors (UNDRR,2024).

Applying this conceptual framework to flood risk, flood risk is perceived as the interaction of physical or environmental processes that trigger flooding and exposure, vulnerability and capacity factors shaped by the socioeconomic and political context within which flood risk is perceived.

The following analysis examines these components that contribute to flood risk, recognizing that their conceptual understanding is crucial for effective flood risk management.

#### 2.2.2.1. Flood Hazard

UNDRR (2017) defines Hazard as:

*"A process, phenomenon or human activity that may cause loss of life, injury or other health impacts, property damage, social and economic disruption or environmental degradation."*

Based on the above definition, flood hazard refers to hydrometeorological events that have the potential to cause damage. Like all types of hazards, flood hazards are characterized by their location, intensity, frequency and probability (UNDRR, 2017). However, flood hazard only is perceived as risk when it interacts with exposed and vulnerable elements.

#### 2.2.2.2. Flood Exposure

UNDRR (2017) defines Exposure as:

*"The situation of people, infrastructure, housing, production capacities and other tangible human assets located in hazard-prone areas."*

Based on the above definition, flood exposure refers to the presence of populations, infrastructure and assets in flood-prone areas. It is also implied that while exposure alone does not determine the flood risk (as its impact also depends on vulnerability) it is necessary for risk to occur. Therefore, reducing exposure is a fundamental step for flood risk reduction.

#### 2.2.2.3. Flood Vulnerability

UNDRR (2017) defines a Vulnerability as:

*"The conditions determined by physical, social, economic and environmental factors or processes which increase the susceptibility of an individual, a community, assets or systems to the impacts of hazards."*

Based on the above definition, flood vulnerability refers to the susceptibility of population, infrastructure and assets to the potential impacts of flooding. Vulnerability is influenced by several factors such as physical, social, economic, environmental and

institutional (ADB, 2016; Bera et al., 2020). In this case, flood vulnerability increases when for example, multiple conditions such as inadequate infrastructure or unplanned settlements (physical vulnerability), marginalized or elderly population (social vulnerability), limited access to resources or poverty (economic vulnerability), degraded ecosystems or land use changes (environmental vulnerability) and absence of operational or participatory planning (institutional vulnerability) coexist.

According to Tabasi et al. (2025), the gradual increase of vulnerability can be explained through Pressure And Release (PAR) model which defines disaster through the progression from root causes that generate dynamic pressures and lead to unsafe conditions. Therefore, when vulnerable elements interact with hazard, disaster risk intensifies, resulting in catastrophic events.

#### 2.2.2.4. Flood Capacity

UNDRR (2017) defines a Capacity as:

*"The combination of all the strengths, attributes and resources available within an organization, community or society to manage and reduce disaster risks and strengthen resilience."*

Based on the above definition, flood capacity refers to the ability of an organization, community or society to manage flood events and enhance their resilience. Alternatively, capacity is related to the ability of the elements to absorb, anticipate, prevent, adapt or transform to manage hazardous events (Manyena et al., 2019). Therefore, capacity is associated with resilience, which is perceived as a positive parameter that mitigates vulnerability and contributes to reducing the overall flood risk (Tabasi et al., 2025).

Flood risk is affected by the continuous interaction of hazard, exposure, vulnerability and capacity. Contemporary floods increasingly deviate from historical patterns along with neglect early warnings (UNDRR, 2019; UNDRR, 2024). Addressing these challenges requires strategies that combine scientific analysis with local knowledge. Learning from past catastrophic events and being adaptable to changing conditions is crucial for efficient flood risk mitigation and building resilience (UNDRR, 2024).

### 2.2.3. Flood Risk Parameters

Flood risk assessments apply several methods to analyze and evaluate flood risk based on influencing factors and variables (Díez-Herrero & Garrote, 2020). The effectiveness of these assessments depends on the selection of parameters that reflect hazard, exposure and vulnerability/capacity and capture the unique characteristics of the study area. Selecting the most appropriate parameters is a challenging process, as it requires careful consideration of the factors influencing flood risk. One critical process is balancing comprehensiveness with simplicity (Abdullah et al., 2021). While there is no standard number of parameters that need to be included in flood risk assessments, their selection should be made strategically. Particularly, many parameters can provide a more detailed and holistic understanding of flood risk but may also increase the complexity of decision-making and a limited number of parameters may overlook crucial factors, potentially resulting in incomplete or insufficient assessments (Abdullah et al., 2021).

Given the potential constraints associated with the required data, the most effective approach is selecting a set of parameters that are relevant, feasible and reliable (Abdullah et al., 2021). Additionally, the selection of analysis scale -whether employing a localized approach that focuses on study area's conditions or a systematic approach that examines broader factors- can significantly influence the assessments (Abdullah et al., 2021).

Previous studies that use MCDA in flood risk assessments have shown significant variation in the number of chosen parameters, ranging from a few to many (Abdullah et al., 2021). These studies also differ in scope, with some focusing mainly on flood hazard while others integrate additional components such as exposure, vulnerability and/or capacity. Díez-Herrero and Garrote (2020) observed in their extensive research that flood risk assessments often place disproportionate emphasis on hazard analysis while less emphasis is given on vulnerability and to a greater extent on exposure. They also highlighted the importance of adopting a more balanced approach that equally integrates all risk components and analyzes their associated uncertainties (Díez-Herrero & Garrote, 2020).

To systematize the existing literature on flood risk assessment, a comprehensive review of 28 peer-reviewed studies was conducted, focusing on the parameters frequently used. These were classified into four categories: flood hazard, flood exposure, flood vulnerability and flood resilience (or capacity) parameters. The review identified 405 parameters which resulted in 220 parameters after removing duplicates. Among these parameters, 83 were related to vulnerability, 40 to hazard, 34 to capacity-resilience and 24 to exposure. Additionally, 18 parameters were identified from studies that did not clearly categorize them into flood risk components, adopting a more hazard-based approach. Furthermore, some parameters were observed to overlap across multiple components: 7 were shared between exposure and vulnerability concepts, 6 between vulnerability and capacity-resilience, 3 between hazard and exposure, 3 between hazard and vulnerability. While 2 parameters were categorized under the general umbrella of flood risk.

The following section presents these parameters representing flood risk components.

#### 2.2.3.1. Flood Hazard Parameters

The analysis of flood hazard parameters is divided into two categories: studies that adopt a more technical or hazard-based approach without clearly defining other components of flood risk and those that employ a more comprehensive approach integrating exposure, vulnerability or capacity parameters. In the second case, flood hazard is treated as one distinct flood risk component among others.

In this context, commonly used parameters in reviewed hazard-based studies include horizontal and vertical overland flow distance, aspect, modified Fournier index, topographic position index and stream power index.

*Table 1 Hazard parameters identified in reviewed hazard-based studies (Source: see sources cited, own processing)*

| Hazard Parameter (non-distinct) | References |
|---|---|
| **horizonal overland flow distance** | Stefanidis et al., 2021; Feloni et al., 2019; Papaioannou et al., 2015; Kanani-Sadat et al., 2019 |
| **vertical overland flow distance** | Stefanidis et al., 2021; Feloni et al., 2019; Papaioannou et al., 2015; Kanani-Sadat et al., 2019 |

| | |
|---|---|
| **aspect** | Feloni et al., 2019; Papaioannou et al., 2015; Tehrany et al., 2019 |
| **modified Fournier index** | Feloni et al., 2019; Papaioannou et al., 2015; Kanani-Sadat et al., 2019 |
| **topographic position index** | Stefanidis et al., 2021; Papaioannou et al., 2015; Kanani-Sadat et al., 2019 |
| **stream power index** | Tehrany et al., 2019; Wang et al., 2015 |

In addition to these commonly used parameters, several others have also been used in hazard-based studies including: available water capacity (Kourgialas & Karatzas, 2017), building area (Xu et al., 2018), height above nearest drainage (Ashfaq et al. 2025), length of drainage conduits (Xu et al., 2018), maximum 3-day precipitation (Wang et al., 2015), precipitation index (Taoukidou et al., 2025), precipitation time (Wang et al., 2024), runoff depth (Wang et al., 2015), sediment transport index (Tehrany et al., 2019), soil erodibility (Kourgialas & Karatzas, 2017), topographic roughness index (Tehrany et al., 2019) and typhoon frequency (Wang et al., 2015).

Hazard parameters identified in the reviewed comprehensive risk-based studies include hydrological (e.g. precipitation, flood depth, duration, velocity and curve number), topographic and terrain (e.g. topographic wetness index and curvature) as well as geological (e.g. geology) parameters.

*Table 2 Hazard parameters identified in reviewed comprehensive risk-based studies (Source: see sources cited, own processing)*

| Hazard Parameter (distinct) | References |
|---|---|
| **topographic wetness index** | Ashfaq et al. 2025; Hossain et al., 2023; Sharker et al., 2025; Gupta & Dixit, 2022; Lappas & Kallioras, 2019; Khan et al., 2025; Stefanidis et al., 2021; Feloni et al., 2019; Papaioannou et al., 2015; Kanani-Sadat et al., 2019; Tehrany et al., 2019; Wang et al., 2015 |
| **precipitation** | Ashfaq et al. 2025; Hossain et al., 2023; Sharker et al., 2025; Khan et al., 2025; Nahin et al., 2023; Yang et al., 2013; Theochari et al., 2021 |
| **curve number** | Stefanidis et al., 2021; Ekmekcioğlu et al., 2020; Feloni et al., 2019; Papaioannou et al., 2015; Kanani-Sadat et al., 2019 |

| | |
|---|---|
| **geology** | Gupta & Dixit, 2022; Lappas & Kallioras, 2019; Khan et al., 2025; Taoukidou et al., 2025; Tehrany et al., 2019 |
| **curvature** | Ashfaq et al. 2025; Khan et al., 2025; Feloni et al., 2019; Tehrany et al., 2019 |
| **flood depth** | Wang et al., 2024; Foudi et al., 2015; Cai et al., 2019; Xu et al., 2018 |
| **precipitation intensity** | Gupta & Dixit, 2022; Lappas & Kallioras, 2019; Lin et al., 2019; Kourgialas & Karatzas, 2017 |
| **flood duration** | Rana & Routray, 2017; Cai et al., 2019 |
| **flood velocity** | Foudi et al., 2015; Xu et al., 2018 |
| **precipitation frequency** | Lin et al., 2019; Wang et al., 2024 |

Additionally, several less widely applied parameters have been identified in comprehensive risk-based studies including: dam break (Yang et al., 2013), damages of previous flood (Rana & Routray, 2017), debris (Foudi et al., 2015), discharge (Gain et al., 2015), distance to embankment breach locations (Gupta & Dixit, 2022), drainage capacity (Wang et al., 2024), erosion and sedimentation (Khan et al., 2025), erosive force of water flow (Khan et al., 2025), flood area (Cai et al., 2019), floodplain (Foudi et al., 2015), fractional vegetation cover (Wang et al., 2024), frequency of flood in the neighborhood (Rana & Routray, 2017), frequency of flood inside the house (Rana & Routray, 2017), geomorphology (Gupta & Dixit, 2022), height of flood measured from local roads (Rana & Routray, 2017), height of flood measured from residence ground floor (Rana & Routray, 2017), imperviousness (Theochari et al., 2021), likelihood of inundation (Rana & Routray, 2017), number of rainy days in a year (Ekmekcioğlu et al., 2020), probability (Foudi et al., 2015), precipitation erosivity factor (Gupta & Dixit, 2022), return period of a storm event (Ekmekcioğlu et al., 2020), river cross section (Gain et al., 2015), runoff coefficient (Gupta & Dixit, 2022), spot height (Gain et al., 2015), storm water pipe network (Ekmekcioğlu et al., 2020), topographic relief (Wang et al., 2024), tsunami (Yang et al., 2013), typhoon (Yang et al., 2013) and water level (Gain et al., 2015).

Additionally, slope, elevation and normalized difference vegetation index are frequently used parameters shared between flood hazard and exposure contexts.

*Table 3 Hazard/ exposure parameters identified in reviewed studies (Source: see sources cited, own processing)*

| Hazard/ Exposure Parameter | References |
|---|---|
| **slope** | Ashfaq et al. 2025; Hossain et al., 2023; Sharker et al., 2025; Gupta & Dixit, 2022; Lappas & Kallioras, 2019; Khan et al., 2025; Lin et al., 2019; Nahin et al., 2023; Danumah et al., 2016; Stefanidis et al., 2021; Ekmekcioglu et al., 2020; Feloni et al., 2019; Papaioannou et al., 2015; Taoukidou et al., 2025; Theochari et al., 2021; Kourgialas & Karatzas, 2017; Kanani-Sadat et al., 2019; Wang et al., 2024; Tehrany et al., 2019; Jun et al., 2013; Cai et al., 2019; Xu et al., 2018; Wang et al., 2015 |
| **elevation** | Ashfaq et al. 2025; Hossain et al., 2023; Sharker et al., 2025; Gupta & Dixit, 2022; Lappas & Kallioras, 2019; Khan et al., 2025; Lin et al., 2019; Nahin et al., 2023; Danumah et al., 2016; Feloni et al., 2019; Papaioannou et al., 2015; Yang et al., 2013; Taoukidou et al., 2025; Theochari et al., 2021; Kourgialas & Karatzas, 2017; Kanani-Sadat et al., 2019; Tehrany et al., 2019; Cai et al., 2019; Xu et al., 2018 |
| **normalized difference vegetation index** | Ashfaq et al. 2025; Hossain et al., 2023; Sharker et al., 2025; Khan et al., 2025; Lin et al., 2019; Kanani-Sadat et al., 2019; Wang et al., 2015 |

Correspondingly, distance from river, drainage density and soil type are frequently used parameters that appear either as hazard or as vulnerability factors.

*Table 4 Hazard/ vulnerability parameters identified in reviewed studies (Source: see sources cited, own processing)*

| Hazard/ Vulnerability Parameter | References |
|---|---|
| **distance from river** | Ashfaq et al. 2025; Sharker et al., 2025; Gupta & Dixit, 2022; Lappas & Kallioras, 2019; Khan et al., 2025; Lin et al., 2019; Nahin et al., 2023; Taoukidou et al., 2025; Tehrany et al., 2019; Xu et al., 2018; Wang et al., 2015 |
| **drainage density** | Ashfaq et al. 2025; Sharker et al., 2025; Gupta & Dixit, 2022; Khan et al., 2025; Lin et al., 2019; Nahin et al., 2023; Danumah et al., 2016; Yang |

| | |
|---|---|
| | et al., 2013; Taoukidou et al., 2025 |
| **soil type** | Ashfaq et al. 2025; Sharker et al., 2025; Gupta & Dixit, 2022; Lappas & Kallioras, 2019; Khan et al., 2025; Nahin et al., 2023; Danumah et al., 2016; Tehrany et al., 2019; Wang et al., 2015 |

#### 2.2.3.2. Flood Exposure Parameters

The most frequently used exposure parameters (distinctively defined as exposure parameters) are grouped into socioeconomic and household, environmental/ climate and land use/ infrastructure factors for the analysis purposes of this study.

Socioeconomic and household factors include housing type (Khan et al., 2025; Rana & Routray, 2017), building construction materials (Rana & Routray, 2017), building height (Rana & Routray, 2017), dependent population (Khan et al., 2025), family type (Rana & Routray, 2017), house prices (Wang et al., 2024), household size (Rana & Routray, 2017), household with injury/ death in previous floods (Rana & Routray, 2017), household's did not receive warning about last floods (Rana & Routray, 2017), household's level of understanding national warning system (Rana & Routray, 2017), humans (Foudi et al., 2015), location of the house (Rana & Routray, 2017) and people dependent on agriculture (Gain et al., 2015).

Environmental and climatic factors include 5-day maximum precipitation (Jun et al., 2013), daily maximum precipitation (Jun et al., 2013), days over 80mm precipitation (Jun et al., 2013), ecosystems (Foudi et al., 2015), summer precipitation (June-September) (Jun et al., 2013) and surface runoff (Jun et al., 2013).

Land use and infrastructure factors include monetary value of land use and land cover types (Gain et al., 2015), non-residential (Foudi et al., 2015), number of bridges (Khan et al., 2025), number of garments industry (Gain et al., 2015) and number of total cars (Gain et al., 2015).

Seven parameters identified across the reviewed studies are shared between exposure and vulnerability concepts. These include land use and land cover, population density, total population, building age, agriculture, impermeability and residential parameters. While the parameters shared between hazard and exposure have been discussed in the previous hazard parameters section.

*Table 5 Exposure/ vulnerability parameters identified in reviewed studies (Source: see sources cited, own processing)*

| Exposure/ Vulnerability Parameter | References |
|---|---|
| **land use land cover** | Ashfaq et al. 2025; Hossain et al., 2023; Sharker et al., 2025; Gupta & Dixit, 2022; Lappas & Kallioras, 2019; Khan et al., 2025; Lin et al., 2019; Nahin et al., 2023; Ekmekcioğlu et al., 2020; Taoukidou et al., 2025; Theochari et al., 2021; Kourgialas & Karatzas, 2017; Gain et al., 2015; Tehrany et al., 2019; Wang et al., 2015 |
| **population density** | Gupta & Dixit, 2022; Khan et al., 2025; Lin et al., 2019; Nahin et al., 2023; Danumah et al., 2016; Moreira et al., 2021; Ekmekcioğlu et al., 2020; Yang et al., 2013; Wang et al., 2024; Jun et al., 2013 |
| **total population** | Khan et al., 2025; Moreira et al., 2021; Gain et al., 2015; Jun et al., 2013 |
| **building age** | Moreira et al., 2021; Gain et al., 2015; Rana & Routray, 2017 |
| **agriculture** | Gain et al., 2015; Foudi et al., 2015 |
| **impermeability** | Cai et al., 2019 |
| **residential** | Foudi et al., 2015 |

#### 2.2.3.3. Flood Vulnerability Parameters

Recognizing the importance of integrating multiple flood risk components into flood risk assessments and acknowledging the limitations of the strictly technical or hazard-based approaches that often underestimate socioeconomic dimensions, several studies have adopted more holistic methodologies. Some studies integrate vulnerability along with hazard (Nahin et al., 2023; Danumah et al., 2016) while others integrate hazard, exposure and/or vulnerability parameters (Cai et al., 2019; Foudi et al., 2015; Gain et al., 2015). Several studies adopt the conceptual framework proposed by UNDRR (2017) which includes capacity as an additional component of flood risk (Jun et al., 2013; Rana & Routray, 2017; Wang et al., 2024). While other studies such as the study of Moreira et al. (2021) focus exclusively on vulnerability, offering a focused analysis on this flood risk component. The identified vulnerability parameters are grouped into the following categories for the analysis purposes of this study:

- Hydrological and topographical parameters include among others: flow accumulation (Gupta & Dixit, 2022; Lappas & Kallioras, 2019; Stefanidis et al., 2021; Papaioannou et al., 2015; Taoukidou et al., 2025; Kourgialas &

Karatzas, 2017; Kanani-Sadat et al., 2019), relief ratio of terrain (Lin et al., 2019), distance from stream confluence (Gupta & Dixit, 2022), area ratio with the banks (Jun et al., 2013), low-lying area of less than 10m (Jun et al., 2013), low-lying household of less than 10m (Jun et al., 2013).

- Structural parameters include among others: building density (Gupta & Dixit, 2022; Cai et al., 2019), building material (Moreira et al., 2021; Gain et al., 2015), building structure (Foudi et al., 2015), building type (Moreira et al., 2021), building location (Moreira et al., 2021), built year of vulnerable structures (Ekmekcioğlu et al., 2020), road network (Moreira et al., 2021).
- Social and demographic parameters include among others: education level (Moreira et al., 2021; Ekmekcioğlu et al., 2020; Rana & Routray, 2017), female rate (Moreira et al., 2021; Rana & Routray, 2017), male rate (Rana & Routray, 2017), age of vulnerable population (Ekmekcioğlu et al., 2020), elderly rate (Moreira et al., 2021), persons with disabilities (Moreira et al., 2021), population poor (Moreira et al., 2021), vulnerable population (Gupta & Dixit, 2022), distance to vulnerable populations (Wang et al., 2024).
- Household parameters include among others: household with more than four family members (Gupta & Dixit, 2022), family members (Moreira et al., 2021), households having no means of transportation (Rana & Routray, 2017), households without safe water (Moreira et al., 2021), households without electricity (Moreira et al., 2021; Rana & Routray, 2017), households without sanitation (Moreira et al., 2021; Rana & Routray, 2017).
- Economic parameters include among others employment rate (Gupta & Dixit, 2022; Moreira et al., 2021), household income (Moreira et al., 2021), cost of flood damage last three years (Jun et al., 2013), industrial production (Yang et al., 2013), occupation of household head (Rana & Routray, 2017), population of flood damage last three years (Jun et al., 2013).
- Infrastructure and access include among others distance from road (Ashfaq et al. 2025; Sharker et al., 2025; Gupta & Dixit, 2022; Khan et al., 2025; Tehrany et al., 2019), no. of health personnel (Nahin et al., 2023), no. of shelters (Nahin et al., 2023), education facilities (Khan et al., 2025), number of hospitals (Moreira et al., 2021), own vehicle (Moreira et al., 2021), poi density (Cai et al., 2019), number of bus stops (Ekmekcioğlu et al., 2020).
- Early Warning Systems include early warning system's information content,

lead time and reliability (Gain et al., 2015), speed on onset (Foudi et al., 2015).

- Land use and land cover include among others: vegetation coverage (Yang et al., 2013), % of easily flooded farmland (Yang et al., 2013), agriculture, forestry, animal husbandry and fishing production (Yang et al., 2013), urban area (Moreira et al., 2021).

Shared parameters between hazard and vulnerability and between exposure and vulnerability are described in the previous flood hazard parameters and flood exposure parameters sections, respectively. Moreover, six parameters have been identified as shared between vulnerability and capacity-resilience concepts. These include GDP, literacy rate, dependency rate, distance from hospital, early warning system and income level parameters.

*Table 6 Vulnerability/ capacity-resilience parameters defined in reviewed studies (Source: see sources cited, own processing)*

| Vulnerability/ capacity-resilience Parameter | References |
|---|---|
| **GDP** | Lin et al., 2019; Moreira et al., 2021; Wang et al., 2024; Jun et al., 2013 |
| **literacy rate** | Khan et al., 2025; Nahin et al., 2023; Moreira et al., 2021; Gain et al., 2015 |
| **dependency rate** | Moreira et al., 2021; Gain et al., 2015; Rana & Routray, 2017 |
| **distance from hospital** | Gupta & Dixit, 2022; Wang et al., 2024; Rana & Routray, 2017 |
| **early warning system** | Foudi et al., 2015 |
| **income level** | Ekmekcioğlu et al., 2020; Gain et al., 2015 |

#### 2.2.3.4. Flood Capacity Parameters

The most frequently used capacity/ resilience parameters are grouped into coping, adaptive and transformative capacity factors for the analysis purposes of this study:

- Coping capacity, which relates to elements' ability to respond to and manage flood risk or disasters, include parameters such as infrastructure (Lin et al., 2019), medical (Lin et al., 2019), number of civil servants per population (Jun

et al., 2013), number of civil servants related to water (Jun et al., 2013), financial independence (Jun et al., 2013), flood insurance (Moreira et al., 2021), households having any kind of savings, average monthly household's savings, housing having building insurance, housing having insurance, number of earning members in household, households having family member who can swim, households having family member who has first aid knowledge, households having households with family member employed outside flood-prone area, households having land/ house outside the flood-prone community, households having multiple sources of livelihood options, households having relatives outside the city (Rana & Routray, 2017) and distance to fire station (Wang et al., 2024).

- Adaptive capacity, which relates to element's ability to learn from previous experiences and adjust accordingly, include parameters such as past flood experience (Moreira et al., 2021; Rana & Routray, 2017), frequency of public awareness programs/ drills attended, availability and circulation of emergency plans to households, households aware of emergency shelter, households aware of evacuation routes, community having land use/zoning laws and HH following them, households that have not gone to their local government for assistance in the past twelve months, strength of community cooperation in disaster response (Rana & Routray, 2017), emergency committee (Moreira et al., 2021) and per capita resident savings (Wang et al., 2024).
- Transformative capacity, which relates to element's ability to change enhancing its resiliency and reducing its vulnerability, include parameters such as accuracy of flood dispatching (Yang et al., 2013), flood control standard (Yang et al., 2013), flood controllability of reservoirs (Jun et al., 2013), capacity of drainage facilities (Jun et al., 2013), disaster relief agencies (Yang et al., 2013), ratio of improved river section (Jun et al., 2013), community having land use/zoning laws and HH following them (Rana & Routray, 2017) and strength of community cooperation in disaster response (Rana & Routray, 2017).

Additionally, six parameters identified across the reviewed studies as shared between vulnerability and capacity-resilience are presented in the corresponding section of flood vulnerability parameters.

### 2.3. Review of related studies using MCDA for flood risk assessment

Flood risk is influenced by multiple factors and underlying conditions that interact in systematic and cumulative way, often leading to catastrophic events. Its multidimensional nature renders flood risk challenging to interpret and, in some cases, difficult to assess particularly when further exacerbated by climate change, which increases the frequency and intensity of precipitation, as well as by population growth and land use changes, which intensify exposure and vulnerability (UNDRR, 2020).

Flood risk assessment requires a holistic evaluation of multiple interrelated parameters such hazard, exposure, vulnerability and capacity. To address these challenges, various methodological approaches have been developed over time. These include the historical disaster statistical method, multi-criteria index system method, remote sensing and GIS coupling method, scenario simulation evaluation method and machine learning-based algorithms (Tabasi et al., 2025; Wang et al., 2024).

Multi-Criteria Decision Analysis (MCDA) has been recognized as essential methodological framework. MCDA methods are applied to support decision-making in complex, multifaceted and time sensitive contexts such as flood risk management (Taoukidou et al., 2025). These methods integrate and prioritize diverse parameters into structured decision-making processes, enhancing transparency and accuracy (Abdullah et al., 2021).

Several methods have been applied in flood risk assessments, particularly in the mitigation phase of disaster risk management where decisions are made on developing strategic and operational planning (Abdullah et al., 2021). Although many studies apply a single MCDA method, there is a growing increase in hybrid methods applications. These hybrid methods aim to overcome limitations of single MCDA methods and are selected each time based on spatial scale, data availability, data quality, accuracy requirements and resource constraints of different studies (Abdullah et al., 2021).

The integration of MCDA with Geographic Information Systems (GIS) is another improvement in flood risk assessment. GIS enhances MCDA by providing capabilities of data analysis and visualization, enabling the creation of detailed flood risk maps that support early warning and mitigation efforts (Gupta & Dixit, 2022; Khan et al., 2025;

Taoukidou et al., 2025). By integrating diverse spatial and non-spatial datasets corresponding to examined parameters, GIS-based MCDA offers a better understanding of flood risk and facilitates decision-making processes (Taoukidou et al., 2025; Lin et al., 2019). However, GIS is mainly used passively for storing data and creating maps rather than for comprehensive analysis (Díez-Herrero & Garrote, 2020). This occurs given the absence of standardized data formats which limit systematic analysis within GIS as well as the software flexibility to adapt to diverse geographic contexts (Díez-Herrero & Garrote, 2020). These limitations undermine the potential capacity of GIS to function as main analytical tool within flood risk management.

A review of relevant literature provides several methodological paradigms applied in flood risk assessment, which combine GIS with MCDA methods such as AHP, ANP, WLC, TOPSIS, fuzzy TOPSIS and Artificial Neural Networks (ANNs), often along with other tools (Jun et al., 2013; Kourgialas & Karatzas, 2017; Xu et al., 2018; Kanani-Sadat et al., 2019; Theochari et al., 2021; Ashfaq et al., 2025). These approaches in some cases attempt to assess flood risk by using not only hazard but also vulnerability and exposure parameters to create relative maps and support decision-making. Many of these approaches apply mixed or advanced MCDA methods to overcome limitations of single methods, particularly in scarce or ungauged data and across different geographic scales. However, they include limitations like remaining subjectivity in expert judgement (Jun et al., 2013; Kanani-Sadat et al.; 2019; Theochari et al., 2021; Ashfaq et al., 2025), data availability and quality constraints (Xu et al., 2018; Theochari et al., 2021; Ashfaq et al., 2025) and omission of critical socioeconomic parameters (Xu et al., 2018; Theochari et al., 2021). To enhance model accuracy and decision-making, they often recommend comprehensive vulnerability analysis (Jun et al., 2013; Xu et al., 2018), fuzzy logic involvement (Kanani-Sadat et al.; 2019), artificial intelligence (Kourgialas & Karatzas, 2017), hydrological and hydraulic modeling (Kanani-Sadat et al.; 2019; Theochari et al., 2021) and high-resolution and quality datasets (Ashfaq et al., 2025; Xu et al., 2018). Table 7 presents several paradigms of single and hybrid MCDA approaches along with methodology details, their strengths and limitations as well as improvement recommendations.

*Table 7 Overview of MCDA (single and hybrid) methods applications in flood risk assessment (Source: see sources cited, own processing)*

| Author | Location | Method/ tools | Validation | Strengths | Limitations | Improvement recommendations |
|---|---|---|---|---|---|---|
| **Jun et al. (2013)** | South Korea | Delphi technique, Climate Scenarios (CCSM3 + SRES), WSM, TOPSIS, fuzzy TOPSIS | -Comparison of WSM, TOPSIS and fuzzy TOPSIS<br>-Spearman rank correlation coefficients | -Considers impacts under different climate change scenarios<br>-Addresses uncertainty using fuzzy concept (weighting)<br>-Combines climate change scenarios and MCDA methods for comparison purposes (ranking) | -Delphi results depend on the selection of experts<br>-Ranking differences between TOPSIS, fuzzy TOPSIS and WSM<br>-Remaining uncertainty requires vulnerability assessment | -Conduct extensive analysis of uncertainty in vulnerability assessments<br>-Integrate vulnerability framework within MCDM field |
| **Kourgialas & Karatzas (2017)** | Greece | GIS-based MCDA using Artificial Neural Networks (ANNs) | 100 historical flood events | -Addresses gap in ungauged or poorly gauged basins<br>-High mapping accuracy with ANNs<br>-Objective weighting<br>-Adaptability at different scales<br>-Policy and measures recommendation | -Black box nature of ANNs (lack of physical meaning)<br>-Data training dependency | -Use of ANNs with GIS<br>-Training models to improve extrapolation |
| **Xu et al. (2018)** | China | Entropy weight & AHP, TOPSIS, k-means, GIS, PCWMM | Historical flood damage data | -Data driven approach (no requirement in classification standards)<br>-Integrates objective (entropy weight) and subjective (AHP) weights | -Accuracy depends on data availability<br>-Overlooks/ underestimates socioeconomic factors<br>-Pre-determination of optimal number of classes | -Use comprehensive index system including socioeconomic factors<br>-Use reliable/ available data<br>-Prioritization of low impact infrastructures |

| | | | | | | |
|---|---|---|---|---|---|---|
| **Kanani-Sadat et al. (2019)** | Iran | GIS-based Hybrid MCDM using fuzzy DEMATEL ANP, AHP | Receiver Operating Characteristic (ROC) Curve, Area Under the Curve (AUC), kappa statistics, historical data | -Addresses uncertainty and subjectivity in expert judgement using fuzzy logic<br>-Adaptable in data-scarce and ungauged areas<br>-Considers linkage and interdependencies of criteria using fuzzy DEMATEL<br>-Sensitivity analysis | -Subjectivity given the dependance on expert judgment<br>-Cannot replace hydraulic and hydrologic models | -Use fuzzy logic and AI for addressing subjectivity<br>-Integrate with hydrologic and hydraulic models for accurate mapping |
| **Theochari et al. (2021)** | Greece | GIS-based MCDA using AHP, WLC and HEC-HMS hydraulic modelling | No specific method | -Includes multiple environmental/ physical and socioeconomic parameters<br>-Proposed parameters by decision makers<br>-Uses AHP for weighting and WLC for integration | -Subjectivity in weighting<br>-Non-spatial data are excluded from GIS analysis<br>-Standardization method affects results<br>-Data inaccuracy affects hydraulic simulation | -Conduct sensitivity analysis<br>-Hydrological analysis for improved predictions |
| **Ashfaq et al. (2025)** | Pakistan | GIS-based MCDA AHP, Frequency Ratio (FR), Remote Sensing | ROC, AUC, 108 flood inventory points | -Integrates multiple key flood risk parameters<br>-Uses transferable methodology applicable to diverse regions<br>-Effectively identifies flood-prone areas<br>-High AHP and FR models accuracy | -AHP depends on subjective judgement<br>-FR depends on limited and unreliable flood inventory data<br>-Medium-resolution DEM (30m)<br>-Does not simulate real time flood processes | -Use high resolution data<br>-Integrate fuzzy logic and advanced machine learning<br>-Combine existing approaches with physical hydraulic modeling<br>-Improve flood protection infrastructure<br>-Implement land use policies in high-risk flood areas |

The Analytic Hierarchy Process (AHP) is widely recognized as the most common MCDA method in flood risk assessment given its structured approach, ease of application and strong compatibility with GIS (Khan et al., 2025; Taoukidou et al., 2025; Ashfaq et al., 2025). AHP's ability to systematically compare and prioritize flood-related parameters, makes it particularly effective for identifying flood-prone areas and creating accurate flood risk maps (Lin et al., 2019; Taoukidou et al., 2025; Ashfaq et al., 2025). When integrated with GIS, AHP enables the organization of spatial and non-spatial parameters, enhancing the understanding of their relationships and supporting their management (Papaioannou et al., 2015; Lin et al., 2019). This integration is especially beneficial as it enables efficient spatial analysis and mapping of diverse datasets, producing precise and visually interpretable outputs, supporting effective interaction among decision-makers (Khan et al., 2025; Taoukidou et al., 2025). This approach is also valuable in data scarce areas where GIS-based MCDA (AHP) provides a practical solution for flood risk mapping (Taoukidou et al., 2025). To effectively address uncertainty and subjectivity in expert judgements, the method has been extended by integrating fuzzy logic (Papaioannou et al., 2015; Feloni et al., 2019; Ekmekcioğlu et al., 2020; Taoukidou et al., 2025). This extension, known as Fuzzy AHP or FAHP offers increased objectivity and flexibility by using a more relaxed numerical representation of expert preferences that AHP may fail to manage (Taoukidou et al., 2025). Although FAHP addresses some limitations of AHP, the literature also highlights that it can introduce additional complexity which could be avoided in other cases (Taoukidou et al., 2025).

Several studies in related literature have applied AHP and Fuzzy AHP (FAHP) methods within GIS framework to assess flood risk. Papaioannou et al. (2015) developed a GIS-based MCDA (AHP, FAHP) framework to identify flood-prone areas in the Xerias River watershed in Greece which has experienced repeated flood. They suggested an AHP-FAHP approach that effectively minimized uncertainty and mainstreamed expert knowledge, though some clustering methods proved unstable. In the end, they recommended normalizing criteria and using clustering methods to improve the approach. Lin et al. (2019) suggested a GIS-based MCDA (AHP) framework to evaluate the potential areas prone to urban pluvial flooding in Zhengzhou city in China. They integrated multiple parameters such geographic, hydrologic and socioeconomic along with capacity parameters. However, their approach is characterized by

subjectivity in expert judgement and data gaps. They finally recommended improvement in weighting methods and real-time assessments. Feloni et al. (2019) introduced a GIS-based hybrid MCDA (AHP, FAHP, MLC) framework to identify flood-prone areas within Attica region in Greece. The authors by comparing AHP and FAHP methods produced similar results, with FAHP showing better performance in addressing uncertainty and reducing processing time. While they effectively classified flood vulnerability using k-means clustering and developed an appropriate approach for ungauged areas, they faced challenges due to the limited data availability as well as the time consuming and complex nature of standardization. They also recommended the application of sensitivity analysis, the use of high-quality UAV-based data and the validation with historical satellite data. Ekmekcioğlu et al. (2020) applied GIS-based FAHP and sensitivity analysis to evaluate flood risk across different districts in Turkey. While their method showed robustness, it heavily depended on expert judgment and was less effective in complex geological settings. They also recommended integrating additional updated datasets and additional experts' perspectives in analysis. Gupta and Dixit (2022) applied a flexible AHP for comprehensive regional flood risk assessment in Assam, India, integrating hazard and vulnerability parameters. The authors observed the lack of data quality and historical flood records and recommended the use of multi-sensor SAR imaginary and AI and machine learning for improved assessments. Taoukidou et al. (2025) applied a GIS-based MCDA framework to evaluate flood hazard in regions of Chalkidiki, Greece. AHP and FAHP proved appropriate methods particularly in areas lacking flood data and Frequency Ratio was recognized for its predictive ability especially when quality data are available. However, they noted that FAHP introduced additional complexity and FR's effectiveness is limited due to unavailable and low-quality data. Instead, they recommended integrating larger and higher quality datasets and using advanced machine learning techniques. Finally, Khan et al. (2025) applied AHP to assess flood risk in Pakistan by integrating flood hazard, vulnerability and exposure parameters. They emphasized the omission of climate change scenarios integration in their approach and recommended addressing this limitation by integrating climate change projections, indigenous people insights and flood risk maps into land use planning. Table 8 presents several paradigms of AHP and fuzzy AHP methods along with methodology details, their strengths and limitations as well as improvement recommendations.

*Table 8 Overview of AHP and fuzzy AHP methods in flood risk assessments (Source: see sources cited, own processing)*

| Author | Location | Method/ tools | Validation | Strengths | Limitations | Improvement recommendations |
|---|---|---|---|---|---|---|
| **Papaioannou et al. (2015)** | Greece | GIS-based using AHP, FAHP | Historical flood data | -Effective with limited data<br>-Minimizes uncertainty using low-subjectivity information<br>-Integrates expert knowledge<br>-Verified consistency in results | -GMMC methods were unstable<br>-Natural Breaks had minimal contribution in high-risk zones | -Normalize criteria before MCA application<br>-Use multiple clustering methods to simulate flood-prone areas and evaluate flood hazard |
| **Lin et al. (2019)** | China | GIS-based MCDA using AHP | 74 test locations, ROC curve | -Appropriate for data-scarce areas<br>-First attempt to map flood risk at urban blocks level<br>-Integrate geographic, hydrologic and socioeconomic factors<br>-Introduces resilience/ capacity as key parameter | -Subjectivity in expert judgement<br>-Socioeconomic data gaps<br>-Bias from unreliable expert judgements<br>-Challenges in real time assessment | -Objective weighting methods<br>-Improve real time assessment efficiency |
| **Feloni et al. (2019)** | Greece | GIS-based MCDA using AHP, FAHP, Weighted Linear Combination (MLC), k-means algorithm | Historical flood data | -AHP and FAHP produced similar results<br>-FAHP better addressed uncertainty and reduced processing time (given the zero weights)<br>-Effective classification of flood vulnerability using k-means clustering<br>-Applicable in ungauged areas | -Limited precipitation data (limited rain gauge stations)<br>-Standardization can be time-consuming and complex | -Apply in larger, ungauged or diverse areas<br>-Apply sensitivity analysis on weights<br>-Use UAV-based high-resolution DEM<br>-Validate using historical satellite data |
| **Ekmekcioğlu et al. (2020)** | Turkey | GIS-based MCDA using | Historical flood data | -Integrates hazard and vulnerability criteria | -Depends on expert judgement (subjectivity) | -Integrate additional vulnerability criteria |

| | | | | | | |
|---|---|---|---|---|---|---|
| | | FAHP, Sensitivity Analysis | | -Appropriate for quick, regional and fair budged flood risk assessment<br>-Sensitivity analysis ensured high model reliability | -Performs better in areas with similar geological attributes and less in complex areas<br>-Uses 2020 data while compared floods are based between 2000-2015 | -Integrate perspectives from multiple stakeholders<br>-Use of updated data<br>-Use the method to other cities across the country |
| **Gupta & Dixit (2022)** | India | GIS-based MCDA using AHP | Confusion matrix, relative mean error, root mean square error based on flood data | -Developed based on existing literature and global research<br>-Integration of physical, social and environmental parameters<br>-Regional scale analysis<br>-Flexible and adaptable methodology<br>-Use of statistical measures for validation | -Data quality issues<br>-Limitations in historical flood data<br>-Challenging weighting | -Use of multi-sensor SAR imaginary<br>-Integration of AI and machine learning |
| **Taoukidou et al. (2025)** | Greece | GIS-based MCDA using AHP, FAHP, Frequency Ratio (FR) | AUC, ROC, DSC, Historical flood data | -AHP and FAHP are applicable in areas lacking flood records<br>-FR has high predictive capacity when available data are available<br>-Provides reliable and robust results<br>-AUC ROC correspondence between predicted and historical flood events | -AHP depends on expert judgement (subjectivity)<br>-FAHP adds complexity without improving necessarily results of AHP<br>-FR introduces uncertainties due to data unavailability and quality | -Integrate larger and higher quality datasets (updated flood inventory map, satellite data and high-resolution data)<br>-Use advanced machine learning techniques to improve accuracy<br>-Use outputs to develop adaptation and mitigation strategies |
| **Khan et al. (2025)** | Pakistan | GIS-based MCDA using AHP | AUC | -First comprehensive flood risk assessment for the catchment<br>-Integrates flood hazard, vulnerability and exposure parameters<br>-Applied in wider region | -Climate change scenarios are not integrated though their involvement is suggested<br>-limitations of MCDA method | -Integrate climate change projections<br>-Investigate land use changes' impact on water flow and surface runoff<br>-Involve indigenous' insights<br>-Integrate flood maps into land use planning |

# 3. Methods and Materials

## 3.1. Study Area

The wider area of Thermi has experienced significant urban expansion in recent years due to its proximity to Thessaloniki city in northern Greece. This urban expansion including the growth in residential, commercial and industrial uses has led to land use and land cover changes, replacing natural surfaces and potentially affecting soil infiltration and natural runoff dynamics. Such modifications are of particular concern, as they may increase flood exposure and vulnerability of elements, especially under climate change scenarios that predict increases in both the intensity and frequency of extreme precipitation events. To ensure a comprehensive and methodologically robust analysis, the study area was extended to the boundaries of the Thermi Basin including the settlement of Thermi.

Thermi Basin is located in the southwestern part of Thessaloniki Prefecture in northern Greece and southeast of Thessaloniki city. Administratively, the basin is distributed across Municipalities of Thermi and Pylaia-Chortiatis. Municipality of Thermi includes the Municipal Communities of Thermi, Mikra and Vasilika while Municipality of Pylaia-Chortiatis includes the Municipal Communities of Chortiatis, Panorama, Exochi, Asvestochori and Pylaia based on reforms introduced by Law 3852/2010 (‘Kallikratis Program’). The Municipality of Thermi is bordered by the Municipalities of Pylaia-Chortiatis to the north, Lagkadas to the northeast and Nea Propontida to the southeast and Thermaikos Gulf to the west while the Municipality of Pylaia-Chortiatis is bordered by the Municipalities of Lagkadas to the north and northeast, Thermi to the south, Kalamaria to the southwest, Thessaloniki to the west and Neapoli-Sykies and Pavlos Melas to the northwest.

The study area covers a total of 6203,35ha and is located around 40°34’ N latitude and 23°3’ E longitude. The basin is characterized by diverse conditions that influence its hydrological behavior. Particularly, the terrain is characterized by heterogeneity with higher elevations and steeper slopes identified in the northern and central parts due to the Mt. Chortiatis while low-lying areas are identified in the southern part near Thermi and the coastal zone. The hydrographic network is quite dense, consisting of numerous streams of varying orders (open and culverts). Among these, the Thermi stream is a major water body, draining the long and narrow basin and receiving runoff originating

in the higher altitudes of Panorama and Chortiatis foothills (Ypeka, 2025). The area generally has a mediterranean climate characterized by mild, wet winters and hot, dry summers but also has mainland characteristics with cooler summers and cold/ snowy winters. Precipitation is seasonal with the majority occurring during autumn and winter (Ypeka, 2025). Additionally, the settlements of Thermi, Panorama and Chortiatis are identified within the study area as well as some smaller administrative parts of Municipal Communities of Pylaia, Exochi and Asvestochori.

According to the Flood Risk Management Plan of Central Macedonia (Ypeka, 2025), the southern part of the study area falls within the flood risk zone EL10APSFR008 (Lowland Basin of Regional Trench T66, Loudias, Axios rivers including the area of the former Lake Arjan and Galliko). This zone is the largest flood-prone area in Central Macedonia (3099,38 km²) and includes both hydraulically interconnected basins and independent basins with independent hydraulic function. Under 50-,100 and 1000-year flood return periods, the Plan highlights that parts of the study area (particularly the southern parts, within and around Thermi settlement) are expected to experience impacts of varying extent. Despite the absence of a major river within the basin, such as the Anthemountas River near its southern boundary, the combined characteristics of the study area increase the potential for local flooding, thereby increasing its research interest.

Figure 1 illustrates the study area in relation to the administrative boundaries of the Municipalities and Municipal Communities as well as its key topographical and hydrographical features.

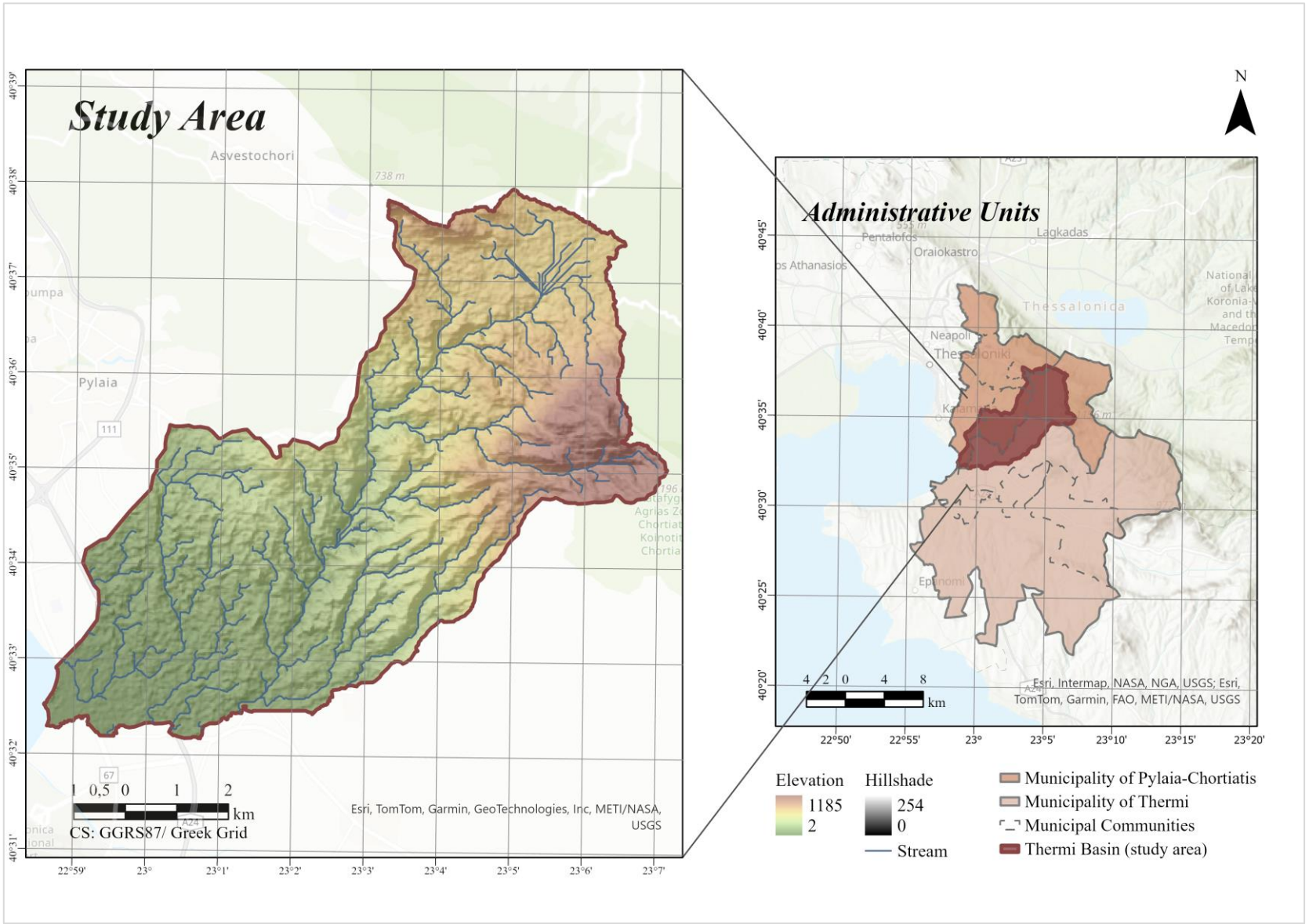


*Figure 1 Study Area & Administrative Units (own processing)*

### 3.2. Methodology

This section presents the methodology adopted by this study to achieve its objectives. Particularly, the study develops a GIS-based Multi-Criteria Analysis (MCDA) framework to identify and map flood risk zones within the Thermi Basin. It combines quantitative (hazard, exposure and vulnerability/ capacity parameters) with qualitative (local expert insights) information to provide a flood risk assessment adapted to the characteristics of the study area. The result of this process is the identification and mapping of flood-prone areas, categorized into different flood risk levels ranging from low to high, along with the estimation of the potential impacts on population, infrastructure and the environment. The flood risk zones are then validated using official Areas of Potential Significant Flood Risk (APSFR) and flood-prone locations and some indicative strategies are proposed.

The methodology includes several steps such as data collection and preparation, selection of flood risk parameters, weighting parameters and spatial analysis in GIS.

#### 3.2.1. Data Collection and Preparation

Seventeen parameters were selected and classified into hazard, exposure and vulnerability/ capacity parameters, following the United Nations Office for Disaster Risk Reduction (UNDRR, 2017) conceptualization of disaster risk. All datasets used in this study were obtained from publicly accessible sources. The study area corresponds to the Thermi Basin whose boundaries were derived using the official geoportal of Flood Risk Management Plans of the Hellenic Ministry of Environment and Energy (Flood Risk Management Plan of Central Macedonia). Administrative boundaries were obtained from the Digital Cartographic Backgrounds provided by the Hellenic Statistical Authority (ELSTAT). DEM was derived from the global Advanced Spaceborne Thermal Emission and Reflection Radiometer (ASTER) Digital Elevation Model (DEM) with an approximate spatial resolution of 30m (27,68m x 27,68m) obtained from NASA's Earth Science data repository. Satellite data were obtained from Landsat 8 imaginary provided by the U.S. Geological Survey (USGS) while yearly precipitation data from Precipitation Estimation from Remotely Sensed Information using Artificial Neural Network Cloud Classification System (PERSIANN-CCS) which is a real time global satellite precipitation product with spatial resolution of 0,04° × 0,04° developed by the Center for Hydrometeorology and Remote Sensing (CHRS)

for the period 2004-2024. Soil type information was obtained from the Soil Map of the World at a scale of 1:5000000 provided by the Food and Agriculture Organization (FAO) of the United Nations. Land use and land cover data were obtained from the CORINE Land Cover 2018 (version 2020) provided by the European Environment Agency's Copernicus Land Monitoring Service for Greece. Socioeconomic and building related information including permanent population, population by age group and buildings (residential) age were obtained from the ELSTAT based on the 2021 Population and Housing Census. Building footprints and road network data were obtained from OpenStreetMap (OSM) for Greece. Qualitative information on the health facilities was derived from the Strategic Development Plans of the Municipalities of Thermi and Pylaia-Chortiatis while emergency shelters information was obtained from the official Civil Protection Plans of the corresponding municipalities. Finally, the boundaries of the official Areas at Potential Significant Flood Risk (APSFR) used for validation purposes, were extracted from the Flood Risk Management Plan of the Region of Central Macedonia, as it is publicly available through the corresponding geoportal. While flood-prone locations were derived from municipal documents.

*Table 9 Data sources (Source: see sources cited, own processing)*

| Parameter | Source | Resolution |
|---|---|---|
| Elevation | ASTER satellite image, NASA | 27,68m x 27,68m |
| Slope, Curvature, TWI, Drainage Density, Distance from stream | Derived from DEM | 27,68m x 27,68m |
| Soil type | FAO, United Nations | - |
| Precipitation | PERSIANN-CCS, CHRS | 0,04° × 0,04° |
| NDVI | Landsat 8 satellite image, USGS | 27,68m x 27,68m |
| Population Density, Dependent Population, Building Age | ELSTAT | - |
| LULC | CORINE Land Cover, Copernicus Land Monitoring Service | - |
| Building Density, Distance from road | OpenStreetMap | - |
| Distance from health facilities | Strategic Development Plans | - |
| Distance from emergency shelter | Civil Protection Plans | - |

### 3.2.2. Selection of Flood Risk Parameters

The selection of parameters was guided by an extensive review of twenty-eight peer-reviewed studies, particularly those employing Multi-Criteria Decision Analysis (MCDA) and Geographic Information Systems (GIS). This GIS-based MCDA framework considers seventeen parameters representing hazard, exposure, vulnerability and capacity. As there is no universally established set of parameters or a strict categorization (Abdullah et al., 2021), their selection was driven by the need to provide a holistic representation of flood risk, ensure a balance between comprehensiveness and manageability and consider available, accessible and relevant datasets. Despite their careful selection based on their conceptual relevance to flood risk, potential underlying interdependencies among parameters are not extensively examined which may introduce some redundancy in the analysis while their categorization is justified according to the definitions adopted in this study.

The selected parameters are divided into three categories as follows:

- Flood hazard parameters include elevation (Ashfaq et al. 2025; Hossain et al., 2023; Sharker et al., 2025; Gupta & Dixit, 2022; Lappas & Kallioras, 2019; Khan et al., 2025), slope (Ashfaq et al. 2025; Hossain et al., 2023; Sharker et al., 2025; Gupta & Dixit, 2022; Lappas & Kallioras, 2019; Khan et al., 2025), soil type (Ashfaq et al. 2025; Sharker et al., 2025; Gupta & Dixit, 2022; Lappas & Kallioras, 2019; Khan et al., 2025; Nahin et al., 2023), curvature (Ashfaq et al. 2025; Khan et al., 2025; Feloni et al., 2019; Tehrany et al., 2019), precipitation (Ashfaq et al. 2025; Hossain et al., 2023; Sharker et al., 2025; Khan et al., 2025; Nahin et al., 2023; Yang et al., 2013; Theochari et al., 2021), Topographic Wetness Index (TWI) (Sharker et al., 2025; Gupta & Dixit, 2022; Lappas & Kallioras, 2019; Khan et al., 2025; Stefanidis et al., 2021; Feloni et al., 2019), drainage density (Khan et al., 2025; Lin et al., 2019; Nahin et al., 2023; Danumah et al., 2016; Yang et al., 2013; Taoukidou et al., 2025) and distance from stream (Lin et al., 2019; Nahin et al., 2023; Taoukidou et al., 2025; Tehrany et al., 2019; Xu et al., 2018; Wang et al., 2015).
- Flood exposure parameters include Normalized Difference Vegetation Index (NDVI) (Hossain et al., 2023; Sharker et al., 2025; Khan et al., 2025; Lin et al., 2019; Kanani-Sadat et al., 2019; Wang et al., 2015), population density (Danumah et al., 2016; Moreira et al., 2021; Ekmekcioğlu et al., 2020; Yang

et al., 2013; Wang et al., 2024; Jun et al., 2013) and Land Use and Land Cover (LULC) (Taoukidou et al., 2025; Theochari et al., 2021; Kourgialas & Karatzas, 2017; Gain et al., 2015; Tehrany et al., 2019; Wang et al., 2015).

- Flood vulnerability/ capacity parameters include dependent population (Moreira et al., 2021; Gain et al., 2015; Rana & Routray, 2017), building density (Gupta & Dixit, 2022; Cai et al., 2019), distance from road (Ashfaq et al. 2025; Sharker et al., 2025; Gupta & Dixit, 2022; Khan et al., 2025; Tehrany et al., 2019), distance from health facilities (Gupta & Dixit, 2022; Wang et al., 2024; Rana & Routray, 2017), distance from emergency shelter (Nahin et al., 2023) and building (residential) age (Moreira et al., 2021; Gain et al., 2015; Rana & Routray, 2017).

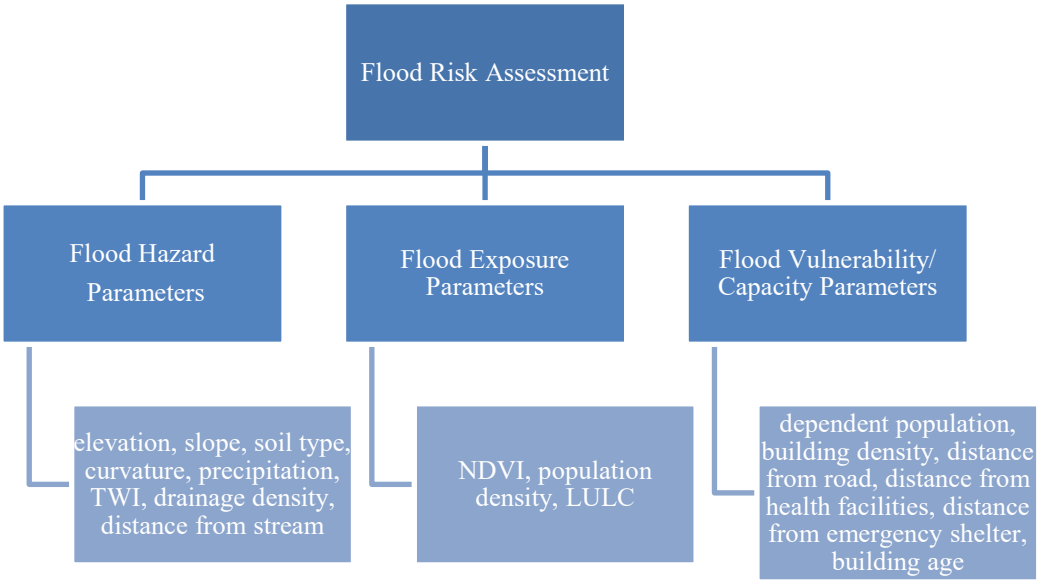


*Figure 2 Flood hazard, exposure and vulnerability/ capacity parameters (own processing)*

The sections below describe each of these parameters and their contribution to the flood risk.

Elevation, defined as the height above mean sea level, is inversely related to flood risk, as low-lying areas are more prone to water accumulation while higher areas drain more efficiently (Asfaq et al., 2025; Hossain et al., 2023; Lappas & Kallioras, 2019; Sharker et al., 2025). Slope, defined as the level of steepness or inclination of the land surface to the horizontal plane is inversely related to flood risk, as gentle slopes or flatter

surfaces promote water accumulation and prolonged inundation while steeper slopes enhance runoff but may increase flash flood and soil erosion (Sharker et al., 2025; Hossain et al., 2023; Ashfaq et al., 2025; Lappas & Kallioras, 2019). Soil type, defined by its texture, composition and infiltration properties, determines surface runoff and flood potential with low permeable soils, such as clay soils, causing water accumulation while permeable soils, such as sandy soils, enhancing infiltration (Ashfaq, 2025; Lappas & Kallioras, 2019; Khan et al., 2025; Sharker et al., 2025). Curvature, defined as the shape of the land surface in either a horizontal or vertical plane, determines the movement of surface water with the flat (values around zero) and concave surfaces (negative values) being more prone to water accumulation compared to convex surfaces (positive values) (Ashfaq et al., 2025; Khan et al., 2025). Precipitation, defined as the deposition of water from the atmosphere to the surface of Earth, is directly related to flood risk as high intensity or prolonged precipitation may produce surplus water and exceed drainage capacity increasing the flood likelihood (Ashfaq et al., 2025; Hossain et al., 2023; Sharker et al., 2025; Khan et al., 2025). TWI, a terrain-based metric used to assess how upstream contributing area and local slope influence soil moisture, is directly related to flood risk, as higher values correspond to drainage depressions and wetter conditions, increasing the likelihood of flooding compared to crests and ridges with well-drained conditions (Ashfaq et al., 2025; Hossain et al., 2023; Sharker et al., 2025; Lappas & Kallioras, 2019; Khan et al., 2025). Drainage density, defined as the ratio of the total length of streams to the area's size, is directly related to flood risk with higher drainage density increasing drainage paths for water movement and runoff, thereby increasing the likelihood of flooding, compared to the areas with lower drainage density (Ashfaq et al., 2025; Sharker et al., 2025; Khan et al., 2025). Distance from stream is inversely related to flood risk, as areas located close to streams are more prone to flooding due to potential overflow during precipitation events, while more distant areas are less likely to be affected (Sharker et al., 2025; Khan et al., 2025).

NDVI reflects the vegetation and soil conditions and is inversely related to flood risk as low values correspond to sparse, unhealthy vegetation and higher exposure due to increased runoff, while high values correspond to dense, healthy vegetation and lower exposure due to infiltration capacity (Lin et., 2019). Population density reflects the number of people potentially affected during a flood event and is directly related to flood risk. Areas with higher population density are more exposed, as a greater number

of individuals are at risk of injury or fatalities, while areas with lower population density are generally less potentially affected (Khan et al., 2025; Lin et al., 2019). LULC reflects the human and environmental characteristics of an area, where different land use and land cover types are associated with varying levels of exposure to flooding. Areas covered by forests and high vegetation show lower exposure due to infiltration capacity while urban or impermeable surfaces show high exposure due to increased runoff (Lin et al., 2019).

Dependent population is a critical parameter in flood risk assessment due to its influence on vulnerability and response capacity. Children, older adults and people with disabilities often perceive and experience physical, social or cultural constraints that limit their ability to respond during flood events, affecting their evacuation and access to services (Khan et al., 2025). A higher dependency rate is associated with a greater part of population potentially affected by flooding. Building density reflects the concentration of structures within an area, with low-density areas providing more open space and facilitating evacuation during flood events while high-density areas limiting movement and increasing evacuation time (Cai et al., 2019). Distance from road affects evacuation and emergency response, with areas closer to road experiencing quicker evacuation and better access to operational support while more distant areas may experience delays and being more susceptible to flood impacts (Khan et al., 2025). Distance from health facilities affects timely medical support during flood events (Khan et al., 2025), with areas closer to health facilities benefiting from timely access to medical care compared to more distant areas. Distance from emergency shelter is important factor in flood risk assessment as shelters function as evacuation points and support emergency response during flood events (Khan et al., 2025). Therefore, communities located closer to shelters can generally respond timely and access related services more easily, while those located farther may face challenges and higher likelihood of being affected by flooding. Building (residential) age affects vulnerability as older buildings that often do not comply with construction standards are more susceptible to flood impacts compared to newer buildings that show greater resistance (Ekmekcioğlu et al., 2020). Therefore, a higher building age rate is associated with a greater number of buildings potentially affected by flooding.

At this stage, it is necessary to present the key limitations and assumptions adopted in this study, particularly those that influence the methodological approach and the interpretation of the results. While additional supporting details for these parameters are provided in Appendix I.

**Precipitation**

Given the absence of meteorological stations within the study area, which limits the efficient application of spatial interpolation methods, annual precipitation data for the period 2004-2024 were derived from the publicly available PERSIANN-CCS dataset. Although this dataset has lower resolution, as the original cell size is larger compared to the cell size of other raster files used in this study, it is considered adequate for the analysis given the extent of the basin and the range of precipitation values.

**DEM**

The analysis is based on the global ASTER DEM (NASA) with an approximate resolution of 30m, as higher-resolution DEM (e.g. 10m) was not publicly available and required additional costs. This relatively lower-resolution dataset may reduce the accuracy of the DEM-derived parameters, such as terrain and hydrographic network representation, particularly near study area's boundaries where inconsistencies with the officially derived boundaries of the basin may occur.

**Population density**

Population density was calculated using 2021 population data and administrative boundaries data from the Hellenic Statistical Authority (ELSTAT) by dividing the permanent population of each municipal community by its respective area. Population density is aggregated at the municipal community level, with a single value assigned to each municipal community which represents the lowest administrative level for which detailed data are available for analysis in Greece. However, this approach may not accurately capture micro-scale variation across municipal communities, particularly for those that are only partially included within the study area (Municipal Communities of

Pylaia, Asvestochori and Exochi), leading to an overestimation of the population density.

**Dependent population**

Dependent population was estimated based on age-based data, particularly 2021 population data from ELSTAT. A dependency rate was calculated to represent the proportion of dependent population as follows:

$$\text{Dependency Rate (\%)} = \left( \frac{Population\ 0{-}14\ years + Population\ 65{+}years}{Population\ 15{-}64\ years} \right) \text{x } 100$$

Dependent population is aggregated at the municipal community level, with a single value assigned to each municipal community which represents the lowest administrative level for which detailed data are available for analysis in Greece. However, this approach may not accurately capture micro-scale variation across municipal communities, particularly for those that are only partially included within the study area (Municipal Communities of Pylaia, Asvestochori and Exochi), leading to an overestimation or underestimation of dependent and non-dependent populations.

**Building (residential) age**

Building age was estimated based on the year of construction of residential buildings, using 2021 housing data from ELSTAT. A building age rate was calculated to represent the proportion of older buildings as follows:

$$\text{Building Age Rate (\%)} = \left( \frac{Buildings\ (residential) before\ 1945 + Buildings\ 1946{-}1980 + Buildings\ 1981{-}1990}{Buildings\ 1991{-}2010 + Buildings\ After\ 2011} \right) \text{x } 100$$

Building age population is aggregated at the municipal community level, with a single value assigned to each municipal community which represents the lowest administrative level for which detailed data are available for analysis in Greece. However, this approach may not accurately capture micro-scale variation across municipal communities, particularly for those that are only partially included within the

study area (Municipal Communities of Pylaia, Asvestochori and Exochi), leading to an overestimation or underestimation of buildings' age.

**Temporal Dimension**

The analysis considers both static (e.g. topography, slope, soil characteristics) and dynamic datasets (e.g. land use/ land cover, population, precipitation) introducing temporal inconsistencies. Particularly, census data represent a single year (2021) while precipitation data correspond to the period 2004-2024. Additionally, the use of historical precipitation data, as derived from the PERSIANN-CCS, does not include climate change projections, limiting the potential to represent future risk scenarios especially in Mediterranean regions where an increase in intensity and frequency of extreme precipitation events is expected.

### 3.2.3. Weighting Parameters

AHP was used to determine the relative importance of the selected parameters contributing to flood risk in the Thermi Basin. AHP, developed by Saaty (1977), is one of the most widely used methods in MCDA given its systematic approach and effectiveness in addressing complex decision problems that involve different competitive parameters (Abdullah et al., 2021; Wang et al., 2024; Khan et al., 2025). The method supports decision-making by deconstructing the problem into a hierarchical structure of criteria, sub-criteria and alternatives to support their weighting and prioritization (Saaty, 1990). Moreover, it enables the evaluation of both qualitative and quantitative parameters through pairwise comparisons, determining their relatively importance as reflected in their assigned weights (Saaty, 1990; Sun et al., 2013). By integrating consistency checks to address potential subjectivity or bias, AHP enhances the reliability of the model, providing a comprehensive framework for informed decision-making. AHP includes three main methodological steps: structuring the decision problem and selecting relevant criteria, assigning weights to these criteria through pairwise comparison and calculating the overall relative scores of alternatives (Saaty, 1990).

**Structuring the decision problem and selecting relevant criteria**

The first methodological step of AHP involves structuring the decision problem by decomposing it into several successive levels. At the top level is the main goal or objective of the decision problem, followed by a set of criteria and sub-criteria and decision alternatives at the bottom level (Saaty, 1990).

One of AHP's advantages is the adaptability and flexibility of this hierarchical structure. As Saaty (1990) states, the process supports non-completeness, meaning that the hierarchy does not require all elements to be directly related or compared to each other. Moreover, the hierarchy can include diverse perspectives on the decision problem, enabling each level to represent different aspects or criteria. Hierarchy also enables flexible management, with elements being selectively included or excluded based on decision makers' specific needs and priorities. Furthermore, the hierarchical structure can be adjusted or reorganized shifting from general to specific concepts while refinement can be applied by removing elements without requiring a complete modification of previous judgments (Saaty, 1990).

**Assigning weights to these criteria through pairwise comparison**

The second methodological step of AHP involves assigning weights to these criteria through pairwise comparison. In this phase, decision-makers by comparing two elements express their relative importance or preference (Saaty, 1990; Lyu et al., 2018). Typically, comparisons apply Saaty's linear scale which ranges from 1 to 9, where 1 represents equal importance and 9 represents extreme importance (Saaty, 1990). However, except from this scale, various alternative scales have been proposed over time to better capture verbal judgments and enhance precision of priorities such as power, geometric, logarithmic, root square, asymptotical (Meesariganda & Ishizaka, 2016).

*Table 10 Fundamental scale of Saaty (Source: Saaty 1990)*

| Intensity of importance or preference | Definition of importance | Description |
|---|---|---|
| **1** | Equal | Equal contribution |
| **3** | Moderate | One activity is slightly favored |
| **5** | Essential | One activity is strongly favored |
| **7** | Very strong | Strongly favored and dominant in practice |
| **9** | Extreme | Absolut importance/ preference |
| **2,4,6,8** | Intermediate | Compromising |

The judgements of decision-makers develop a pairwise comparison matrix in which two elements are compared each time by assessing their relative importance (Meesariganda & Ishizaka, 2016). Particularly, each element $a_{ij}$ in the pairwise comparison matrix represents the relative importance of criterion i compared to criterion j. The matrix applies reciprocal property, meaning that $a_{ji} = \frac{1}{a_{ij}}$, and the diagonal entries are equal to one ($a_{ii} = 1$), reflecting that each criterion is equally important to itself (Saaty, 1990; Vargas, 1990). These axioms of AHP are briefly presented below.

*Table 11 Axioms of AHP (Source: Vargas, 1990, own processing)*

| Axiom of AHP | Description |
|---|---|
| **Reciprocal comparison** | If A is x times preferred to B, then B is 1/x times preferred to A |
| **Homogeneity** | Comparisons use a 1–9 scale; elements must be comparable |
| **Independence** | Preferences for criteria are independent of the alternatives |
| **Expectations** | All relevant criteria and alternatives should be considered |

When the pairwise comparison matrix is completed, the relative criteria weights can be calculated. One common method is the geometric mean method, where the weight $w_i$ of each criterion i is derived as follows (Lyu et al., 2018).

$$w_i = \frac{M_i}{\sum_{i=1}^{n} M_i}$$

where $M_i = \sqrt[n]{\prod_{j=1}^{n} a_{ij}}$

To assess the sensitivity and consistency of the judgement matrix, Consistency Index (CI) and Consistency Ratio (CR) are calculated (Saaty, 1990). CI can be calculated with following formula:

$$CI = \frac{\lambda_{max} - n}{n-1}$$

where $\lambda_{max}$ is the largest eigenvalue of the matrix, can be calculated with the formula:

$$\lambda_{max} = \sum_{i=1}^{n} \frac{\sum_{j=1}^{n} a_{ij} w_i}{n w_i}$$

CR is calculated as follows:

$$CR = \frac{CI}{RI}$$

where Random Index (RI) is the average CI for randomly generated reciprocal matrices. According to Saaty (1990) if CR is <10%, then the matrix is considered consistent.

**Calculating the overall relative scores of alternatives**

The third methodological step of AHP involves the calculation of the global priorities (or overall scores) of the decision alternatives by combining the local priorities of the alternatives under each criterion with the corresponding criterion weights. Particularly, local priorities are organized in a matrix where each column represents a criterion and each row represents an alternative. Each column is multiplied by the weight of the specific criterion and the resulting weighted scores in each row are summed. The sum of the scores refers to the global priority of each alternative. Based on the overall relative scores of the decision alternatives, the alternatives can be ranked under the problem objective. The alternative with the highest global priority is considered as the most appropriate (Saaty, 1990).

Although AHP is widely applied for decision-making, there are several limitations associated with the method. One limitation is the use of consistency ratio (CR) threshold of 0,1 which may not be appropriate for all the cases (Abdullah et al., 2021). Another limitation is the rank change, where the ranking of existing elements in the hierarchical structure may change when a new element is included or excluded, influencing the force of the axiom of independence (Ho & Ma, 2017; Vargas, 1990). Additionally, AHP can become challenging for medium and large decision problems due to the great number of pairwise comparisons applied (Abdullah et al., 2021). The pairwise comparison also introduces imprecision concerns, as it is based on expert judgments who may find difficulty in assigning specific numerical values to their preferences (Liu et al., 2020). Traditional AHP argues that judgments are precise, not adequately capturing the uncertainty and subjectivity in decision makers' preferences (Aruldoss et al., 2013). To address this limitation, Fuzzy AHP was developed by applying fuzzy logic in decision-making (Aruldoss et al., 2013). FAHP (originally introduced by Zadeh in 1965) provides a structured framework for evaluating criteria or alternatives that reflect the uncertainty and vagueness of real-world problems (Aruldoss et al., 2013; Ho & Ma, 2017; Gündoğdu & Kahraman, 2019). Particularly, it translates subjective judgements into linguistic variables represented as fuzzy intervals (zero or near zero weights) to capture the uncertainty in qualitative evaluations and human preferences (Aruldoss et al., 2013; Ho & Ma, 2017). FAHP can explain appropriately problems where information is uncertain, whereas AHP is suitable in cases where judgements are more certain (Aruldoss et al., 2013).

Given the characteristics of the decision problem in this study, AHP was applied to assess and map the flood risk within the study area, integrating parameters that reflect hazard, exposure and vulnerability/ capacity. The seventeen parameters, identified through an extensive literature review as described in previous sections, were organized into a hierarchical structure. At the highest level was set the overall goal or decision objective (assessment and mapping of flood risk), followed by flood risk components (hazard, exposure and vulnerability/ capacity) and the flood risk parameters at the lowest level. Then, pairwise comparisons to determine parameter weights based on expert judgement were applied. For this purpose, a 17x17 Pairwise Comparison Matrix (PCM) was constructed in which each parameter was compared to all other parameters in pairs to evaluate their relative importance in contributing to flood risk.

The comparison process followed the AHP Axioms (Saaty, 1990; Vargas, 1990):

- For each element $a_{ij}$ the reciprocal value $a_{ji} = 1/ a_{ij}$ was automatically assigned and all diagonal elements were set to 1 (reciprocal comparison).
- All comparisons were constructed using Saaty's 1-9 scale, ensuring that all elements were comparable (homogeneity comparison).
- Preferences among parameters of the same hierarchical level were independent of other levels (independence).
- All parameters identified in the literature review were included in the decision hierarchy and considered in the analysis (expectations).

Local experts and stakeholders' participation was essential to ensure that weighting considers scientific knowledge and experience. The PCM was distributed to ten experts and stakeholders. Participation was voluntary and anonymity and confidentiality were ensured throughout the process. A total of five responses (n=5)[1] were collected from experts, researchers and professionals from universities, research institutions, municipal and regional authorities, activating in spatial and environmental planning, hydrology/ hydraulics and disaster management fields.

Table 12 presents the participants' profiles according to their sector, division and proficiency.

*Table 12 Participants' profiles (own processing)*

| Role | Sector | Division | Proficiency |
|---|---|---|---|
| **Professor** | University | Environment | Civil Engineer |
| **Professor** | University | Hydraulics | Civil Engineer |
| **Researcher** | Research Institute | Hydrology | Forest Engineer |
| **Board Advisor** | Regional Authority | Disaster Risk Management | Civil Engineer |
| **Board Advisor** | Municipal Authority | Urban Planning | Topographical Engineer |

[1] The limited participation was mainly attributed to the high workload of potential participants and the specialized nature of the survey. These obstacles represent common challenges in participatory processes. However, they also raise concerns regarding the level of participatory maturity in co-planning.

The five completed PCMs were examined for internal consistency according to AHP methodology. Three responses satisfied the consistency threshold (CR<0,10) while two responses slightly exceeded it. These two matrices were returned to the responders for reassessment. However, only one changed matrix was received while the other was kept without changes. Although two responses showed CR slightly above the threshold, their judgements were retained due to the limited number of responses.

To address potential inconsistencies among experts, individual judgements were aggregated using the geometric mean method. More particularly, for each row i of the combined matrix the geometric mean $M_i$ was calculated. The normalized weight vector $w_i$ was then calculated by dividing each geometric mean $M_i$ by the sum of all geometric means, ensuring that the weights sum to one. Subsequently, the weighed sum vector $A_w$ was calculated by multiplying the combined matrix A by the weight vector w. Each element of $A_w$ was divided by the corresponding weight $w_i$ to calculate the consistency vector, from which the maximum eigenvalue $\lambda_{max}$ was derived. The Consistency Index and Consistency Ratio were then calculated to assess the reliability of the judgements. For n=17, the Random Index is 1,59.

The aggregation of individual judgements applying the geometric mean method reduced individual inconsistencies and resulted in a combined PCM that satisfied the consistency criterion (CR<0,10), confirming the reliability of weights. This approach is widely applied in interdisciplinary studies, particularly in environmental decision-making and spatial planning, where expert-based AHP studies with small sample sizes are common. In this context, the results are based on the consistency of pairwise comparisons and the quality of expert judgements rather than statistical representativeness (e.g. through hypothesis testing). In addition, no extensive sensitivity analysis was applied to further assess the influence of variations in weights and results, given the scope of the study.

### 3.2.4. Spatial Analysis in GIS

The combination of MCDA with GIS is recognized as a significant advancement in flood risk assessment, providing spatial analysis, data management and visualization capabilities to create detailed flood risk maps that can inform early warning systems and support mitigation strategies (Gupta & Dixit, 2022; Khan et al., 2025; Taoukidou

et al., 2025). GIS played a central role across all methodological steps of this study supporting data management, weighted overlay analysis, impact analysis and validation.

#### 3.2.4.1. Data Management

After completing the collection of all required datasets corresponding to flood hazard, exposure and vulnerability/ capacity parameters, data were imported into ArcGIS Pro (version 3.6.0) for analysis. All raster and vector layers were projected into a common coordinate reference system, with the Greek Grid (EPSG:2100) adopted as Projected Coordinate System and GGRS 1987 (EPSG: 4121) as Geographic Coordinate System. Additionally, they were clipped to the boundaries of the Thermi Basin and resampled to a cell size of 27,68m x 27,68m corresponding to analysis resolution. To ensure comparability among parameters expressed in different units (meters, percentage, index values) all datasets were standardized using a min-max normalization and then classified using the Natural Breaks (Jenks) method. The following sections provide a detailed description of the management of each dataset individually.

Elevation data were obtained from the ASTER DEM, specifically from ASTGTMV003_N40E022_dem and ASTGTMV003_N40E023_dem tiles, which were combined to cover the whole study area's extension. The mosaic raster was projected and clipped to the boundaries of the Thermi Basin. Elevation values ranged from 2 to 1185m and were classified into five categories using the Natural Breaks (Jenks) method: 2,001-168m; 168,001-368m; 368,001-573m; 573,001-795m; 795,001-1185m corresponding to 1-5 classes and then assigned flood risk values. Given the inverse relationship between elevation and flood risk, classes were assigned risk values in descending order from 5 (lowest elevation, highest risk) to 1 (highest elevation, lowest risk).

Slope was derived from the DEM using the Slope tool from Spatial Analyst Tools. The raster was projected into the common reference system and clipped to the boundaries of the study area. Slope values ranged from 0 to 57,138° and were classified into five categories using the Natural Breaks (Jenks) method: 0,001-5,826°; 5,827-11,652°; 11,653-18,374°; 18,375-27,113°; 27,114-57,138° corresponding to 1-5 classes and then assigned flood risk values. Given the reverse relationship between slope and flood risk,

classes assigned risk values in descending order from 5 (lowest slope, highest risk) to 1 (steepest slope, lowest risk).

Soil type data (vector format) were obtained from the FAO Digital Soil Map of the World (DSWM). The layer was projected into the common reference system, clipped to the boundaries of the study area and rasterized using the same cell size as the other raster files. Two soil types were identified in the study area including Chromic Luvisols (Lc104-2/3bc) and Calcaric Regosols (Rc49-2ab). The raster was classified into two categorical classes, Calcaric Regosols-Rc49-2ab and Chromic Luvisols-Lc104-2/3bc and then assigned flood risk values. Based on other studies assessing flood risk of Calcaric Regosols and Chromic Luvisols, it is concluded that Calcaric Regosols- Rc49-2ab show low flood risk corresponding to a flood risk value of 2 (Ashfaq et al., 2025) while Chromic Luvisols show moderate flood risk corresponding to flood risk value of 3 (Gebremichael et al., 2025). These flood risk values are similarly adopted in this study.

Curvature was derived from the DEM using the Curvature tool from Spatial Analyst Tools. The raster was projected into the common reference system and clipped to the boundaries of the study area. Curvature values ranged from -14,971 to 18,859 and were classified into five categories using the Natural Breaks (Jenks) method: -14,971 - -3,297; -3,296 - -0,909; -0,908 - 0,949; 0,95-3,469; 3,47-18,859 corresponding to 1-5 classes and then assigned flood risk values. Given that the relationship between curvature and flood risk, flat areas (class 3, near zero) were assigned with the highest risk value of 5, concave surfaces (negative curvature) were assigned risk values of 4 (for 1st class – strongly concave) and 3 (for 2nd class – weakly concave) and convex surfaces (positive curvature) were assigned lower risk values of 2 (for 4th class- weakly convex) and 1 (for 5th class – strongly convex).

Precipitation data were obtained from the PERSIANN-CCS satellite-based dataset of the CHRS for the period 2004-2024. The set of rasters corresponding to each year was projected into the common reference system, clipped to the boundaries of the study area and resampled using the same cell size as the other raster files. It should be noted that the original raster resolution of 0,04° × 0,04° limits the spatial precision of the resulting raster. Average annual precipitation was calculated using the Raster Calculator tool in

Spatial Analyst Tools. Precipitation values ranged from 621,049 to 672,381mm and were classified into five categories using the Natural Breaks (Jenks) method: 621,049-622,859mm; 622,86-640,172mm; 640,173-647,62mm; 647,621-658,491mm; 658,492-672,381mm corresponding to 1-5 classes and then assigned flood risk values. Given the direct relationship between elevation and flood risk, classes were assigned risk values in ascending order from 1 (lowest precipitation, lowest risk) to 5 (highest precipitation, highest risk).

TWI was derived from the DEM following a sequential creation of filled DEM, flow direction and flow accumulation layers (Hydrology tools) and slope calculated in radians. TWI was calculated using the formula:

$$TWI = ln\frac{A_s}{tan\beta}$$

where As is the specific catchment area and β is the local slope (in radians). TWI index was calculated using the Raster Calculator tool. TWI values ranged from 3,203 to 19,232 and were classified into five categories using the Natural Breaks (Jenks) method: 3,204-5,592; 5,593-7,163; 7,164-9,3; 9,301-12,255; 12,256-19,232 corresponding to 1-5 classes and then assigned flood risk values. Given the direct relationship between TWI and flood risk, classes were assigned risk values in ascending order from 1 (lowest TWI value, lowest risk) to 5 (highest TWI value, highest risk).

Drainage density was derived from the DEM following several steps. Firstly, the Stream Order layer was created by applying the respective Spatial Analyst tool and using the same cell size and spatial extent with other raster files. Then, the raster stream network was converted to vector format using the Stream to Feature tool. Only streams with orders greater than 3 were kept and then dissolved based on their stream order. Then, the Line Density tool was used to generate a continuous surface raster representing drainage density across the study area. Drainage density values ranged from 0 to 10,821 and were classified into five categories using the Natural Breaks (Jenks) method: 0,001-1,188; 1,189-2,419; 2,42-3,565; 3,566-5,814; 5,815-10,821 corresponding to 1-5 classes and then assigned flood risk values. Given the direct relationship between drainage density and flood risk, classes were assigned risk values

in ascending order from 1 (lowest drainage density, lowest risk) to 5 (highest drainage density, highest risk).

Distance from stream was calculated using the Euclidean Distance tool based on the dissolved stream network derived from the previous process. Distance from stream values ranged from 0 to 765,683m and were classified into five categories using the Natural Breaks (Jenks) method: 0,001-81,072m; 81,073-168,15m; 168,151-258,23m; 258,231-375,335m; 375,336-765,683m corresponding to 1-5 classes and then assigned flood risk values. Given the reverse relationship between distance from stream and flood risk, classes assigned risk values in descending order from 5 (shortest distance, highest risk) to 1 (greatest distance, lowest risk).

NDVI values were derived from USGS Landsat 8 imaginary (bands 4 and 5; path 184, row 032, Level 1, Collection 2, Tier 1) and the NDVI index was calculated using the Raster Calculator (Spatial Analyst Tool) based on the expression NDVI=NIR-RED/ NIR+RED with red band corresponding to band 4 and NIR band corresponding to band 5. NDVI values ranged from -0,036 to 0,546 and were classified into five categories using the Natural Breaks (Jenks) method: -0,036-0,173; 0,174-0,237; 0,238-0,301; 0,302-0,377; 0,378-0,546 corresponding to 1-5 classes and then assigned flood risk values. Given the reverse relationship between NDVI and flood risk, classes assigned risk values in descending order from 5 (lowest NDVI value, highest risk) to 1 (highest NDVI value, lowest risk).

Population density was calculated by dividing the total population of each municipal community by the area of the corresponding municipal community in hectares (ha), after joining the relevant tables obtained from the 2021 ELSTAT census. Population density values ranged from 0,792 to 15,031 permanent residents per hectare and were classified into four categories using the Natural Breaks (Jenks) method: 0,792-1,852; 1,853-5,258; 5,259-8,106; 8,107-15,031 corresponding to 1-4 classes and then assigned flood risk values. Given the direct relationship between population density and flood risk, classes were assigned risk values in ascending order from 1 (lowest population density, lowest risk) to 4 (highest population density, highest risk). It is noted that the Natural Breaks method couldn’t produce five statistically meaningful classes, therefore in this case only four classes were used.

LULC data (vector format) were derived from CORINE Land Cover dataset provided by the Copernicus Land Monitoring Service. The layer was projected into the common reference system, clipped to the boundaries of the study area and rasterized using the same cell size as the other raster files. Within the study area, nineteen LULC types were identified with sclerophyllous vegetation covering the largest part, followed by transitional woodland-shrub, discontinuous urban fabric and complex cultivation patterns, while smaller areas were covered by other LULC types. These nineteen LULC types were classified into five categorical classes based on their infiltration capacity and contribution to runoff: coastal and marine zones, forested areas, semi-natural grasslands and shrubs, agricultural lands and mixed farming and built-up and industrial urban areas. These categories corresponding to 1-5 classes (1 corresponds to lowest contribution/lowest runoff and 5 corresponds to highest runoff/ lowest infiltration) assigned flood risk values. Given the direct relationship between LULC characteristics and flood risk, classes were assigned risk values in ascending order from 1 (coastal and marine zones, lowest risk) to 5 (built up and industrial urban areas, highest risk).

*Table 13 LULC categorization in the study area based on infiltration capacity and runoff potential (Source: Copernicus, own processing)*

| **Infiltration Capacity/ Runoff** | **Class Value** | **LULC Category based on Copernicus** | **LULC Category in this study** |
|---|---|---|---|
| **Very low infiltration / High runoff** | 5 | Continuous urban fabric, Discontinuous urban fabric, Industrial or commercial units, Airports, Mineral extraction sites, Construction sites | Built-up and industrial urban areas |
| **Low infiltration / Moderate-high runoff** | 4 | Non-irrigated arable land, Permanently irrigated land, Pastures, Complex cultivation patterns, Land principally occupied by agriculture, with significant areas of natural vegetation | Agricultural lands and mixed farming |
| **Medium infiltration** | 3 | Natural grasslands, Sclerophyllous vegetation, Transitional woodland-shrub | Semi-natural grasslands and shrubs |

| | | | |
|---|---|---|---|
| **High infiltration / Low runoff** | 2 | Broad-leaved forest, Coniferous forest, Mixed forest | Forested areas |
| **Little or no additional runoff** | 1 | Salt marshes, Sea and ocean | Coastal and marine zones |

Dependent and non-dependent populations were calculated for each municipal community using age-based data from the 2021 ELSTAT census. The Dependency Rate was used to express the proportion of dependent population (individual aged 0-14 years and 65+ years) to the non-dependent (individuals aged 15-64 years) as a percentage. After joining the census data with the corresponding municipal communities, the index was calculated using the Raster Calculator tool. Dependency Rate values ranged from 49,308 to 57,054% and were classified into four categories using the Natural Breaks (Jenks) method: 49,308-50,188%; 50,189-52,497%; 52,498-54,806%; 54,807-57,054% corresponding to 1-4 classes and then assigned flood risk values. Given the direct relationship between dependency rate and flood risk, classes were assigned risk values in ascending order from 1 (lowest dependency rate, lowest risk) to 4 (highest dependency rate, highest risk). It is noted that the Natural Breaks method couldn't produce five statistically meaningful classes, therefore in this case only four classes were used. The assignment of risk values was since the range of dependency rate values was relatively small. The highest rate values couldn't correspond to the highest possible risk value (5) as this risk value should correspond to higher dependency rate values and therefore, such an assignment couldn't justify the values. Although there is relatively little differentiation among the values, they were assigned different risk values to distinguish their different contribution to the total flood risk.

In case of building density, building polygons were obtained from OpenStreetMap for Greece. Building polygons were projected into the common reference system and clipped to the boundaries of the study area. Centroids were generated from polygons using the Feature to Point tool (Data Management Tools) and then rasterized to create a continuous surface (reclassification into binary values). Subsequently, Focal Statistics (Spatial Analyst Tools) with a 5x5 window was applied to smooth the results by

summing the number of buildings present in each neighborhood. Building density (per hectare) was then calculated using Raster Calculator for the study area. Building density values ranged from 0 to 13,049 and were classified into five categories using the Natural Breaks (Jenks) method: 0-1,023; 1,024-3,121; 3,122-6,243; 6,244-9,415; 9,416-13,049 buildings per hectare corresponding to 1-5 classes and then assigned flood risk values. Given the direct relationship between building density and flood risk, classes were assigned risk values in ascending order from 1 (lowest building density, lowest risk) to 5 (highest building density, highest risk).

Road network was obtained from OpenStreetMap for Greece. Roads were projected into the common reference system and clipped to the boundaries of the study area. Distance to the closest road was calculated using Euclidean Distance tool (Spatial Analyst Tools). Distance from road values ranged from 0 to 1869,598m and were classified into five categories using the Natural Breaks (Jenks) method: 0,001-175,962m; 175,963-469,232m; 469,233-828,488m; 828,489-1275,726m; 1275,727-1869,598m corresponding to 1-5 classes and then assigned flood risk values. Given the direct relationship between distance from road and flood risk, classes were assigned risk values in ascending order from 1 (shortest distance, lowest risk) to 5 (greatest distance, highest risk).

Health facilities data were obtained from Strategic Development Plans of the Municipalities of Thermi and Pylaia-Chortiatis. Their locations identified and manually digitized as point features in GIS. Distance from the closest health facility was then calculated using the Euclidean Distance tool (Spatial Analyst tools). Distance from health facilities values ranged from 0 to 6009,576m and were classified into five categories using the Natural Breaks (Jenks) method: 0-1319,75m; 1319,751-2262,429m; 2262,43-3157,973m; 3157,974-4218,487m; 4218,488-6009,576m corresponding to 1-5 classes and then assigned flood risk values. Given the direct relationship between distance from health facilities and flood risk, classes were assigned risk values in ascending order from 1 (shortest distance, lowest risk) to 5 (greatest distance, highest risk).

Emergency shelter data within the boundaries of the study area were obtained from Civil Protection Plans of the Municipalities of Thermi and Pylaia-Chortiatis. Their

locations identified and manually digitized as point features in GIS. Distance from the closest emergency shelter was then calculated using the Euclidean Distance tool (Spatial Analyst tools). Distance from emergency shelter values ranged from 0 to 4287,341m and were classified into five categories using the Natural Breaks (Jenks) method: 0-790,216m; 790,217-1479,553m; 1479,554-2152,077m; 2152,078-2858,227m; 2858,228-4287,341m corresponding to 1-5 classes and then assigned flood risk values. Given the direct relationship between distance from health facilities and flood risk, classes were assigned risk values in ascending order from 1 (shortest distance, lowest risk) to 5 (greatest distance, highest risk).

Older and newer buildings (residential) were calculated for each municipal community using the construction year from the 2021 ELSTAT census. The Building Age Rate was used to express the proportion of older buildings (before 1945, 1946-1980, 1981-1990) to the newer buildings (1991-2010 and after 2011) as a percentage. After joining the census data with the corresponding municipal communities, the index was calculated using the Raster Calculator tool. Building Age Rate values ranged from 32,08 to 90,646% and were classified into four categories using manual method: 32,08-51,601%; 51,602-71,124%; 71,125-90,646% corresponding to 1-3 classes and then assigned flood risk values. Given the direct relationship between dependency rate and flood risk, classes were assigned risk values in ascending order 2 (lower building age rate, lower risk), 3 (moderate building age rate, moderate risk) and 4 (higher building age rate, higher risk). It is noted that in this case manual classification of the building age rate was chosen due to inability of the Jenks method to produce meaningful classes. This decision ensured that all values were represented and corresponded to a class. Although an attempt was made to classify the values into 5 or 4 classes with Jenks method, this was not possible as some municipal communities were unpresentable. Therefore, the building age rate values were categorized into three classes, reflecting the progression from lower to higher building age rate. In this case, risk values were assigned 2, 3, 4 representing low, moderate and high-risk categories respectively. The absence of risk values 1 (lowest risk) and 5 (highest risk) was justified as values did not reach extremes of 0% and 100% dependency age rate and therefore, the assignment of those values would have been inappropriate. While sensitivity analysis or expert judgement would provide more robustness in such cases, it is considered reasonable given the limited range of the values.

#### 3.2.4.2. Weighted Overlay Analysis

A weighted overlay analysis was applied to assess and map the spatial distribution of flood risk across the study area, considering parameters that represent hazard, exposure and vulnerability/ capacity. As described, all datasets were managed in GIS, projected into a common coordinate reference system (Greek Grid), clipped to the study area boundaries and in case of vector data, converted into raster format.

The resulting raster files were standardized, classified and assigned with risk values ranging from 1 (very low risk) to 5 (very high risk). Then, they were combined using the Weighted Overlay tool (Spatial Analyst tools) in ArcGIS Pro with weights derived from AHP based on expert judgments. During this process, each raster cell value was multiplied by its corresponding weight and summed to produce a final flood risk index. Although the input raster data were classified into total 3-5 classes and assessed through the overlay analysis on a 1-5 scale, the final output (flood risk map) was classified into three categories (low, moderate and high) due to the methods applied (e.g. normalization, classification) and the weighted aggregation of parameters.

The weighted overlay tool combines the raster files to represent flood risk as the cumulative interaction of parameters based on an additive approach. This approach assumes independence among parameters and their linear contribution to flood risk. Therefore, it does not typically capture the differing contributions of hazard, exposure, vulnerability and capacity. To address this constraint of the tool, all datasets were classified and assigned with risk values according to their relationship with flood risk, as described in section 3.2.4.1. (Data Management). Particularly, parameters positively associated with flood risk were assigned risk values in ascending order while parameters negatively associated with flood risk were assigned inverse risk values. This approach was also applied to capacity parameters, where higher capacity values correspond to lower risk values.

#### 3.2.4.3. Impact Analysis

Based on the resulting flood risk map, an impact analysis was conducted to assess the potential impacts on the environment, infrastructure and population within the study area. The quantification of the impacts was mainly performed using Extract by Mask tool, extracting the corresponding parameter values for each flood risk zone.

#### 3.2.4.4. Validation

Validation is essential to assess the plausibility of the model's results. There is a variety of validation methods that are applied in similar studies, with test locations (Lin et al., 2019) and historical flood records being among the most widely used approaches (Papaioannou et al., 2015; Feloni et al., 2019; Ekmekcioğlu et al., 2020; Taoukidou et al., 2025).

Given the absence of publicly available georeferenced historical flood data from the fire department (only the total number of flood-related incidents is recorded), validation was applied through comparison with the official Areas of Potential Significant Flood Risk (APSFR), particularly the zone EL10APSFR008 (Lowland Basin of Regional Trench T66, encompassing the Loudias and Axios rivers, the former Lake Arjan, and Galliko) as identified in the Flood Risk Management Plan of Central Macedonia. Particularly, EL10APSFR008 zone overlaps with the southern part of the study area. APSFRs are generally defined by combining the assessment of significant past floods, the identification of areas likely to be flooded and areas with significant impacts to future floods at strategic level for Central Macedonia (Ypeka, 2025). Additionally, these official zones provide a reliable basis for comparison as they identified in alignment with national regulations and EU flood risk management directives.

For the part of the study area that is not included within the EL10APSFR008 zone, validation was conducted using qualitative data. For this purpose, an application was submitted to the related municipality services to collect information on flood-prone locations. The eighteen identified locations include some representative or main areas showing water accumulation after heavy precipitation events (e.g. due to alterations in stream channels or disrupted stream continuity) as well as stream points where inadequate maintenance is observed.

## 4. Results

The following sections present the results of the methodology application.

### 4.1. Parameters Analysis

The largest part of the area (87%) is located in very low to moderate elevations ranging from 2 to 573m. Lowest elevations are found in the southwest part of the study area given its proximity to sea while low to moderate elevations extend northward. These areas correspond to very high to moderate flood risk. In contrast, the highest elevations (5% of the total area) are located in the northeast where Mt. Chortiatis is and these areas correspond to the lowest flood risk. Additionally, most of the area (62%) has slopes ranging from 0 to 11,652° which are mainly found in the southern and northern parts of the study area, corresponding to higher flood risk. In contrast, steeper slopes (4% of the total area) are located in the central and northeastern parts and these correspond to the lowest flood risk. The largest part of the area (60%) is covered by chromic luvisols found in the central and northern part of the study area. This type is considered moderately susceptible to flooding. 40% of the area is covered by calcaric regosols, in the northern part of the study area which shows low flood risk. As for the curvature, the majority of the area (39%) consists of flat surfaces which show the highest flood risk. Then, follow the concave surfaces (31% of the total area) which show moderate to high flood risk and the convex surfaces (29% of the total area) which correspond to lower flood risk.

Analyzing hydrological parameters, the largest part of the area (40%) receives higher annual precipitation (>647,621mm) mainly in the central and northern parts which corresponds to higher flood risk. This is mainly influenced by the orographic effect due to Mt. Chortiatis. These areas are followed by areas with moderate precipitation (640,173-647,62mm) mainly in the northern part but also in a southern part of the study area corresponding to moderate flood risk. Moreover, the largest part of the study area (71%) shows lower TWI values which correspond to lower susceptibility to flooding, while areas with higher TWI values are limited to 10% of the total study area corresponding to higher flood risk. Regarding drainage density, the largest part of the area (57%) shows from very low to low drainage densities (0-2,419) corresponding to lower flood risk, followed by areas with moderate drainage density covering 28% of the total area (moderate flood risk). While areas with higher drainage density

corresponding to higher flood risk represent 15% of the total area. On the other hand, 66% of the total area is located close to stream (within a distance of 168,15m) corresponding to higher flood risk while only 13% of the area is located in a distance greater than 258,231m corresponding to lower flood risk.

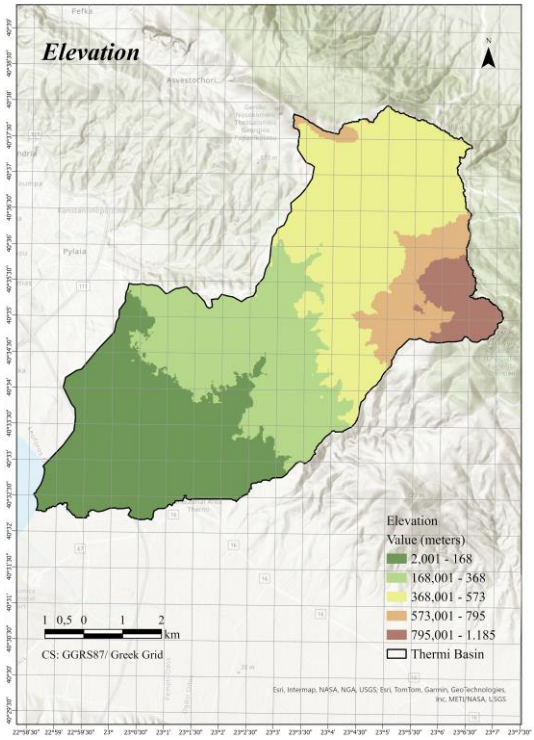


a)

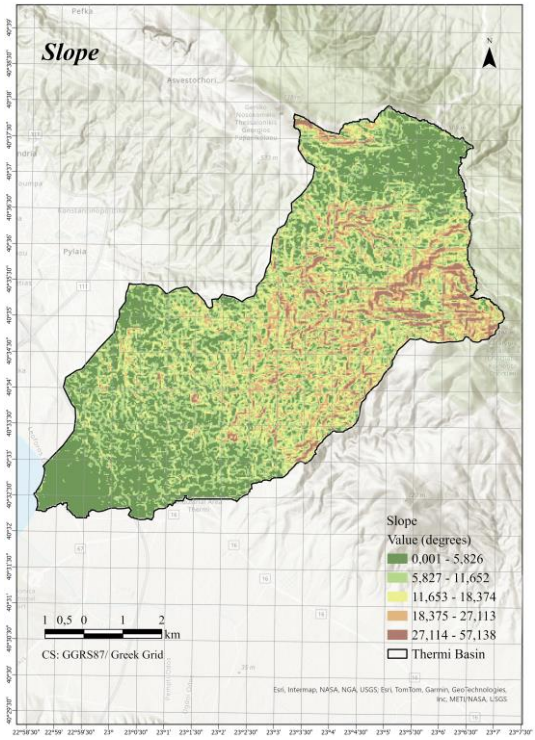


b)

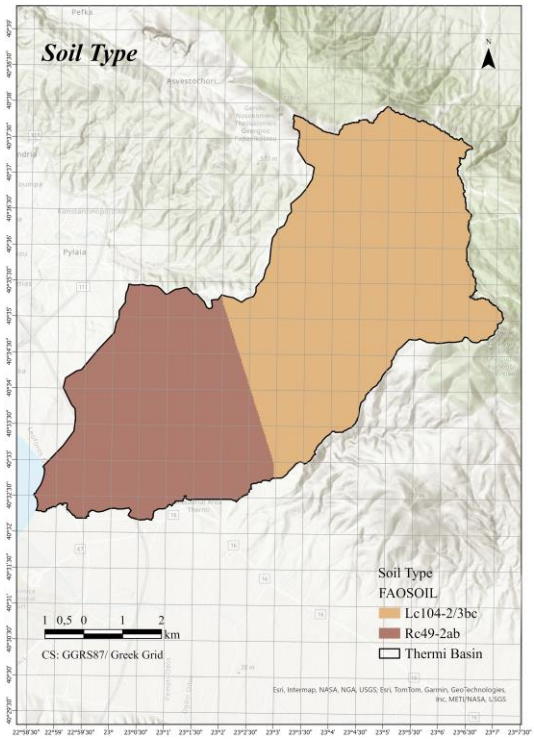


c)

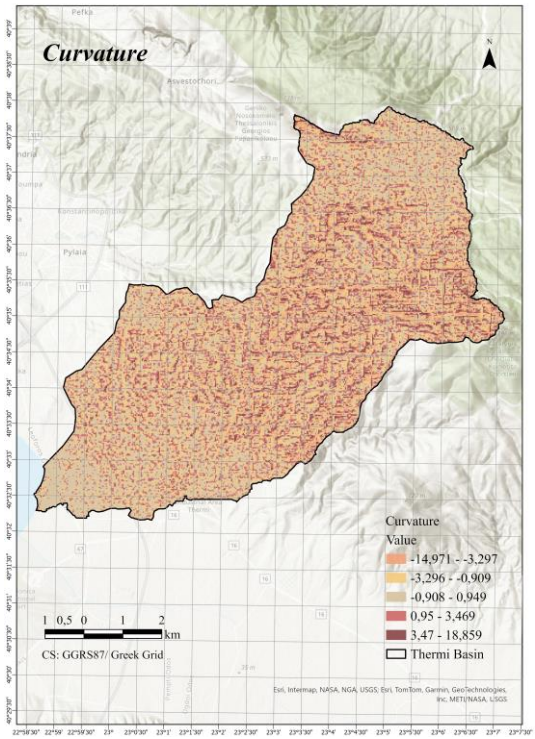


d)

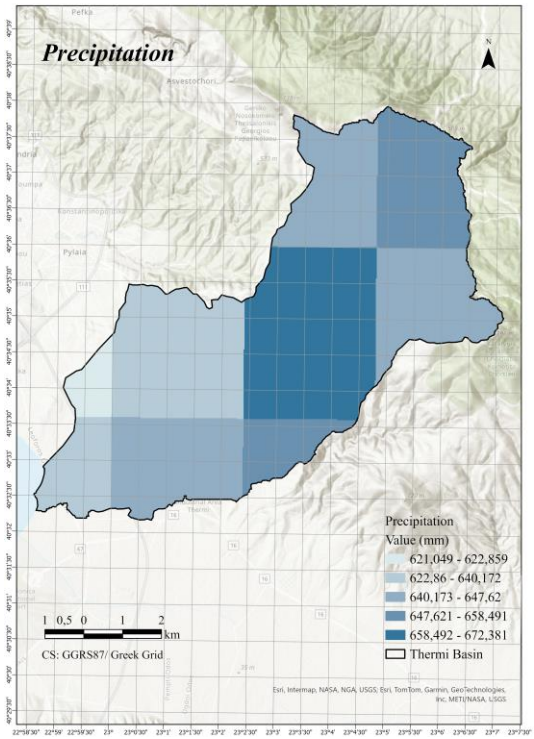


e)

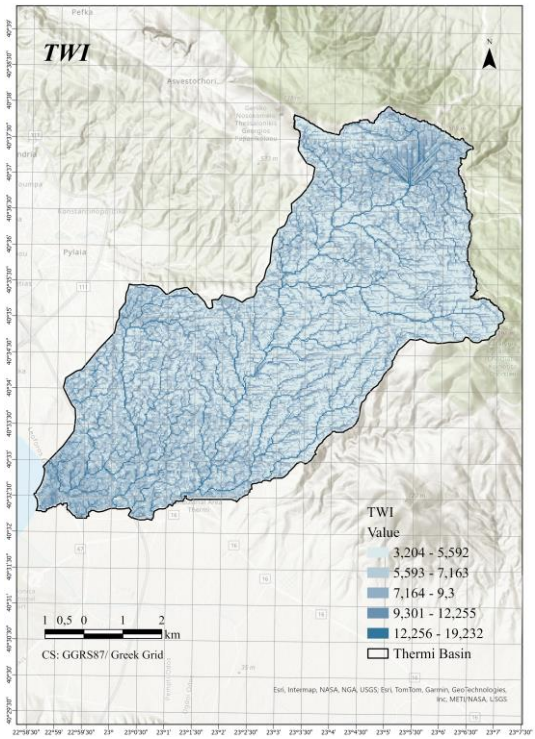


f)

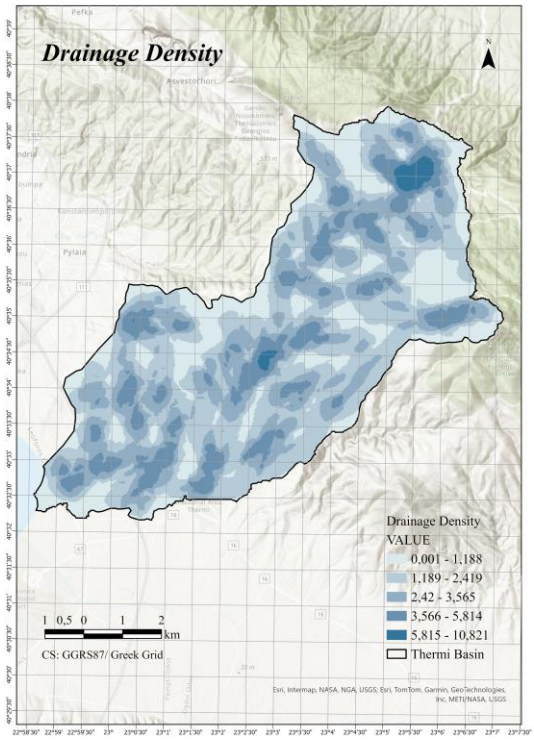


g)

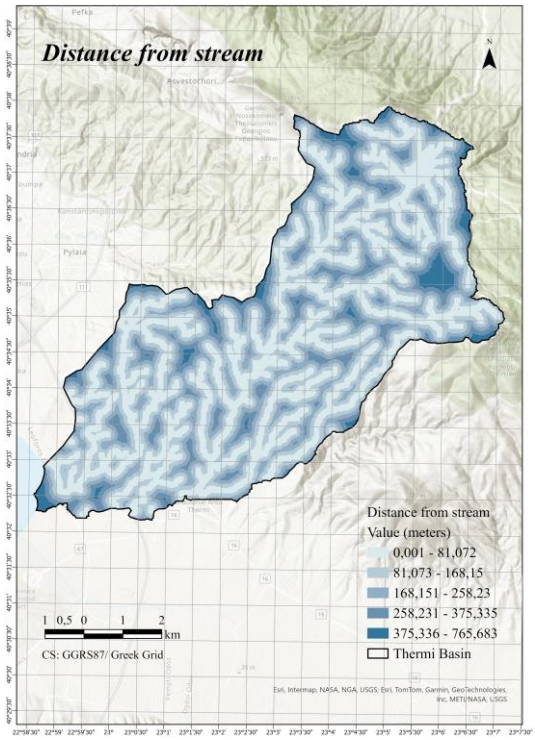


h)

*Figure 3 Flood hazard parameters a) elevation, b) slope, c) soil type, d) curvature, e) precipitation, f) TWI, g) drainage density and h) distance from stream (own processing)*

The largest area (41%) shows lower NDVI values (<0,237) corresponding to higher flood risk. Then follow the areas with moderate NDVI values (31%) mainly identified in the central part while higher NDVI values are observed in the 28% (>0,302) of the study area mainly around Mt. Chortiatis corresponding to lower flood risk.

Regarding population density, the largest area (36%) is characterized by low population density. This class includes the settlement of Thermi in the southern part of the study area which despite rapid development in recent years still shows suburban characteristics compared to Pylaia. The highest population densities are observed in municipal communities located closer to the urban fabric of Thessaloniki, such as Panorama and Pylaia (32% of the total area). The same proportion (32%) correspond to areas with very low population density such Chortiatis.

As for land use and land cover, the largest part of the total area (34%) is covered by semi-natural grasslands and shrubs. Then follow areas covered by agricultural lands and mixed farming (32%), built-up and industrial urban areas (24%) and forested areas (10%). While coastal and marine zones represent a small part of the study area located near Thermaikos Gulf.

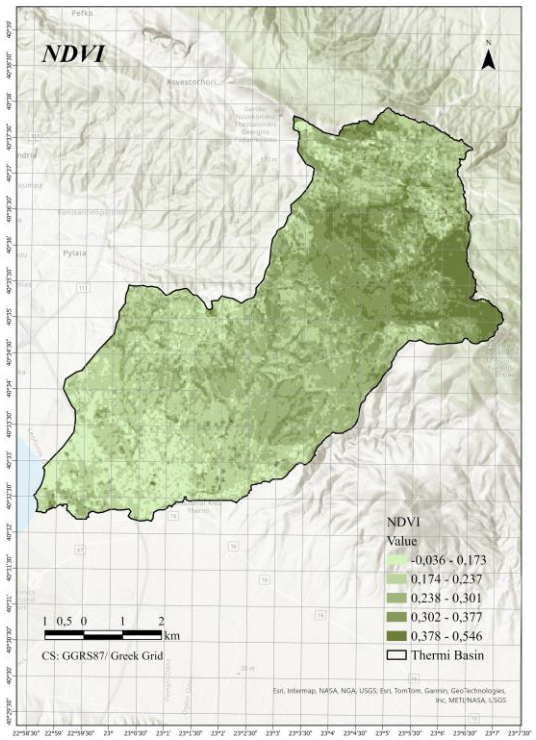


i)

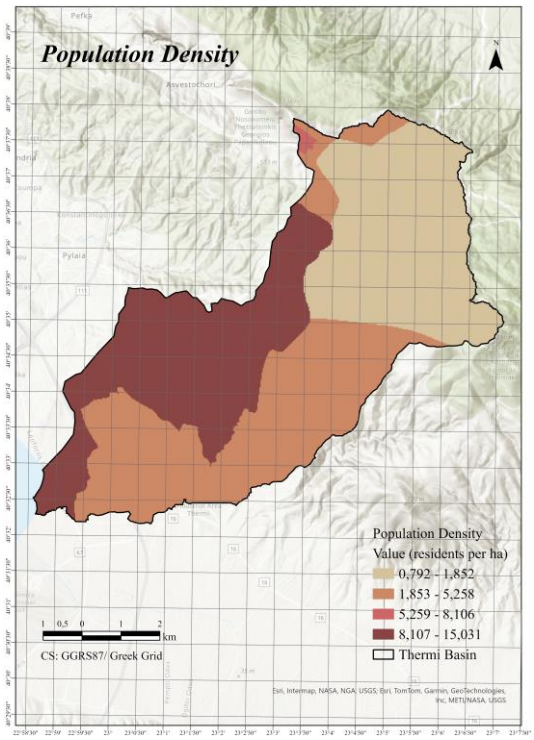


j)

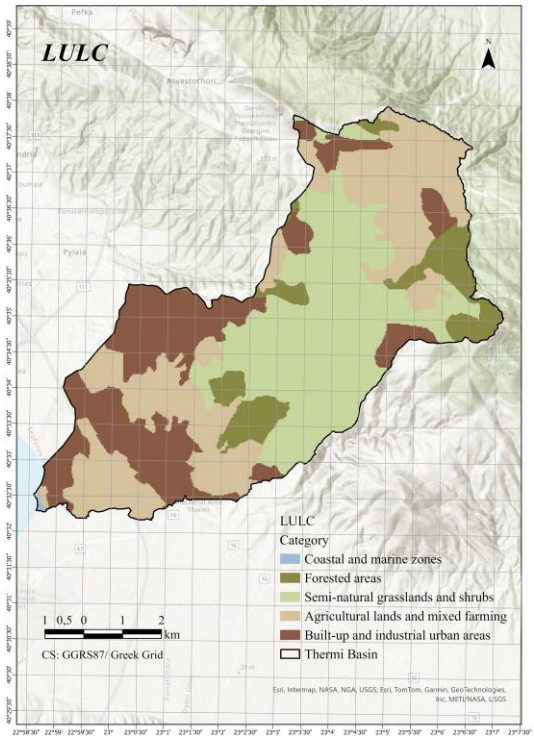


k)

*Figure 4 Flood exposure parameters i) NDVI, j) population density and k) LULC (own processing)*

Dependency rate is higher in the Municipal Community of Exochi corresponding to the higher flood risk. However, the largest area is characterized by low dependency rate (36%) for Municipal Communities of Thermi and Asvestochori corresponding to low flood risk while the lowest and moderate values are observed in the same proportion (32%) for Municipal Communities of Chortiatis, Panorama and Pylaia corresponding to the lowest and moderate flood risk.

Regarding building density, the largest part of the study area (67%) shows very low building density (<1,023 buildings per ha) due to the topography of the region, followed by areas showing low building density (17% of the total area). Higher building densities are mainly observed in the centers of the settlements of Thermi, Panorama and Chortiatis, as well as in parts of Pylaia, Exochi and Triadi near the boundaries of the study area. Thermi has a more concentrated and high-density core while Panorama shows higher density in certain parts. Moderate building densities are smoothly distributed across the settlement. On the other hand, Chortiatis given its smaller size, has more localized building densities in certain parts due to significant development

and expansion over the past decade. Moderate and low building densities are also found along the road network. Overall, the higher densities exceeding 6,244 buildings per ha cover 7% of the total area and correspond to higher flood vulnerability while moderate densities are observed in 9% of the study area.

Analyzing the access to road, emergency services and health care provides the following insights into the flood vulnerability of the study area. Regarding distance from road, the largest part of the study area (78%) is close to road network (<469,232m), corresponding to lower flood risk given the ability for direct access and quicker emergency response. Areas located in moderate distances from roads (469,233-828,488m) correspond to 11% of the total area. The same proportion (11% of the total area) have the areas farther from roads corresponding to higher flood risk. However, these areas are mainly uninhabited due to the topography of the region. Regarding distance from health facilities, most areas (44%) are near health facilities (<2262,429m) corresponding to lower flood risk due to the ability of quicker access to health care. On the other hand, areas located in greater distances from health facilities (>3157,974m) cover 27% of the total area corresponding to higher flood vulnerability. While areas at moderate distances cover the remaining proportion. Regarding distance from emergency shelters, the largest part of the area (47%) is located close to emergency shelters (<1479,553m) corresponding to lower flood vulnerability given direct access to emergency services and protection points. However, relatively high is the proportion of the areas located farther from emergency shelters (>3157,974m) (30%) but may be related to parts of remote and uninhabited regions not exclusively corresponding to higher flood vulnerability.

Finally, building age rate is highest (35%) in the Municipalities of Panorama, Pylaia and Asvestochori, ranging from 71 to 91%, since they are generally older settlements. In contrast, Municipal Communities of Chortiatis which has expanded mainly over the past decade and Thermi, which has experienced rapid development in recent years, have a relatively greater proportion of newer buildings ranging from 32 to 71%, corresponding to more flood-resilient structures and therefore, low and moderate flood risk.

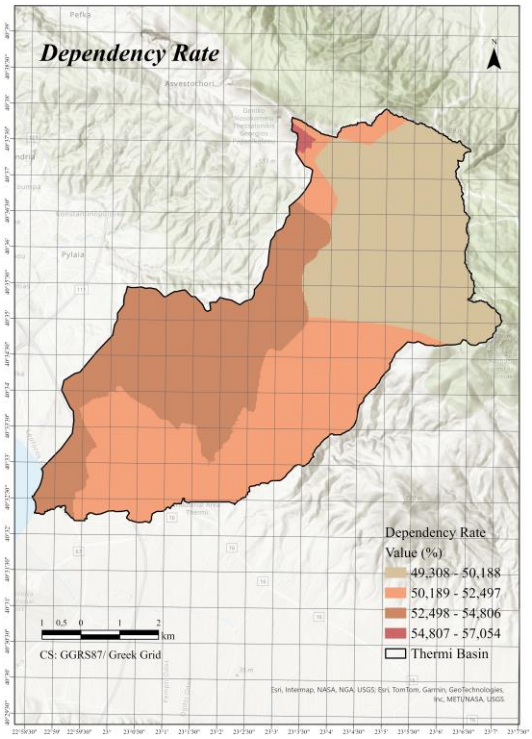
Dependency Rate
Dependency Rate
Value (%)
49,308 - 50,188
50,189 - 52,497
52,498 - 54,806
54,807 - 57,054
Thermi Basin
CS: GGRS87/ Greek Grid
km

l)

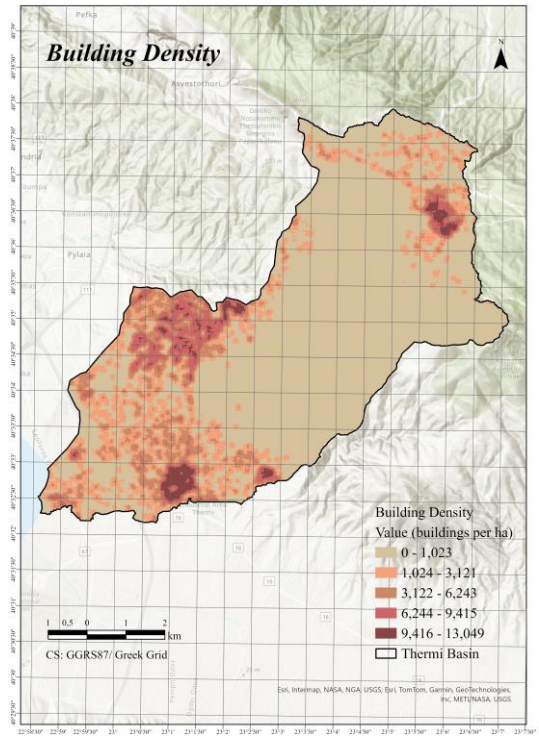
Building Density
Building Density
Value (buildings per ha)
0 - 1,023
1,024 - 3,121
3,122 - 6,243
6,244 - 9,415
9,416 - 13,049
Thermi Basin
CS: GGRS87/ Greek Grid
km

m)

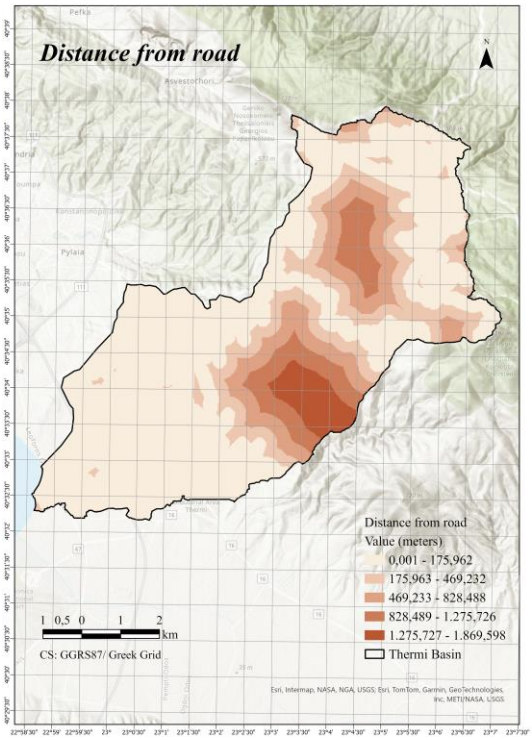
Distance from road
Distance from road
Value (meters)
0,001 - 175,962
175,963 - 469,232
469,233 - 828,488
828,489 - 1.275,726
1.275,727 - 1.869,598
Thermi Basin
CS: GGRS87/ Greek Grid
km

n)

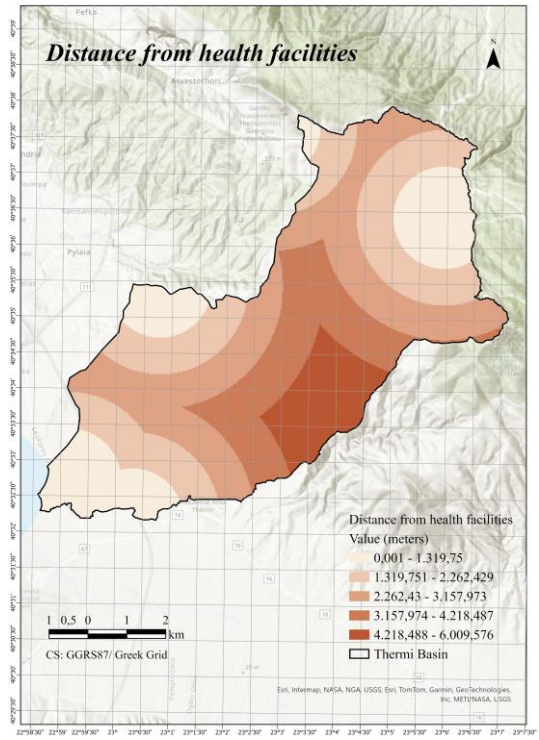
Distance from health facilities
Distance from health facilities
Value (meters)
0,001 - 1.319,75
1.319,751 - 2.262,429
2.262,43 - 3.157,973
3.157,974 - 4.218,487
4.218,488 - 6.009,576
Thermi Basin
CS: GGRS87/ Greek Grid
km

o)

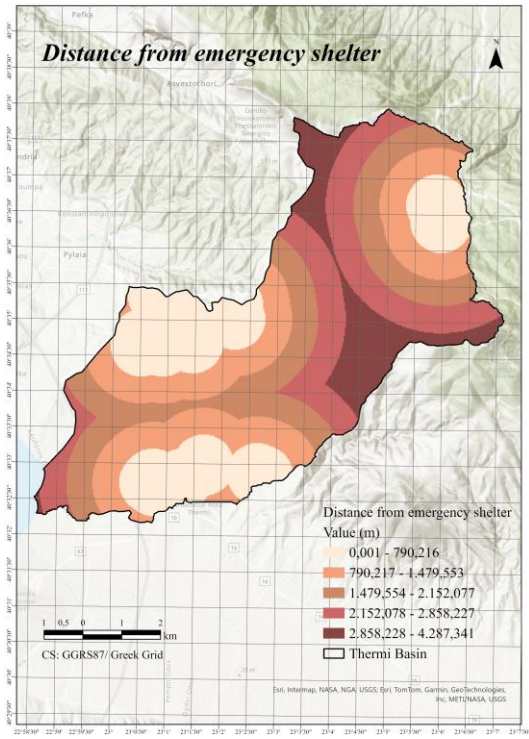


p)

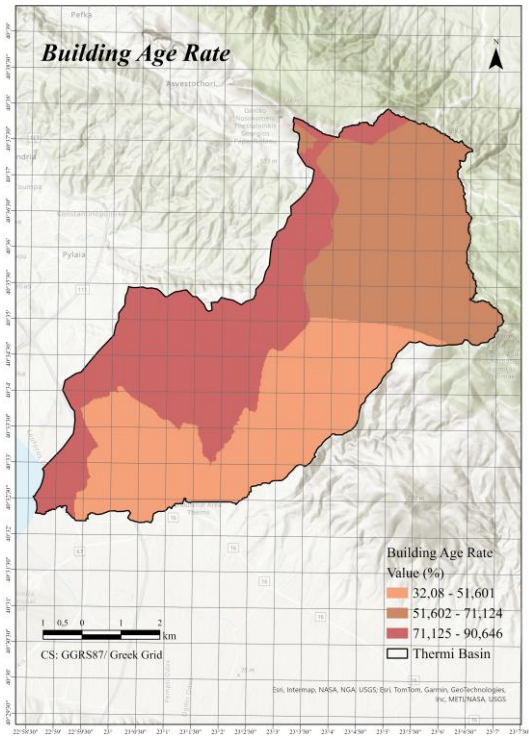


q)

*Figure 5 Flood exposure parameters l) dependency rate, m) building density, n) distance from road, o) distance from health facilities, p) distance from emergency shelter and q) building age rate (own processing)*

The table in Appendix II (Table 23) presents the detailed classification and risk values of the selected parameters as well as area statistics.

### 4.2. AHP Results

Combining the completed 17x17 Pairwise Comparison Matrices as derived from participants, the geometric means, normalized weight vector, weighted sum vector and consistency vector were calculated to derive maximum eigenvalue and compute Consistency Index and Consistency Ratio. Precipitation received the highest weight (0,1528), followed by slope (0,1257), distance from stream (0,1022), soil type (0,0730), TWI (0,0656), drainage density (0,0588), land use and land cover (0,0584), curvature (0,0569), population density (0,0554), dependent population (0,0520), elevation (0,0508), building density (0,0380), NDVI (0,0313), distance from road (0,0234), distance from health facilities (0,0222), distance from emergency shelter (0,0202) and building age (0,0132). Given the CI is calculated 0,0696 and CR 0,0438 which is below the threshold of 0,10 (for n=17, RI=1,59) the comparisons are consistent and therefore reliable. Table 14 presents the combined matrix of pairwise comparisons and the calculated weights.

*Table 14 Combined Pairwise Comparison Matrix (PCM) and calculated weights (own processing)*

| Parameters | P1 | P2 | P3 | P4 | P5 | P6 | P7 | P8 | P9 | P10 | P11 | P12 | P13 | P14 | P15 | P16 | P17 | Weights (Wi) |
|---|---|---|---|---|---|---|---|---|---|---|---|---|---|---|---|---|---|---|
| **P1** | 1,0 | 0,44 | 1,15 | 1,52 | 0,48 | 0,86 | 0,93 | 0,45 | 1,58 | 0,76 | 0,57 | 0,90 | 0,95 | 1,40 | 2,41 | 2,11 | 3,94 | 0,0508 |
| **P2** | 2,3 | 1,00 | 3,47 | 3,65 | 0,88 | 3,16 | 3,39 | 1,48 | 5,01 | 2,12 | 1,55 | 1,93 | 2,74 | 3,80 | 3,28 | 4,08 | 6,11 | 0,1257 |
| **P3** | 0,9 | 0,29 | 1,00 | 2,85 | 1,25 | 1,43 | 1,97 | 0,78 | 2,85 | 1,12 | 1,00 | 1,11 | 1,52 | 2,51 | 2,59 | 3,23 | 4,83 | 0,0730 |
| **P4** | 0,7 | 0,27 | 0,35 | 1,00 | 1,08 | 1,58 | 1,63 | 0,78 | 2,45 | 1,23 | 0,96 | 0,85 | 1,38 | 2,05 | 2,27 | 2,46 | 2,85 | 0,0569 |
| **P5** | 2,1 | 1,13 | 0,80 | 0,92 | 1,00 | 5,35 | 4,99 | 2,24 | 6,72 | 3,71 | 4,83 | 3,18 | 4,52 | 6,15 | 5,84 | 6,47 | 7,22 | 0,1528 |
| **P6** | 1,2 | 0,32 | 0,70 | 0,63 | 0,19 | 1,00 | 1,84 | 0,64 | 3,68 | 1,48 | 1,32 | 1,01 | 1,95 | 4,08 | 3,90 | 3,90 | 5,52 | 0,0656 |
| **P7** | 1,1 | 0,29 | 0,51 | 0,61 | 0,20 | 0,54 | 1,00 | 0,82 | 4,48 | 1,64 | 1,38 | 1,25 | 1,95 | 2,91 | 3,13 | 2,95 | 4,66 | 0,0588 |
| **P8** | 2,2 | 0,68 | 1,29 | 1,28 | 0,45 | 1,55 | 1,21 | 1,00 | 4,55 | 2,11 | 2,95 | 2,95 | 3,06 | 5,72 | 4,17 | 4,17 | 6,11 | 0,1022 |
| **P9** | 0,6 | 0,20 | 0,35 | 0,41 | 0,15 | 0,27 | 0,22 | 0,22 | 1,00 | 0,68 | 1,00 | 0,84 | 1,27 | 2,27 | 1,64 | 2,27 | 2,67 | 0,0313 |
| **P10** | 1,3 | 0,47 | 0,89 | 0,81 | 0,27 | 0,67 | 0,61 | 0,47 | 1,48 | 1,00 | 1,58 | 1,43 | 2,04 | 2,83 | 2,24 | 2,63 | 3,71 | 0,0554 |
| **P11** | 1,7 | 0,64 | 1,00 | 1,05 | 0,21 | 0,76 | 0,72 | 0,34 | 1,00 | 0,63 | 1,00 | 2,02 | 2,61 | 4,52 | 2,93 | 2,93 | 4,15 | 0,0584 |
| **P12** | 1,1 | 0,52 | 0,90 | 1,18 | 0,31 | 0,99 | 0,80 | 0,34 | 1,18 | 0,70 | 0,50 | 1,00 | 1,70 | 3,47 | 2,79 | 2,79 | 3,47 | 0,0520 |
| **P13** | 1,1 | 0,37 | 0,66 | 0,72 | 0,22 | 0,51 | 0,51 | 0,33 | 0,79 | 0,49 | 0,38 | 0,59 | 1,00 | 2,85 | 2,18 | 2,24 | 3,84 | 0,0380 |
| **P14** | 0,7 | 0,26 | 0,40 | 0,49 | 0,16 | 0,25 | 0,34 | 0,17 | 0,44 | 0,35 | 0,22 | 0,29 | 0,35 | 1,00 | 2,04 | 2,04 | 3,47 | 0,0234 |
| **P15** | 0,4 | 0,31 | 0,39 | 0,44 | 0,17 | 0,26 | 0,32 | 0,24 | 0,61 | 0,45 | 0,34 | 0,36 | 0,46 | 0,49 | 1,00 | 1,52 | 2,09 | 0,0222 |
| **P16** | 0,5 | 0,24 | 0,31 | 0,41 | 0,15 | 0,26 | 0,34 | 0,24 | 0,44 | 0,38 | 0,34 | 0,36 | 0,45 | 0,49 | 0,66 | 1,00 | 2,54 | 0,0202 |
| **P17** | 0,3 | 0,16 | 0,21 | 0,35 | 0,14 | 0,18 | 0,21 | 0,16 | 0,37 | 0,27 | 0,24 | 0,29 | 0,26 | 0,29 | 0,48 | 0,39 | 1,00 | 0,0132 |

*Where P1: elevation, P2: slope, P3: soil type, P4: curvature, P5: precipitation, P6: topographic wetness index, P7: drainage density, P8: distance from stream, P9: normalized difference vegetation index, P10: population density, P11: land use and land cover, P12: dependent population, P13: building density, P14: distance from road, P15: distance from health facilities, P16: distance from emergency shelter and P17: building age.*

### 4.3. Flood Risk Assessment

The weighted overlay analysis was applied to create a flood risk map using the weights derived from AHP. The resulting map classifies the study area into three categories: low, moderate and high flood risk. Most of the area is characterized by moderate flood risk, followed by low and high-risk areas. Particularly, of the total area, 503 ha (8,26%) are classified as low-risk, 5114 ha (83,94%) as moderate-risk and 476 ha (7,80%) as high-risk[2].

Analyzing the spatial distribution of flood risk within the study area several variations are observed. Initially, most areas of all municipal communities are classified as moderate flood risk. The largest proportions of moderate-risk areas are observed in Municipal Communities of Thermi (29,82% of the area), Chortiatis (23,61%) and Panorama (22,08%). High flood risk areas are mainly observed in Municipal Community of Thermi (2,96% of the total area), followed by Panorama (2,78%) and Chortiatis (1,08%) while the remaining municipal communities have smaller proportions. Areas classified as low flood risk are comparatively limited, with Municipal Community of Chortiatis showing the largest proportion (7,14%) while the other municipal communities show smaller proportions.

Table 15 shows the distribution of flood risk across municipal communities.

*Table 15 Flood risk categories per municipal community (own processing)*

| Municipal Community | Low | | | Moderate | | | High | | |
|---|---|---|---|---|---|---|---|---|---|
| | Cells Count | Area (ha) | % total area | Cells Count | Area (ha) | % total area | Cells Count | Area (ha) | % total area |
| **Asvestochori** | 308 | 23,60 | 0,39 | 2166 | 165,99 | 2,72 | 41 | 3,14 | 0,05 |
| **Exochi** | 5 | 0,38 | 0,01 | 222 | 17,01 | 0,28 | 29 | 2,22 | 0,04 |
| **Thermi** | 278 | 21,30 | 0,35 | 23705 | 1816,67 | 29,82 | 2354 | 180,40 | 2,96 |
| **Panorama** | 221 | 16,94 | 0,28 | 17555 | 1345,36 | 22,08 | 2214 | 169,67 | 2,78 |
| **Pylaia** | 81 | 6,21 | 0,10 | 4316 | 330,76 | 5,43 | 709 | 54,34 | 0,89 |
| **Chortiatis** | 5673 | 434,76 | 7,14 | 18767 | 1438,24 | 23,61 | 858 | 65,75 | 1,08 |

[2] During raster processing and clipping a slight difference in boundaries was observed between the original basin extent (6203,35ha) and the final analyzed area (6092,76ha). Therefore, only cells within the final extent were kept and all were classified into flood risk categories.

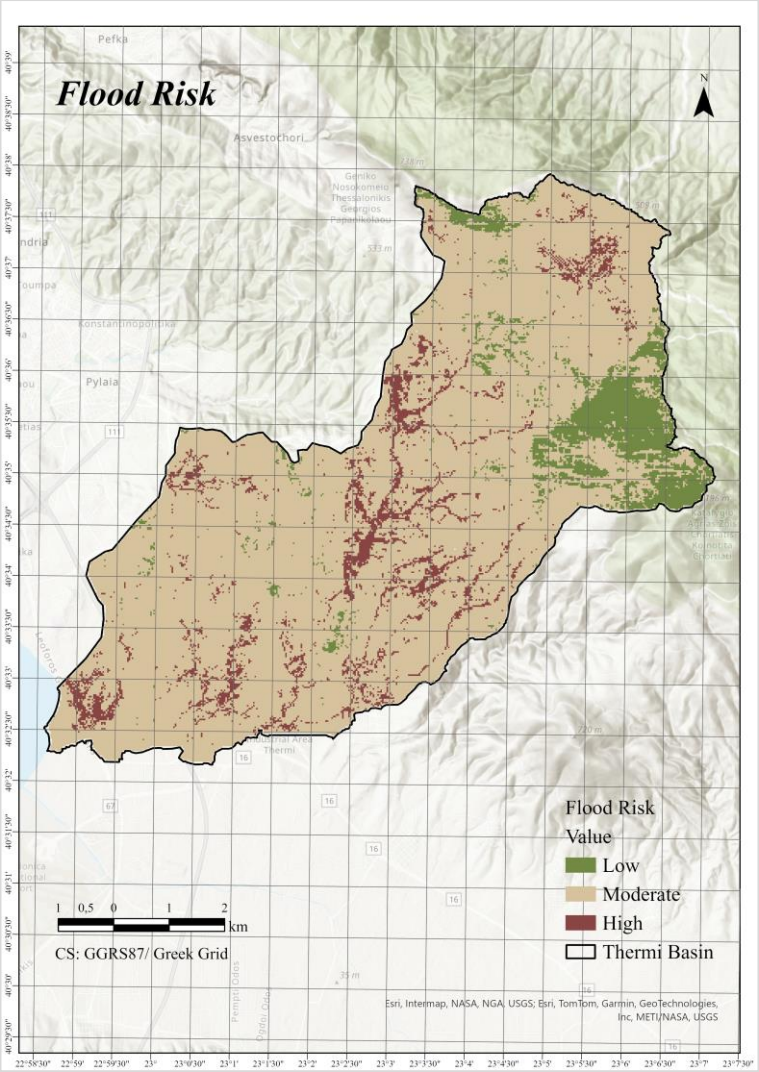


*Figure 6 Flood risk within the study area (own processing)*

**Low Flood Risk Zone**

Most areas in the low flood risk zone are located at high elevations with a mean of 731,91m and on steeper slopes with a mean of 22,44° corresponding to low flood risk. The main soil type is Chromic Luvisols with a minority of Calcaric Regosols. There, curvature has a mean of 0,95 and precipitation a mean of 645,71mm, which are related to low and moderate flood risk respectively. TWI has a mean of 5,18 and drainage density a mean of 1,24 corresponding to very low and low flood risk, while the mean distance from streams is 235,71m corresponding to moderate flood risk. Regarding exposure, the mean NDVI is 0,36 indicating dense and healthy vegetation and land use/ land cover is mainly forested corresponding to low flood risk. Population density is very low with a mean of 1,38 residents per hectare. Regarding vulnerability/ capacity parameters, these areas show a mean population dependency rate of 49,74% and

building density of 0,23 buildings per hectare corresponding to very low flood risk. The mean distance from road is approx. 232m and from health facilities is 2078m, indicating a low vulnerability. On the other hand, the mean distance from emergency shelters is 2006m and building age rate has a mean of 62,38% corresponding to moderate flood vulnerability. The combination of these parameters along with their flood risk values results in the classification of the areas as low flood risk.

**Moderate Flood Risk Zone**

Most areas in the moderate flood risk zone are located at lower elevations with a mean of 306,34m and on smoother slopes with a mean of 10,03° reflecting high flood risk. The main soil type is Chromic Luvisols with a minority of Calcaric Regosols. There, curvature has a mean of -0,02 and precipitation a mean of 649,66mm, which are related to very high and high flood risk respectively. TWI has a mean of 6,54 and drainage density a mean of 2,28 corresponding to low flood risk, while the mean distance from streams is 136,21m corresponding to high flood risk. Regarding exposure, the mean NDVI is 0,25 indicating moderately dense and healthy vegetation and land use/ land cover is mainly semi-natural grasslands and shrubs corresponding to moderate flood risk. Population density is low with a mean of 4,66 residents per hectare. Regarding vulnerability/ capacity parameters, these areas show a mean population dependency rate of 52,26% and building density of 1,35 buildings per hectare corresponding to low flood risk. The mean distance from road is approx. 279m and from health facilities 2495m indicating low and moderate vulnerability respectively. On the other hand, the mean distance from emergency shelters is 1572m and building age rate has a mean of 56,66% corresponding to moderate flood vulnerability. The combination of these parameters along with their flood risk values results in the classification of the areas as moderate flood risk.

**High Flood Risk Zone**

Most areas in the high flood risk zone are located at low elevations with a mean of 231,68m and on flat slopes with a mean of 5,25° reflecting high and very high flood risk susceptibility respectively. The main soil type is Chromic Luvisols with a minority of Calcaric Regosols. There, curvature has a mean of -0,92 and precipitation a mean of

656,51mm, which are related to moderate and high flood risk respectively. TWI has a mean of 9,55 and drainage density a mean of 3,52 corresponding to high and moderate flood risk respectively, while the mean distance from streams is 46,86m corresponding to very high flood risk. Regarding exposure, the mean NDVI is 0,24 indicating moderately dense and healthy vegetation and land use/ land cover is mainly semi-natural grasslands and shrubs corresponding to moderate flood risk. Population density is moderate with a mean of 6,09 residents per hectare. Regarding vulnerability/ capacity parameters, these areas show a mean population dependency rate of 53,08% and building density of 1,44 buildings per hectare corresponding to moderate and low risk respectively. The mean distance from road is approx. 355m and from health facilities 2706m indicate a low and moderate vulnerability respectively. On the other hand, the mean distance from emergency shelters is 1460m and building age rate has a mean of 57,22% corresponding to low and moderate flood vulnerability respectively. The combination of these parameters along with their flood risk values results in the classification of the areas as high flood risk.

### 4.4. Impact Analysis

The potential impacts on exposed environment, infrastructure and population are assessed in this section. Particularly, land use and land cover, infrastructure (building and roads) and population parameters are quantified for each flood risk zone to evaluate the potential damages and losses.

#### 4.4.1. Impact on the Environment

Most areas are located within the moderate flood risk zone. In this zone, agricultural land and mixed farming (1760,88ha) is the most potentially affected LULC category given its exposure, followed by semi-natural grasslands and shrubs (1713,59ha), built-up and industrial urban areas (1303,82ha), forested areas (332,14ha) and coastal and marine zone (3,60ha).

The low flood risk zone covers the second largest area. In this area, forested areas (226,77ha) are the most potentially affected, followed by semi-natural grasslands and shrubs (162,09ha), agricultural lands and mixed farming (78,63ha) and built-up and industrial urban areas (35,71ha).

The high flood risk zone covers the smallest area. In this zone, semi-natural grasslands and shrubs (196,73ha) are the most potentially affected, followed by built-up and industrial urban areas (137,33ha), agricultural lands and mixed farming (127,68ha) and forested areas (13,79ha).

*Table 16 Potentially affected land use and land cover by flood risk level (own processing)*

| LULC category | Low flood risk zone | | Moderate flood risk zone | | High flood risk zone | |
|---|---|---|---|---|---|---|
| | Cells Count | Area (ha) | Cells Count | Area (ha) | Cells Count | Area (ha) |
| **Built-up and industrial urban areas** | 466 | 35,71 | 17013 | 1303,82 | 1792 | 137,33 |
| **Agricultural lands and mixed farming** | 1026 | 78,63 | 22977 | 1760,88 | 1666 | 127,68 |
| **Semi-natural grasslands and shrubs** | 2115 | 162,09 | 22360 | 1713,59 | 2567 | 196,73 |
| **Forested areas** | 2959 | 226,77 | 4334 | 332,14 | 180 | 13,79 |
| **Coastal and marine zones** | 0 | 0 | 47 | 3,60 | 0 | 0 |

### 4.4.2. Impact on Infrastructure

Infrastructure potentially most affected due to its exposure is located within the moderate flood risk zone. In this zone, the exposed roads cover an area of 967,31ha and buildings cover 200,02ha. Critical infrastructure is located in this zone, including Trans-Balkan Medical Center (partially), Saint Luke's General Clinic and Chortiatis Municipal Health Center. The second most potentially affected infrastructure is located within the high flood risk zone. In this zone, the roads cover an area of 101,54ha and buildings cover 20ha. Additionally, Trans-Balkan Medical Center is identified partially in this zone. Finally, potentially affected infrastructure is located within the low flood risk with roads covering an area of 42ha and buildings covering 2,76ha.

*Table 17 Potentially affected infrastructure by flood risk level (own processing)*

| Infrastructure Type | Low flood risk zone | | Moderate flood risk zone | | High flood risk zone | |
|---|---|---|---|---|---|---|
| | Cells Count | Area (ha) | Cells Count | Area (ha) | Cells Count | Area (ha) |
| **Buildings** | 36 | 2,76 | 2610 | 200,02 | 261 | 20,00 |
| **Roads** | 548 | 42,00 | 12622 | 967,31 | 1325 | 101,54 |

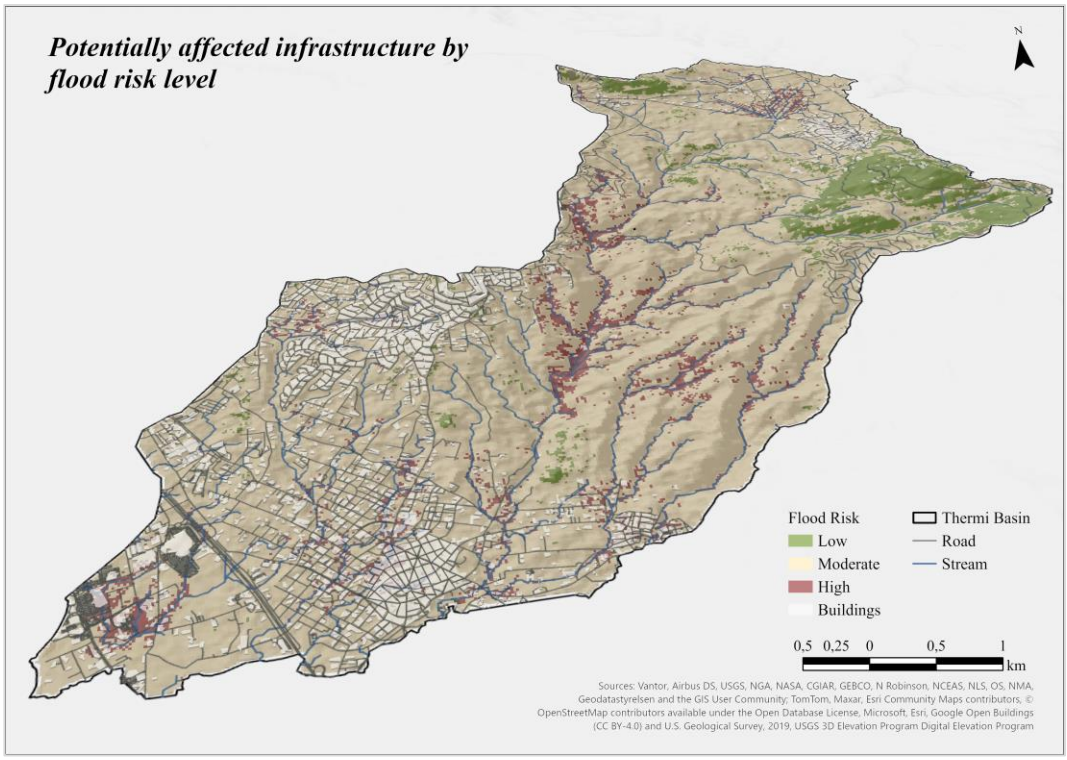


*Figure 7 Potentially affected infrastructure by flood risk level (own processing)*

### 4.4.3. Impact on Population

The exposed populations were assessed using census data at the municipal community level. As noted in the methodology section, a single value is assigned to each municipal community, therefore the approach does not capture micro-scale variation. However, flood risk is expected to affect the exposed population more locally rather than the total population of the municipal community. Particularly:

- The population of Municipal Community of Thermi is 19602 residents and the dependent population is 6747 residents based on 2021 census. Most of this population is exposed to moderate flood risk while some areas particularly in the central and northwestern as well as eastern expansions of the settlement are in high risk zones, potentially affecting residents in these parts more intensively.
- The population of Municipal Community Chortiatis is 4512 and the dependent population is 1495. Most of this population is exposed to moderate flood risk while some parts especially in the center of the settlement and its western expansion are at high risk. However given the lower population density in these high risk zones, the number of exposed people potentially affected is smaller.

- The population of Municipal Community Panorama is 17680 and the dependent population is 6261. Most of this population is exposed to moderate flood risk with some western and eastern parts located in high risk zones. Other parts, particularly in the south are exposed to low flood risk.
- A larger area in the southern part of the study area close to coast line is exposed to high flood risk. This area is mainly characterized by commercial and third sector activities, as well as critical infrastructure and some industrial uses. As a result, there is no permanent population at risk in this part.
- A part of the Municipal Community of Pylaia located within the study area near the Panorama is potentially affected since it is classified as high-risk. However, the exposed populations in this area as well as in small parts of Asvestochori and Exochi are affected proportionally.

### 4.5. Validation Results

An area of 614,01ha of the APSFR EL10APSFR008 (Lowland Basin of Regional Trench T66, encompassing the Loudias and Axios rivers, the former Lake Arjan, and Galliko) overlaps with the southern part of the study area. By comparing the APSFR zone with the flood risk zones of this study, it is observed that the EL10APSFR008 zone is mainly included in moderate and high-risk areas, while a smaller part is included in the low-risk areas. More particularly, the majority of the APSFR zone is classified as moderate risk based on the proposed flood risk zones by this study (526,34ha), followed by the high-risk (87,06ha) and low-risk (0,61ha). The areas represent 10,29% of the total moderate risk zone, 18,31% of the total high-risk zone and 0,12% of the total low risk zone in the study area. These indicate that the model generally identifies those flood-prone areas defined by the official APSFR.

Although the part of the APSFR included in the study area covers approx. 10% of the total study area, this result is expected due to methodological differences between two applications. Particularly, APSFR are defined by combining the assessment of significant floods, the identification of areas likely to be flooded and areas with significant impacts to future floods at strategic level. On the other hand, the methodology of this study is applied at basin level considering smaller streams as well as hazard, exposure and vulnerability/ capacity parameters to categorize flood risk from low to high.

For the part of the study area not included within the EL10APSFR008 zone, validation was conducted using eighteen documented potentially flooding locations as recorded from municipal services. All these points are included in the moderate flood risk zone, supporting the reliability of the model's results given the absence of publicly available and independent past flood events.

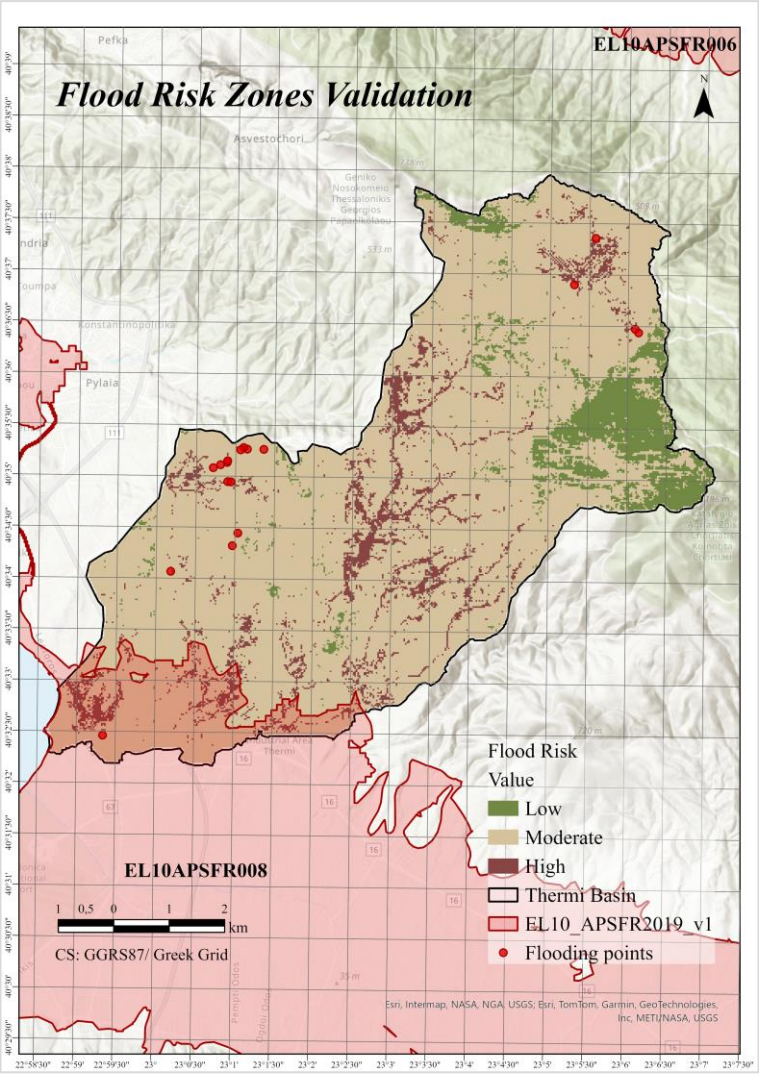


*Figure 8 Flood Risk Zones Validation (own processing)*

## 5. Discussion

This GIS-based MCDA framework considers seventeen parameters representing hazard, exposure and vulnerability/ capacity components, following the internationally recognized conceptualization of flood risk proposed by UNDRR (2017). The approach aligns with recent studies that recognize the need for more comprehensive flood risk assessments that beyond hazard consider exposure, vulnerability and capacity parameters. While no comprehensive flood risk assessments have been identified in the wider area, several studies in Greece have partially integrated hazard with exposure and vulnerability, although capacity aspect has generally underestimated. In this context, the study addresses this gap by developing a framework that covers all these components and highlights their cumulative contribution to flood risk.

An additional advantage of the study is the involvement of local expert and stakeholder knowledge through Analytical Hierarchy Process (AHP), a widely used method in flood risk assessments. The results of the weighting process indicate that precipitation is the most influential parameter followed by slope, distance from stream, soil type, topographic wetness index, drainage density, land use and land cover, curvature, population density, dependent population, elevation, building density, normalized difference vegetation index, distance from road, distance from health facilities, distance from emergency shelter and building age. Prioritization shows that hazard parameters are the main influential factors for flood occurrence while exposure and vulnerability parameters are less influential. This finding is consistent with other Mediterranean studies, where physical/ environmental parameters are identified as the main determinants of flood risk.

The resulting flood risk map shows that the largest part of the study area is classified as moderate flood risk (83,94%) followed by low (8,26%) and high (7,80%) risk-areas. This distribution reflects not only the interactions among these specific parameters but also the effects of methodological choices. Particularly, the use of min-max normalization and Natural Breaks (Jenks) classification may affect results, as these methods tend to be sensitive to outliers and minimize variance within classes and maximize variance between classes (Papaioannou et al., 2015). Moreover, although weights are assigned independently, they influence the flood risk distribution through the weighted overlay analysis in GIS. This approach also provides a linear and additive

rather than a dynamic representation of flood risk that captures synergistic or antagonistic interactions among parameters. While the GIS-based MCDA framework provides a structured and transparent approach for mapping flood risk distribution and prioritizing risk areas, it remains less predictive than physics-based simulation models. Therefore, the results should be interpreted accordingly.

In addition, validation generally supports the plausibility of the model's results, particularly the consistency between the flood risk zones and the EL10APSFR008 zone defined in Flood Risk Management Plan of Central Macedonia as well as the eighteen documented locations of water accumulation and inadequate maintenance. However, the use of APSFR may introduce a risk of circular validation, as these zones are potentially derived from underlying data sources that may overlap with those used in this study.

Several additional methodological limitations should be acknowledged. The approach simplifies complex hydrological processes into linear relationships, highlighting a limitation of MCDA compared to hydraulic and hydrological models (e.g. HEC-RAS or MIKE) or machine learning, which typically provide higher predictive accuracy. Parameters selection introduces uncertainty as some parameters may show partial underlying interdependence (e.g. distance from stream and TWI), potentially leading to redundancy in the analysis. Furthermore, the applied normalization and classification methods may influence the distribution of values and consequently affect the results. Additional limitations related to data include the use of datasets with different temporal characteristics (static e.g. topography, slope and dynamic e.g. LULC, population data, precipitation), the absence of climate change projections as well as limitations in data resolution and availability. For example, the relatively low-resolution DEM may have influenced the accuracy of DEM-derived parameters such as terrain and hydrographic network, particularly near boundaries where inconsistencies with the study area derived from official sources may occur. Additionally, the use of low-resolution publicly available precipitation data, due to the absence of local meteorological stations within the study area, affects the precise representation of local precipitation variability. Similarly, the aggregation of socioeconomic data (e.g. population density, dependency ratio) at municipal community level, reduces the model's ability to identify micro-scale variation, introducing further uncertainty. Finally, the relatively small number of

participants (n=5) involved in the weighting process may limit the representativeness of the results and introduce potential bias, such as groupthink, due to their similar field of expertise. Finally, no extensive sensitivity analysis was applied to assess how variations in weights (e.g. ±10–20% variation) influence the robustness of the results.

Based on these methodological limitations, future improvements may focus on combining the results with information derived from hydraulic and hydrological models (such as HEC-RAS or MIKE) as well as machine learning that efficiently capture complex interactions and provide higher predictive accuracy. However, given that these models may introduce additional complexity, particularly in strategic planning, their use should be carefully assessed depending on the decision-making context. Although parameters selection was based on their conceptual relevance to flood risk and supported by literature, uncertainty related to potential underlying interdependencies and redundancy in the analysis could be reduced through extensive parameters analysis (e.g. correlation analysis). Additionally, the influence of normalization and classification methods on the results could be examined through comparison with other methods. This could confirm if the spatial distribution of flood risk is driven by the interaction among these specific parameters or by the methodological choices. The use of higher resolution datasets (e.g. UAV-based high-resolution DEM) and climate change projections would also enhance the quality and reliability of the results (mapping). Increasing participation in the AHP and applying sensitivity analysis to assess how weights variations affect results could reduce subjectivity and improve the accuracy of weights. Moreover, the use of independent datasets (e.g. historical satellite data) could reduce potential circular validation.

Finally, the study provides a transferable methodology that can support decision-makers to identify and prioritize risk areas using publicly available datasets. However, its application requires adaptation to local conditions. In this case, the study area is characterized by a Mediterranean climate, specific topography and socioeconomic characteristics while application in different contexts, such as Nordic climate or a region with different socioeconomic structure, would require additional adjustments (e.g. in parameters selection and weighting).

## 6. Conclusions

This study developed a comprehensive GIS-based MCDA framework for flood risk assessment in the Thermi Basin in northern Greece, considering seventeen parameters that represent hazard, exposure and vulnerability/ capacity. The Analytic Hierarchy Process (AHP) was applied to assign weights through expert judgments and the weighted parameters were aggregated in GIS using the Weighted Overlay Tool to create a flood risk map. The map classified the study area into low, moderate and high flood risk zones and revealed that most of the area is classified as moderate-risk, followed by low and high-risk. Moderate flood risk areas are generally expected to be the most affected due to their extent and relatively high exposure of assets and population, while high flood risk areas, although covering the smallest area, intersect some critical infrastructure and parts of settlements, indicating potential considerable impacts. Validation against APSFR and eighteen documented flood-prone locations was also applied, generally confirming the plausibility of the model's results.

The framework enabled the simultaneous consideration of multiple and diverse parameters in a simplified and transparent approach. Although it is based on a additive representation of flood risk and is less predictive compared to physics-based simulation models, it provided a prioritization of flood risk areas that can support decision-makers in formulating informed and differentiated strategies, particularly in data-scarce and ungauged regions. Indicatively, given that moderate-risk areas represent a balanced yet dynamic system, they require preventive strategies including land-use planning and infrastructure completion, upgrading or maintenance. Low-risk areas, characterized by limited flood potential, should prioritize conservation and nature-based solutions to maintain their risk level while high-risk areas require more targeted mitigation strategies including stormwater drainage system improvement, sediment management and stream boundary regulation. In addition, horizontal measures such as long-term monitoring and early warning systems, sustainable spatial planning, flood risk management regulations and public awareness initiatives could enhance sustainability across the study area. However, these strategies are indicative and serve only as a basis for planners to further develop specific measures based on local needs.

In addition, the results should be interpreted based on the methodological assumptions and limitations including the simplified approach of the framework compared to

physics-based models, potential interdependencies among parameters, methodological choices' influence on results, data resolution issues, absence of climate change projections, potential circularity in validation, potential bias due to the limited participation in AHP (n=5) and absence of extensive sensitivity analysis. Future studies could combine the results with those from higher-predictive approaches (depending on the context), use higher-resolution data and climate change projections, increase AHP participation, apply sensitivity analysis and parameters analysis as well as use more independent datasets for validation.

## 7. References


Abdullah, M. F., Siraj, S., & Hodgett, R. E. (2021). An overview of multi-criteria decision analysis (MCDA) application in managing water-related disaster events: Analyzing 20 years of literature for flood and drought events. *Water, 13*(10), 1358. https://doi.org/10.3390/w13101358

Akram, M., Zahid, K., & Alcantud, J. C. R. (2022). A new outranking method for multicriteria decision-making with complex Pythagorean fuzzy information. *Neural Computing and Applications*, *34*(10), 8069–8102. https://doi.org/10.1007/s00521-021-06847-1

Akram, M., & Bibi, R. (2023). Multi-criteria group decision-making based on an integrated PROMETHEE approach with 2-tuple linguistic Fermatean fuzzy sets. *Granular Computing*, *8*(5), 917–941. https://doi.org/10.1007/s41066-022-00359-6

Amirteimoori, A., Kordrostami, S., & Sarparast, M. (2006). Modeling undesirable factors in data envelopment analysis. *Applied Mathematics and Computation*, *180*(2), 444–452. https://doi.org/10.1016/j.amc.2005.12.029

Aruldoss, M., Lakshmi, T. M., & Venkatesan, V. P. (2013). A survey on multi criteria decision-making methods and its applications. *American Journal of Information Systems*, *1*(1), 31–43. https://doi.org/10.12691/ajis-1-1-5

Ashfaq, S., Tufail, M., Niaz, A., Muhammad, S., Alzahrani, H., & Tariq, A. (2025). Flood susceptibility assessment and mapping using GIS-based analytical *hierarchy process and frequency ratio models. Global and Planetary Change, 251,* 104831. https://doi.org/10.1016/j.gloplacha.2025.104831

Asian Development Bank. (2016). *Reducing disaster risk by managing urban land use: Guidance notes for planners.* https://www.adb.org/publications/reducing-disaster-risk-urban-land-use-guidance-notes

Balali, A., Yunusa-Kaltungo, A., & Edwards, R. (2022). A systematic review of passive energy consumption optimisation strategy selection for buildings through multiple criteria decision-making techniques. *Renewable and Sustainable Energy Reviews*, *171*, 113013. https://doi.org/10.1016/j.rser.2022.113013

Bera, S., Guru, B., & Oommen, T. (2020). Indicator-based approach for assigning physical vulnerability of the houses to landslide hazard in the Himalayan region of India. *International Journal of Disaster Risk Reduction, 50*, 101891. https://doi.org/10.1016/j.ijdrr.2020.101891

Cai, T., Li, X., Ding, X., Wang, J., & Zhan, J. (2019). Flood risk assessment based on hydrodynamic model and fuzzy comprehensive evaluation with GIS technique. *International Journal of Disaster Risk Reduction*, *35*, 101077. https://doi.org/10.1016/j.ijdrr.2019.101077

Cheng, E. W., & Li, H. (2005). Application of ANP in process models: An example of strategic partnering. *Building and Environment*, *42*(1), 278–287. https://doi.org/10.1016/j.buildenv.2005.07.031

CHRS (n.d.). *Data portal*. Center for Hydrometeorology and Remote Sensing. https://chrsdata.eng.uci.edu

Colapinto, C., Jayaraman, R., & Marsiglio, S. (2015). Multi-criteria decision analysis with goal programming in engineering, management and social sciences: a state-of-the art review. *Annals of Operations Research*, *251*, 7–40. https://doi.org/10.1007/s10479-015-1829-1

Copernicus. (n.d.). *CORINE land cover 2018*. https://land.copernicus.eu/en/products/corine-land-cover/clc2018

Crichton, D. (1999). The risk triangle. *Natural Disaster Management, 102*(3), 102-103.

Danumah, J. H., Odai, S. N., Saley, B. M., Szarzynski, J., Thiel, M., Kwaku, A., Kouame, F. K., & Akpa, L. Y. (2016). Flood risk assessment and mapping in Abidjan district using multi-criteria analysis (AHP) model and geoinformation techniques. *Geoenvironmental Disasters*, *3*(10). https://doi.org/10.1186/s40677-016-0044-y

Dell'Ovo, M., Oppio, A., & Capolongo, S. (2020). Structuring the decision problem. A spatial multi-methodological approach. In *SpringerBriefs in applied sciences and technology* (pp. 29–51). https://doi.org/10.1007/978-3-030-50173-0_2

Dervishaj, G., Cimellaro, G. P., & Agrawal, A. (2017). A new decision-making method to select priority interventions after extreme events. *COMPDYN, 2017*, 4546–4561. https://doi.org/10.7712/120117.5743.18664

Díez-Herrero, A., & Garrote, J. (2020). Flood Risk Analysis and Assessment, Applications and Uncertainties: A bibliometric review. *Water, 12*(7), 2050. https://doi.org/10.3390/w12072050

Dwanoko, Y. S., Habibi, F. Y., Purwanto, H. L., Swastika, I. K., & Hudha, M. N. (2018). The smart method to support a decision based on multi attributes identification. *IOP Conference Series Materials Science and Engineering*, *434*,

012037. https://doi.org/10.1088/1757-899x/434/1/012037

Ekmekcioğlu, Ö., Koc, K., & Özger, M. (2020). District based flood risk assessment in Istanbul using fuzzy analytical hierarchy process. *Stochastic Environmental Research and Risk Assessment*, *35*, 617–637. https://doi.org/10.1007/s00477-020-01924-8

Elstat. (n.d.). *2021 Population and Housing Census.* Hellenic Statistical Authority. https://www.statistics.gr/en/statistics/pop

EM-DAT. (n.d.). *Emergency events database*. Centre for Research on the Epidemiology of Disasters (CRED). https://public.emdat.be

FAO. (n.d.). *FAO/ UNESCO soil map of the world*. Food and Agriculture Organization of the United Nations. https://www.fao.org/soils-portal/data-hub/soil-maps-and-databases/faounesco-soil-map-of-the-world/en/

Feizizadeh, B., & Kienberger, S. (2017). Spatially explicit sensitivity and uncertainty analysis for multicriteria-based vulnerability assessment. *Journal of Environmental Planning and Management, 60*(11), 2013–2035. http://dx.doi.org/10.1080/09640568.2016.1269643

Feloni, E., Mousadis, I., & Baltas, E. (2019). Flood vulnerability assessment using a GIS-based multi-criteria approach - The case of Attica region. *Journal of Flood Risk Management, 13*(1). https://doi.org/10.1111/jfr3.12563

Foudi, S., Osés-Eraso, N., & Tamayo, I. (2015). Integrated spatial flood risk assessment: The case of Zaragoza. *Land Use Policy*, *42*, 278–292. https://doi.org/10.1016/j.landusepol.2014.08.002

Gain, A. K., Mojtahed, V., Biscaro, C., Balbi, S., & Giupponi, C. (2015). An integrated approach of flood risk assessment in the eastern part of Dhaka City. *Natural Hazards*, *79*(3), 1499–1530. https://doi.org/10.1007/s11069-015-1911-7

Gebremichael, A., Gebremariam, E., & Desta, H. (2025). GIS-based mapping of flood hazard areas and soil erosion using analytic hierarchy process (AHP) and the universal soil loss equation (USLE) in the Awash River Basin, Ethiopia. *Geoscience Letters*, *12*(12). https://doi.org/10.1186/s40562-025-00382-w

Greene, R., Devillers, R., Luther, J. E., & Eddy, B. G. (2011). GIS-Based Multiple-Criteria Decision Analysis. *Geography Compass, 5*(6), 412–432. https://doi.org/10.1111/j.1749-8198.2011.00431.x

Gupta, L., & Dixit, J. (2022). A GIS-based flood risk mapping of Assam, India, using

the MCDA-AHP approach at the regional and administrative level. *Geocarto International,* *37*(26), 11867-11899. https://doi.org/10.1080/10106049.2022.2060329

Guitouni, A., & Martel, J. (1998). Tentative guidelines to help choosing an appropriate MCDA method. *European Journal of Operational Research, 109*(2), 501–521. https://doi.org/10.1016/s0377-2217(98)00073-3

Gündoğdu, F. K., & Kahraman, C. (2019). A novel spherical fuzzy analytic hierarchy process and its renewable energy application. *Soft Computing*, *24*, 4607–4621. https://doi.org/10.1007/s00500-019-04222-w

Gütmen, S., Roy, S. K., & Weber, G. (2024). An overview of weighted goal programming: a multi-objective transportation problem with some fresh viewpoints. *Central European Journal of Operations Research*, *32*, 557–568. https://doi.org/10.1007/s10100-023-00861-5

Ho, W., & Ma, X. (2017). The state-of-the-art integrations and applications of the analytic hierarchy process. *European Journal of Operational Research*, *267*(2), 399–414. https://doi.org/10.1016/j.ejor.2017.09.007

Hodgett, R. E., & Siraj, S. (2018). SURE: A method for decision-making under uncertainty. *Expert Systems with Applications*, *115*, 684–694. https://doi.org/10.1016/j.eswa.2018.08.048

Hossain, A. B. M. S., Rasel, H. M., Ahad, S. M. A. A., Bari, M. N., Alam, M.Z., & Chowdhury, A. (2023). *Assessing flood vulnerability at Chilmari Upazilla in Bangladesh through GIS and AHP approaches.* International Conference on Planning, Architecture and Civil Engineering, Rajshahi University of Engineering & Technology, Rajshahi, Bangladesh. https://www.researchgate.net/publication/375604616

Jun, K., Chung, E., Kim, Y., & Kim, Y. (2013). A fuzzy multi-criteria approach to flood risk vulnerability in South Korea by considering climate change impacts. *Expert Systems With Applications*, *40*(4), 1003–1013. https://doi.org/10.1016/j.eswa.2012.08.013

Kahraman, C., & Kaya, I. (2012). A fuzzy multiple attribute utility model for intelligent building assessment. *Journal of Civil Engineering and Management*, *18*(6), 811–820. https://doi.org/10.3846/13923730.2012.720932

Kanani-Sadat, Y., Arabsheibani, R., Karimipour, F., & Nasseri, M. (2019). A new approach to flood susceptibility assessment in data-scarce and ungauged regions

based on GIS-based hybrid multi criteria decision-making method. *Journal of Hydrology*, *572*, 17–31. https://doi.org/10.1016/j.jhydrol.2019.02.034

Khalafalla, M., & Rueda-Benavides, J. A. (2024). Value for money-based project selection framework using multi-attribute utility theory. *Construction Research Congress 2022*, 50–59. https://doi.org/10.1061/9780784485286.006

Khan, N. A., Alzahrani, H., Bai, S., Hussain, M., Tayyab, M., Ullah, S., Ullah, K., & Khalid, S. (2025). Flood risk assessment in the Swat river catchment through GIS-based multi-criteria decision analysis. *Frontiers in Environmental Science, 13*. https://doi.org/10.3389/fenvs.2025.1567796

Kourgialas, N. N., & Karatzas, G. P. (2017). A national scale flood hazard mapping methodology: The case of Greece – Protection and adaptation policy approaches. *Science of the Total Environment, 601–602*, 441–452. https://doi.org/10.1016/j.scitotenv.2017.05.197

Lappas, I., & Kallioras, A. (2019). Flood Susceptibility Assessment through GIS-Based Multi-Criteria Approach and Analytical Hierarchy Process (AHP) in a River Basin in Central Greece. *International Research Journal of Engineering and Technology (IRJET), 6*(3), 738-751. https://www.irjet.net/archives/V6/i3/IRJET-V6I3137.pdf

Lin, L., Wu, Z., & Liang, Q. (2019). Urban flood susceptibility analysis using a GIS-based multi-criteria analysis framework. *Natural Hazards*, *97*, 455–475. https://doi.org/10.1007/s11069-019-03615-2

Liu, Y., Eckert, C. M., & Earl, C. (2020). A review of fuzzy AHP methods for decision-making with subjective judgements. *Expert Systems with Applications*, *161*, 113738. https://doi.org/10.1016/j.eswa.2020.113738

Lyu, H., Sun, W., Shen, S., & Arulrajah, A. (2018). Flood risk assessment in metro systems of mega-cities using a GIS-based modeling approach. *The Science of The Total Environment, 626*, 1012–1025. https://doi.org/10.1016/j.scitotenv.2018.01.138

Manyena, B., Machingura, F., & O'Keefe, P. (2019). Disaster Resilience Integrated Framework for Transformation (DRIFT): A new approach to theorising and operationalising resilience. *World Development, 123*, 104587. https://doi.org/10.1016/j.worlddev.2019.06.011

Mateo, J. R. S. C. (2012a). Multi-Attribute utility theory. In *Green energy and technology* (pp. 63–72). https://doi.org/10.1007/978-1-4471-2346-0_10

Mateo, J. R. S. C. (2012b). PROMETHEE. In *Green energy and technology* (pp. 23–32). https://doi.org/10.1007/978-1-4471-2346-0_5

Meesariganda, B. R., & Ishizaka, A. (2016). Mapping verbal AHP scale to numerical scale for cloud computing strategy selection. *Applied Soft Computing*, *53*, 111–118. https://doi.org/10.1016/j.asoc.2016.12.040

Moreira, L. L., De Brito, M. M., & Kobiyama, M. (2021). Review article: A systematic review and future prospects of flood vulnerability indices. *Natural Hazards and Earth System Sciences*, *21*(5), 1513–1530. https://doi.org/10.5194/nhess-21-1513-2021

Municipality of Pylaia-Chortiati. (n.d.). Official website of Municipality of Pylaia-Chortiatis. https://pilea-hortiatis.gr/en/

Municipality of Thermi. (n.d.). Official website of Thermi. https://thermi.gr/en/

Nahin, K. T. K., Islam, S. B., Mahmud, S., & Hossain, I. (2023). Flood vulnerability assessment in the Jamuna river floodplain using multi-criteria decision analysis: A case study in Jamalpur district, Bangladesh. *Heliyon*, *9*(3), e14520. https://doi.org/10.1016/j.heliyon.2023.e14520

NASA. (n.d.). Earthdata search. https://search.earthdata.nasa.gov/search

OpenStreetMap. (n.d.). https://www.openstreetmap.org/#map=7/38.359/23.810

Papaioannou, G., Vasiliades, L., & Loukas, A. (2015). Multi-Criteria Analysis Framework for potential flood prone areas mapping. *Water Resources Management*, *29*(2), 399–418. https://doi.org/10.1007/s11269-014-0817-6

Papathanasiou, J., & Ploskas, N. (2018). PROMETHEE. In *Springer optimization and its applications* (pp. 57–89). https://doi.org/10.1007/978-3-319-91648-4_3

Rana, I. A., & Routray, J. K. (2017). Integrated methodology for flood risk assessment and application in urban communities of Pakistan. *Natural Hazards*, *91*, 239–266. https://doi.org/10.1007/s11069-017-3124-8

Saaty, T. L. (1977). A scaling method for priorities in hierarchical structures. *Journal of Mathematical Psychology, 15*(3), 234–281. https://doi.org/10.1016/0022-2496(77)90033-5

Saaty, T. L. (1990). How to make a decision: The analytic hierarchy process. *European Journal of Operational Research*, *48*(1), 9–26. https://doi.org/10.1016/0377-2217(90)90057-i

Sánchez-Garrido, A., Navarro, I., García, J., & Yepes, V. (2022). An Adaptive ANP & ELECTRE IS-Based MCDM Model Using Quantitative Variables.

*Mathematics*, *10*(12), 2009. https://doi.org/10.3390/math10122009

Seneviratne, S.I., Zhang, X., Adnan, M., Badi, W., Dereczynski, C., Di Luca, A., Ghosh, S., Iskandar, I., Kossin, J., Lewis, S., Otto, F., Pinto, I., Satoh, M., Vicente-Serrano, S.M., Wehner, M., & Zhou, B. (2021). Weather and Climate Extreme Events in a Changing Climate. In *Climate Change 2021: The Physical Science Basis. Contribution of Working Group I to the Sixth Assessment Report of the Intergovernmental Panel on Climate Change (*pp. 1513–1766). https://doi:10.1017/9781009157896.013

Sharker, R., Islam, M. R., Hosen, M. B., Kader, Z., Aziz, M. T., Tahera-Tun-Humayra, U., Hossain, M. A., Pervin, R., Hasan, M., & Roy, A. (2025). GIS-based AHP approach to flood susceptibility assessment in Tangail district, Bangladesh. *Journal of Earth System Science*, *134*. https://doi.org/10.1007/s12040-024-02480-3

Stefanidis, S., Kalantzi, G., Chatzichristaki, Ch., & Karystinakis, K. (2021). *A GIS-based flash flood hazard mapping and vulnerability assessment*. Eighth International Conference on Environmental Management, Engineering, Planning & Economics (CEMEPE 2021) and SECOTOX Conference. https://www.researchgate.net/publication/353513871

Sun, Z., Pan, L., Wang, Y., & Zhang, D. (2013). The purchase house choice research based on the Analytic Hierarchy Process (AHP). In *Springer eBooks* (pp. 897–902). https://doi.org/10.1007/978-3-642-38391-5_95

Tabasi, N., Fereshtehpour, M., & Roghani, B. (2025). A review of flood risk assessment frameworks and the development of hierarchical structures for risk components. *Discover Water*, *5*. https://doi.org/10.1007/s43832-025-00193-2

Taoukidou, N., Karpouzos, D., & Georgiou, P. (2025). Flood Hazard Assessment through AHP, Fuzzy AHP, and Frequency Ratio Methods: A Comparative analysis. *Water*, *17*(14), 2155. https://doi.org/10.3390/w17142155

Tehrany, M. S., Jones, S., & Shabani, F. (2019). Identifying the essential flood conditioning factors for flood prone area mapping using machine learning techniques. *CATENA*, *175*, 174–192. https://doi.org/10.1016/j.catena.2018.12.011

Theochari, A., Develekou, M., & Baltas, E. (2021). GIS-based multi-criteria approach

towards sustainability of flood-susceptible areas in Giofiros River Basin, Greece. *Circular Economy and Sustainability*, *2*, 1615–1626. https://doi.org/10.1007/s43615-021-00096-z

UNDRR. (2009). *2009 UNISDR terminology on disaster risk reduction*. United Nations Office for Disaster Risk Reduction. https://www.undrr.org/publication/2009-unisdr-terminology-disaster-risk-reduction

UNDRR. (2017). *Report of the open-ended intergovernmental expert working group on indicators and terminology relating to disaster risk reduction*. United Nations Office for Disaster Risk Reduction. https://www.undrr.org/publication/report-open-ended-intergovernmental-expert-working-group-indicators-and-terminology

UNDRR. (2020). *Words into Action: Engaging for resilience in support of the Sendai Framework for Disaster Risk Reduction 2015-2030*. United Nations Office for Disaster Risk Reduction. https://www.undrr.org/words-into-action/implementation-guide-land-use-and-urban-planning

UNDRR. (2024). *GAR Special Report 2024 Forensic insights for future resilience: Learning from past disasters*. United Nations Office for Disaster Risk Reduction. https://www.undrr.org/gar/gar2024-special-report

UNDRR. (2025). *Global Assessment Report on Disaster Risk Reduction 2025: Resilient pays: financing and investing for our future.* United Nations Office for Disaster Risk Reduction. https://www.undrr.org/gar

USGS. (n.d.). *EarthExplorer*. https://earthexplorer.usgs.gov

Vargas, L. G. (1990). An overview of the analytic hierarchy process and its applications. *European Journal of Operational Research*, *48*(1), 2–8. https://doi.org/10.1016/0377-2217(90)90056-h

Vahdani, B., Jabbari, A. H. K., Roshanaei, V., & Zandieh, M. (2010). Extension of the ELECTRE method for decision-making problems with interval weights and data. *The International Journal of Advanced Manufacturing Technology*, *50*, 793–800. https://doi.org/10.1007/s00170-010-2537-2

Yang, X., Ding, J., & Hou, H. (2013). Application of a triangular fuzzy AHP approach for flood risk evaluation and response measures analysis. *Natural Hazards*, *68*, 657–674. https://doi.org/10.1007/s11069-013-0642-x

Ypeka. (2025). *1st Revision of Flood Risk Management Plan of the River Basins of the Water District of Central Macedonia (EL10).* General Secretariat for Natural Environment and Water General Directorate for Water. *https://floods.ypeka.gr/wp-content/uploads/2025/05/EL10_FEK_2480_B_2025.pdf*

Wang, Z., Lai, C., Chen, X., Yang, B., Zhao, S., & Bai, X. (2015). Flood hazard risk assessment model based on random forest. *Journal of Hydrology*, *527*, 1130–1141. https://doi.org/10.1016/j.jhydrol.2015.06.008

Wang, Y., Zhang, Q., Lin, K., Liu, Z., Liang, Y., Liu, Y., & Li, C. (2024). A novel framework for urban flood risk assessment: Multiple perspectives and causal analysis. *Water Research, 256*, 121591. https://doi.org/10.1016/j.watres.2024.121591

Zadeh, L. (1965). Fuzzy sets. *Information and Control*, *8*(3), 338–353. https://doi.org/10.1016/s0019-9958(65)90241-x

Xu, H., Ma, C., Lian, J., Xu, K., & Chaima, E. (2018). Urban flooding risk assessment based on an integrated k-means cluster algorithm and improved entropy weight method in the region of Haikou, China. *Journal of Hydrology*, *563*, 975–986. https://doi.org/10.1016/j.jhydrol.2018.06.060

# 8. Appendices

## Appendix I

### Precipitation

Within the boundaries of the study area, no meteorological stations provided by the national meteorological service are available for measuring annual precipitation. The closest station, the one located within the regional unit, is approximately 10km away. However, the development of reliable precipitation maps requires a greater number of stations for spatial interpolation. Such data could potentially be obtained by combining datasets from various stations by different institutions or agencies having meteorological stations within the wider study area. However, considering the required time for data collection from different sources, the potential costs and the study's requirements, annual precipitation data was obtained from publicly access PERSIANN-CCS dataset. It should be noted that these data present limitations related to their spatial resolution as the original cell size is larger than the cell size of the other raster files used in this study. However, this resolution is considered adequate for the analysis given the extent of the basin and the range of precipitation values.

### Population density

In this study, population density was calculated by dividing the permanent number of residents in each municipal community by the corresponding area of each municipal community, using 2021 census data from ELSTAT and spatial information from the ELSTAT Digital Cartographic Backgrounds. The table below presents the total population, area and population density of municipal communities within the study area.

*Table 18 Total population, area and population density of each municipal community within the study area (Source: ELSTAT, own processing)*

| Municipal Community | Total Population 2021 | Area (ha) | Population Density (people/ha) |
|---|---|---|---|
| **Asvestochori** | 6553 | 3517,33 | 1,86 |
| **Exochi** | 1267 | 240,63 | 5,27 |
| **Thermi** | 19602 | 5592,82 | 3,50 |
| **Panorama** | 17680 | 2174,38 | 8,13 |

| | | | |
|---|---|---|---|
| **Pylaia** | 36843 | 2451,15 | 15,03 |
| **Chortiatis** | 4512 | 5707,13 | 0,79 |

**Dependent population**

In this study, the dependent population was analyzed solely based on populations' age groups (dependent population: 0-14years and 65+ years, non-dependent population: 15-64 years) using municipal community level data from the 2021 ELSTAT census and spatial information from the ELSTAT Digital Cartographic Backgrounds. The disability dimension, although recognized as critical factor for inclusive flood risk assessments, was not included due to data limitations. The following present some conclusions drawn from the research of the relevant datasets. ELSTAT does not provide data on the total population with disabilities due to the sensitivity of such information. Additionally, Municipal Social Services are often unaware of the exact population with disabilities in their municipalities or the relevant information is fragmented across different municipal departments, requiring significant time to concentrate such information. In Greece, the number of people with disabilities is officially recorded only for those receiving disability allowances, a measure that does not represent their actual population. Therefore, the disability aspect was excluded from this analysis. In this study it is considered appropriate to analyze the dependent population using the total dependency rate, which combines dependent and non-dependent populations into a single index (also for effective use in GIS analysis). The dependency rate was calculated using the following formula:

$$\text{Dependency Rate (\%)} = \left( \frac{Population\ 0{-}14\ years + Population\ 65{+}years}{Population\ 15{-}64\ years} \right) \text{x } 100$$

The total number of dependent and non-dependent populations along with the dependency rate is presented in the table below.

*Table 19 Dependent population, non-dependent population and dependency rate of each municipal community within the study area (Source: ELSTAT, own processing)*

| Municipal Community | Total population 2021 | Dependent Population 2021 | Non-Dependent Population 2021 | Dependency Rate (%) |
|---|---|---|---|---|
| **Asvestochori** | 6553 | 2188 | 4359 | 50,195 |
| **Exochi** | 1267 | 461 | 808 | 57,054 |
| **Thermi** | 19602 | 6747 | 12853 | 52,494 |
| **Panorama** | 17680 | 6261 | 11426 | 54,796 |
| **Pylaia** | 36843 | 12958 | 23879 | 54,265 |
| **Chortiatis** | 4512 | 1495 | 3032 | 49,307 |

**Health facilities**

Within the study area, two facilities were identified including the Chortiatis Municipal Health Center and the Trans-Balkan Medical Center (private clinic). Due to their size and regional significance, additional facilities on the boundaries of the study area were also considered including Saint Luke's General Clinic (private clinic), Thermi Municipal Health Center and slightly beyond the study area boundaries Georgios Papanikolaou General Regional Hospital.

The table below presents the health facilities identified within, on the boundaries or very close to the boundaries of the study area as derived from Strategic Development Plans of the Municipalities of Thermi and Pylaia-Chortiatis.

*Table 20 Health facilities identified within or very close to the study area (Source: Strategic Development Plans, own processing)*

| Municipal Community | Health Facility | X (Greek Grid) | Y (Greek Grid) |
|---|---|---|---|
| **Chortiatis** | Chortiatis Municipal Health Center | 423787,98 | 4495528,67 |
| **Pylaia** | Trans-Balkan Medical Center | 414137,82 | 4488795,24 |
| **Panorama** | Saint Luke's General Clinic | 416472,59 | 4493775,53 |
| **Thermi** | Thermi Municipal Health Center | 415752,40 | 4487749,46 |
| **Exochi** | Georgios Papanikolaou General Regional Hospital | 419261,50 | 4497850,77 |

**Emergency shelters**

The table below presents the emergency shelters identified within the boundaries of the study area as derived from Civil Protection Plans of the Municipalities of Thermi and Pylaia-Chortiatis.

*Table 21 Emergency shelters within the study area based on their type (Source: Civil Protection Plans, own processing)*

| Municipal Community | n. Points | Assembly Point | Camp site | Shelter point | Disposal Area |
|---|---|---|---|---|---|
| **Asvestochori** | - | - | - | - | - |
| **Exochi** | - | - | - | - | - |
| **Thermi** | 7 | 3 | - | 4 | - |
| **Panorama** | 15 | 3 | 1 | 10 | 1 |
| **Pylaia** | - | - | - | - | - |
| **Chortiatis** | 3 | 1 | 1 | 1 | - |

**Building (residential) age**

In this study, building (residential) age was analyzed using municipal community level data from the 2021 ELSTAT census. The data includes the total number of residential buildings (empty and occupied) constructed across five time periods: before 1945, 1946-1980, 1981-1990, 1991-2010 and after 2011, referred to municipal community level. In this study it is considered appropriate to analyze the building (residential) age using the building age rate, which combines older and newer buildings into a single index (also for effective use in GIS analysis). The building age rate was calculated using the following formula:

$$\text{Building Age Rate (\%)} = \left( \frac{Buildings\ (residential) before\ 1945 + Buildings\ 1946-1980 + Buildings\ 1981-1990}{Buildings\ 1991-2010 + Buildings\ After\ 2011} \right) \times 100$$

The total number of buildings (residential) based on their year of construction along with the dependency rate is presented in the table below.

*Table 22 Number of buildings based on their construction year and building age rate of each municipal community within the study area (Source: ELSTAT, own processing)*

| Municipal Community | Total residential | Before 1945 | 1946-1980 | 1981-1990 | 1991-2010 | After 2011 | Building Age Rate (%) |
|---|---|---|---|---|---|---|---|
| **Asvestochori** | 2768 | 115 | 709 | 494 | 1368 | 86 | 90,646 |
| **Exochi** | 611 | 11 | 135 | 103 | 271 | 91 | 68,785 |
| **Thermi** | 7273 | 27 | 744 | 993 | 4532 | 967 | 32,079 |
| **Panorama** | 7250 | 37 | 1316 | 1767 | 3879 | 263 | 75,326 |
| **Pylaia** | 16245 | 113 | 2998 | 3926 | 8359 | 849 | 76,423 |
| **Chortiatis** | 2169 | 20 | 318 | 489 | 1301 | 41 | 61,624 |

## Appendix II

*Table 23 Classification and risk values of the selected parameters and area statistics (own processing)*

| Parameter | Natural Breaks (Jenks) | Class Value | Risk Value | Cells Count | Area (ha) | % of the total area (ha) |
|---|---|---|---|---|---|---|
| **Elevation** | 2,001-168 | 1 | 5 | 24845 | 1904,04 | 31 |
| | 168,001-368 | 2 | 4 | 20362 | 1560,47 | 25 |
| | 368,001-573 | 3 | 3 | 25418 | 1947,95 | 31 |
| | 573,001-795 | 4 | 2 | 6451 | 494,38 | 8 |
| | 795,001-1185 | 5 | 1 | 3849 | 294,97 | 5 |
| **Slope** | 0,001-5,826 | 1 | 5 | 26093 | 1999,68 | 32 |
| | 5,827-11,652 | 2 | 4 | 24459 | 1874,46 | 30 |
| | 11,653-18,374 | 3 | 3 | 16114 | 1234,92 | 20 |
| | 18,375-27,113 | 4 | 2 | 9279 | 711,11 | 11 |
| | 27,114-57,138 | 5 | 1 | 3570 | 273,59 | 4 |
| **Soil Type** | Rc49-2ab 14 | 1 | 2 | 32158 | 2464,48 | 40 |
| | Lc104-2/3bc 9 | 2 | 3 | 48777 | 3738,10 | 60 |
| **Curvature** | -14,971 - -3,297 | 1 | 4 | 5059 | 387,70 | 6 |
| | -3,296 - -0,909 | 2 | 3 | 20134 | 1543,00 | 25 |
| | -0,908 - 0,949 | 3 | 5 | 31921 | 2446,32 | 39 |
| | 0,95-3,469 | 4 | 2 | 18931 | 1450,81 | 23 |
| | 3,47-18,859 | 5 | 1 | 4879 | 373,91 | 6 |
| **Precipitation** | 621,049-622,859 | 1 | 1 | 2238 | 171,51 | 3 |
| | 622,86-640,172 | 2 | 2 | 18755 | 1437,32 | 23 |
| | 640,173-647,62 | 3 | 3 | 27828 | 2132,64 | 34 |
| | 647,621-658,491 | 4 | 4 | 13566 | 1039,65 | 17 |

| | | | | | | |
|---|---|---|---|---|---|---|
| | 658,492-672,381 | 5 | 5 | 18427 | 1412,18 | 23 |
| **TWI** | 3,204-5,592 | 1 | 1 | 27726 | 2124,83 | 34 |
| | 5,593-7,163 | 2 | 2 | 29850 | 2287,60 | 37 |
| | 7,164-9,3 | 3 | 3 | 13487 | 1033,60 | 17 |
| | 9,301-12,255 | 4 | 4 | 6047 | 463,42 | 7 |
| | 12,256-19,232 | 5 | 5 | 2405 | 184,31 | 3 |
| **Drainage density** | 0,001-1,188 | 1 | 1 | 17412 | 1334,40 | 22 |
| | 1,189-2,419 | 2 | 2 | 29088 | 2229,21 | 36 |
| | 2,42-3,565 | 3 | 3 | 22327 | 1711,07 | 28 |
| | 3,566-5,814 | 4 | 4 | 11094 | 850,21 | 14 |
| | 5,815-10,821 | 5 | 5 | 1024 | 78,48 | 1 |
| **Distance from stream** | 0,001-81,072 | 1 | 5 | 27878 | 2136,48 | 34 |
| | 81,073-168,15 | 2 | 4 | 25748 | 1973,24 | 32 |
| | 168,151-258,23 | 3 | 3 | 16744 | 1283,20 | 21 |
| | 258,231-375,335 | 4 | 2 | 8023 | 614,86 | 10 |
| | 375,336-765,683 | 5 | 1 | 2557 | 195,96 | 3 |
| **NDVI** | -0,036-0,173 | 1 | 5 | 8601 | 659,15 | 11 |
| | 0,174-0,237 | 2 | 4 | 24507 | 1878,13 | 30 |
| | 0,238-0,301 | 3 | 3 | 25151 | 1927,49 | 31 |
| | 0,302-0,377 | 4 | 2 | 16306 | 1249,64 | 20 |
| | 0,378-0,546 | 5 | 1 | 6133 | 470,01 | 8 |
| **Population density** | 0,792-1,852 | 1 | 1 | 25542 | 1957,45 | 32 |
| | 1,853-5,258 | 2 | 2 | 29493 | 2260,24 | 36 |
| | 5,259-8,106 | 3 | 3 | 296 | 22,68 | 0,37 |
| | 8,107-15,031 | 4 | 4 | 25593 | 1961,36 | 32 |

| | | | | | | |
|---|---|---|---|---|---|---|
| **LULC** | Coastal and marine zones | 1 | 1 | 79 | 6,05 | 0,10 |
| | Forested areas | 2 | 2 | 7695 | 589,72 | 10 |
| | Semi-natural grasslands and shrubs | 3 | 3 | 27249 | 2088,27 | 34 |
| | Agricultural lands and mixed farming | 4 | 4 | 26091 | 1999,53 | 32 |
| | Built-up and industrial urban areas | 5 | 5 | 19818 | 1518,78 | 24 |
| **Dependent Population (Dependency Rate)** | 49,308-50,188 | 1 | 1 | 25552 | 1958,22 | 32 |
| | 50,189-52,497 | 2 | 2 | 29511 | 2261,62 | 36 |
| | 52,498-54,806 | 3 | 3 | 25587 | 1960,90 | 32 |
| | 54,807-57,054 | 4 | 4 | 295 | 22,61 | 0,36 |
| **Building Density** | 0-1,023 | 1 | 1 | 54608 | 4184,97 | 67 |
| | 1,024-3,121 | 2 | 2 | 13975 | 1071,00 | 17 |
| | 3,122-6,243 | 3 | 3 | 7060 | 541,05 | 9 |
| | 6,244-9,415 | 4 | 4 | 3765 | 288,54 | 5 |
| | 9,416-13,049 | 5 | 5 | 1536 | 117,71 | 2 |
| **Distance from road** | 0,001-175,962 | 1 | 1 | 50480 | 3868,62 | 62 |
| | 175,963-469,232 | 2 | 2 | 12662 | 970,37 | 16 |
| | 469,233-828,488 | 3 | 3 | 8799 | 674,33 | 11 |
| | 828,489-1275,726 | 4 | 4 | 5938 | 455,07 | 7 |
| | 1275,727-1869,598 | 5 | 5 | 3071 | 235,35 | 4 |
| **Distance from health facilities** | 0,001-1319,75 | 1 | 1 | 15473 | 1185,80 | 19 |
| | 1319,751-2262,429 | 2 | 2 | 20515 | 1572,20 | 25 |

| | | | | | | |
|---|---|---|---|---|---|---|
| | 2262,43-3157,973 | 3 | 3 | 23411 | 1794,14 | 29 |
| | 3157,974-4218,487 | 4 | 4 | 14022 | 1074,60 | 17 |
| | 4218,488-6009,576 | 5 | 5 | 7524 | 576,61 | 9 |
| **Distance from emergency shelter** | 0-790,216 | 1 | 1 | 19617 | 1503,38 | 24 |
| | 790,217-1479,553 | 2 | 2 | 18615 | 1426,59 | 23 |
| | 1479,554-2152,077 | 3 | 3 | 18335 | 1405,13 | 23 |
| | 2152,078-2858,227 | 4 | 4 | 15682 | 1201,82 | 19 |
| | 2858,228-4287,341 | 5 | 5 | 8701 | 666,82 | 11 |
| **Building age (Building Age Rate)** | 32,08-51,601 | 1 | 2 | 26846 | 2057,39 | 33 |
| | 51,602-71,124 | 2 | 3 | 25847 | 1980,83 | 32 |
| | 71,125-90,646 | 3 | 4 | 28252 | 2165,14 | 35 |

**Appendix III**

Series from Lund University

## Department of Physical Geography and Ecosystem Science

### Master Thesis in Geographical Information Science

1. *Anthony Lawther:* The application of GIS-based binary logistic regression for slope failure susceptibility mapping in the Western Grampian Mountains, Scotland (2008).
2. *Rickard Hansen:* Daily mobility in Grenoble Metropolitan Region, France. Applied GIS methods in time geographical research (2008).
3. *Emil Bayramov:* Environmental monitoring of bio-restoration activities using GIS and Remote Sensing (2009).
4. *Rafael Villarreal Pacheco:* Applications of Geographic Information Systems as an analytical and visualization tool for mass real estate valuation: a case study of Fontibon District, Bogota, Columbia (2009).
5. *Siri Oestreich Waage:* a case study of route solving for oversized transport: The use of GIS functionalities in transport of transformers, as part of maintaining a reliable power infrastructure (2010).
6. *Edgar Pimiento:* Shallow landslide susceptibility – Modelling and validation (2010).
7. *Martina Schäfer:* Near real-time mapping of floodwater mosquito breeding sites using aerial photographs (2010).
8. *August Pieter van Waarden-Nagel:* Land use evaluation to assess the outcome of the programme of rehabilitation measures for the river Rhine in the Netherlands (2010).
9. *Samira Muhammad:* Development and implementation of air quality data mart for Ontario, Canada: A case study of air quality in Ontario using OLAP tool. (2010).
10. *Fredros Oketch Okumu*: Using remotely sensed data to explore spatial and temporal relationships between photosynthetic productivity of vegetation and malaria transmission intensities in selected parts of Africa (2011).
11. *Svajunas Plunge:* Advanced decision support methods for solving diffuse water pollution problems (2011).
12. *Jonathan Higgins:* Monitoring urban growth in greater Lagos: A case study using GIS to monitor the urban growth of Lagos 1990 - 2008 and produce future growth prospects for the city (2011).
13. *Mårten Karlberg:* Mobile Map Client API: Design and Implementation for Android (2011).
14. *Jeanette McBride:* Mapping Chicago area urban tree canopy using color infrared imagery (2011).
15. *Andrew Farina:* Exploring the relationship between land surface temperature and vegetation abundance for urban heat island mitigation in Seville, Spain (2011).
16. *David Kanyari*: Nairobi City Journey Planner: An online and a Mobile Application (2011).

17. *Laura V. Drews:* Multi-criteria GIS analysis for siting of small wind power plants - A case study from Berlin (2012).
18. *Qaisar Nadeem:* Best living neighborhood in the city - A GIS based multi criteria evaluation of ArRiyadh City (2012).
19. *Ahmed Mohamed El Saeid Mustafa:* Development of a photo voltaic building rooftop integration analysis tool for GIS for Dokki District, Cairo, Egypt (2012).
20. *Daniel Patrick Taylor*: Eastern Oyster Aquaculture: Estuarine Remediation via Site Suitability and Spatially Explicit Carrying Capacity Modeling in Virginia's Chesapeake Bay (2013).
21. *Angeleta Oveta Wilson:* A Participatory GIS approach to *unearthing* Manchester's Cultural Heritage '*gold mine'* (2013).
22. *Ola Svensson:* Visibility and Tholos Tombs in the Messenian Landscape: A Comparative Case Study of the Pylian Hinterlands and the Soulima Valley (2013).
23. *Monika Ogden:* Land use impact on water quality in two river systems in South Africa (2013).
24. *Stefan Rova:* A GIS based approach assessing phosphorus load impact on Lake Flaten in Salem, Sweden (2013).
25. *Yann Buhot:* Analysis of the history of landscape changes over a period of 200 years. How can we predict past landscape pattern scenario and the impact on habitat diversity? (2013).
26. *Christina Fotiou:* Evaluating habitat suitability and spectral heterogeneity models to predict weed species presence (2014).
27. *Inese Linuza:* Accuracy Assessment in Glacier Change Analysis (2014).
28. *Agnieszka Griffin:* Domestic energy consumption and social living standards: a GIS analysis within the Greater London Authority area (2014).
29. *Brynja Guðmundsdóttir:* Detection of potential arable land with remote sensing and GIS - A Case Study for Kjósarhreppur (2014).
30. *Oleksandr Nekrasov:* Processing of MODIS Vegetation Indices for analysis of agricultural droughts in the southern Ukraine between the years 2000-2012 (2014).
31. *Sarah Tressel:* Recommendations for a polar Earth science portal in the context of Arctic Spatial Data Infrastructure (2014).
32. *Caroline Gevaert:* Combining Hyperspectral UAV and Multispectral Formosat-2 Imagery for Precision Agriculture Applications (2014).
33. *Salem Jamal-Uddeen:* Using GeoTools to implement the multi-criteria evaluation analysis - weighted linear combination model (2014).
34. *Samanah Seyedi-Shandiz:* Schematic representation of geographical railway network at the Swedish Transport Administration (2014).
35. *Kazi Masel Ullah:* Urban Land-use planning using Geographical Information System and analytical hierarchy process: case study Dhaka City (2014).
36. *Alexia Chang-Wailing Spitteler:* Development of a web application based on MCDA and GIS for the decision support of river and floodplain rehabilitation projects (2014).
37. *Alessandro De Martino:* Geographic accessibility analysis and evaluation of potential changes to the public transportation system in the City of Milan (2014).
38. *Alireza Mollasalehi:* GIS Based Modelling for Fuel Reduction Using Controlled Burn in Australia. Case Study: Logan City, QLD (2015).

39. *Negin A. Sanati:* Chronic Kidney Disease Mortality in Costa Rica; Geographical Distribution, Spatial Analysis and Non-traditional Risk Factors (2015).
40. *Karen McIntyre:* Benthic mapping of the Bluefields Bay fish sanctuary, Jamaica (2015).
41. *Kees van Duijvendijk:* Feasibility of a low-cost weather sensor network for agricultural purposes: A preliminary assessment (2015).
42. *Sebastian Andersson Hylander:* Evaluation of cultural ecosystem services using GIS (2015).
43. *Deborah Bowyer:* Measuring Urban Growth, Urban Form and Accessibility as Indicators of Urban Sprawl in Hamilton, New Zealand (2015).
44. *Stefan Arvidsson:* Relationship between tree species composition and phenology extracted from satellite data in Swedish forests (2015).
45. *Damián Giménez Cruz*: GIS-based optimal localisation of beekeeping in rural Kenya (2016).
46. *Alejandra Narváez Vallejo:* Can the introduction of the topographic indices in LPJ-GUESS improve the spatial representation of environmental variables? (2016).
47. *Anna Lundgren:* Development of a method for mapping the highest coastline in Sweden using breaklines extracted from high resolution digital elevation models (2016).
48. *Oluwatomi Esther Adejoro:* Does location also matter? A spatial analysis of social achievements of young South Australians (2016).
49. *Hristo Dobrev Tomov:* Automated temporal NDVI analysis over the Middle East for the period 1982 - 2010 (2016).
50. *Vincent Muller:* Impact of Security Context on Mobile Clinic Activities A GIS Multi Criteria Evaluation based on an MSF Humanitarian Mission in Cameroon (2016).
51. *Gezahagn Negash Seboka:* Spatial Assessment of NDVI as an Indicator of Desertification in Ethiopia using Remote Sensing and GIS (2016).
52. *Holly Buhler:* Evaluation of Interfacility Medical Transport Journey Times in Southeastern British Columbia. (2016).
53. *Lars Ole Grottenberg*: Assessing the ability to share spatial data between emergency management organisations in the High North (2016).
54. *Sean Grant:* The Right Tree in the Right Place: Using GIS to Maximize the Net Benefits from Urban Forests (2016).
55. *Irshad Jamal:* Multi-Criteria GIS Analysis for School Site Selection in Gorno-Badakhshan Autonomous Oblast, Tajikistan (2016).
56. *Fulgencio Sanmartín:* Wisdom-volkano: A novel tool based on open GIS and time-series visualization to analyse and share volcanic data (2016).
57. *Nezha Acil:* Remote sensing-based monitoring of snow cover dynamics and its influence on vegetation growth in the Middle Atlas Mountains (2016).
58. *Julia Hjalmarsson:* A Weighty Issue: Estimation of Fire Size with Geographically Weighted Logistic Regression (2016).
59. *Mathewos Tamiru Amato:* Using multi-criteria evaluation and GIS for chronic food and nutrition insecurity indicators analysis in Ethiopia (2016).
60. *Karim Alaa El Din Mohamed Soliman El Attar:* Bicycling Suitability in Downtown, Cairo, Egypt (2016).

61. *Gilbert Akol Echelai:* Asset Management: Integrating GIS as a Decision Support Tool in Meter Management in National Water and Sewerage Corporation (2016).
62. *Terje Slinning:* Analytic comparison of multibeam echo soundings (2016).
63. *Gréta Hlín Sveinsdóttir:* GIS-based MCDA for decision support: A framework for wind farm siting in Iceland (2017).
64. *Jonas Sjögren:* Consequences of a flood in Kristianstad, Sweden: A GIS-based analysis of impacts on important societal functions (2017).
65. *Nadine Raska:* 3D geologic subsurface modelling within the Mackenzie Plain, Northwest Territories, Canada (2017).
66. *Panagiotis Symeonidis*: Study of spatial and temporal variation of atmospheric optical parameters and their relation with PM 2.5 concentration over Europe using GIS technologies (2017).
67. *Michaela Bobeck:* A GIS-based Multi-Criteria Decision Analysis of Wind Farm Site Suitability in New South Wales, Australia, from a Sustainable Development Perspective (2017).
68. *Raghdaa Eissa*: Developing a GIS Model for the Assessment of Outdoor Recreational Facilities in New Cities Case Study: Tenth of Ramadan City, Egypt (2017).
69. *Zahra Khais Shahid*: Biofuel plantations and isoprene emissions in Svea and Götaland (2017).
70. *Mirza Amir Liaquat Baig*: Using geographical information systems in epidemiology: Mapping and analyzing occurrence of diarrhea in urban - residential area of Islamabad, Pakistan (2017).
71. *Joakim Jörwall*: Quantitative model of Present and Future well-being in the EU-28: A spatial Multi-Criteria Evaluation of socioeconomic and climatic comfort factors (2017).
72. *Elin Haettner*: Energy Poverty in the Dublin Region: Modelling Geographies of Risk (2017).
73. *Harry Eriksson*: Geochemistry of stream plants and its statistical relations to soil- and bedrock geology, slope directions and till geochemistry. A GIS-analysis of small catchments in northern Sweden (2017).
74. *Daniel Gardevärn:* PPGIS and Public meetings – An evaluation of public participation methods for urban planning (2017).
75. *Kim Friberg:* Sensitivity Analysis and Calibration of Multi Energy Balance Land Surface Model Parameters (2017).
76. *Viktor Svanerud:* Taking the bus to the park? A study of accessibility to green areas in Gothenburg through different modes of transport (2017).
77. *Lisa-Gaye Greene*: Deadly Designs: The Impact of Road Design on Road Crash Patterns along Jamaica's North Coast Highway (2017).
78. *Katarina Jemec Parker*: Spatial and temporal analysis of fecal indicator bacteria concentrations in beach water in San Diego, California (2017).
79. *Angela Kabiru*: An Exploratory Study of Middle Stone Age and Later Stone Age Site Locations in Kenya's Central Rift Valley Using Landscape Analysis: A GIS Approach (2017).
80. *Kristean Björkmann*: Subjective Well-Being and Environment: A GIS-Based Analysis (2018).
81. *Williams Erhunmonmen Ojo*: Measuring spatial accessibility to healthcare for people living with HIV-AIDS in southern Nigeria (2018).

82. *Daniel Assefa*: Developing Data Extraction and Dynamic Data Visualization (Styling) Modules for Web GIS Risk Assessment System (WGRAS). (2018).
83. *Adela Nistora*: Inundation scenarios in a changing climate: assessing potential impacts of sea-level rise on the coast of South-East England (2018).
84. *Marc Seliger*: Thirsty landscapes - Investigating growing irrigation water consumption and potential conservation measures within Utah's largest master-planned community: Daybreak (2018).
85. *Luka Jovičić*: Spatial Data Harmonisation in Regional Context in Accordance with INSPIRE Implementing Rules (2018).
86. *Christina Kourdounouli*: Analysis of Urban Ecosystem Condition Indicators for the Large Urban Zones and City Cores in EU (2018).
87. *Jeremy Azzopardi*: Effect of distance measures and feature representations on distance-based accessibility measures (2018).
88. *Patrick Kabatha*: An open source web GIS tool for analysis and visualization of elephant GPS telemetry data, alongside environmental and anthropogenic variables (2018).
89. *Richard Alphonce Giliba*: Effects of Climate Change on Potential Geographical Distribution of Prunus africana (African cherry) in the Eastern Arc Mountain Forests of Tanzania (2018).
90. *Eiður Kristinn Eiðsson*: Transformation and linking of authoritative multi-scale geodata for the Semantic Web: A case study of Swedish national building data sets (2018).
91. *Niamh Harty*: HOP!: a PGIS and citizen science approach to monitoring the condition of upland paths (2018).
92. *José Estuardo Jara Alvear*: Solar photovoltaic potential to complement hydropower in Ecuador: A GIS-based framework of analysis (2018).
93. *Brendan O'Neill*: Multicriteria Site Suitability for Algal Biofuel Production Facilities (2018).
94. *Roman Spataru*: Spatial-temporal GIS analysis in public health – a case study of polio disease (2018).
95. *Alicja Miodońska*: Assessing evolution of ice caps in Suðurland, Iceland, in years 1986 - 2014, using multispectral satellite imagery (2019).
96. *Dennis Lindell Schettini*: A Spatial Analysis of Homicide Crime's Distribution and Association with Deprivation in Stockholm Between 2010-2017 (2019).
97. *Damiano Vesentini*: The Po Delta Biosphere Reserve: Management challenges and priorities deriving from anthropogenic pressure and sea level rise (2019).
98. *Emilie Arnesten*: Impacts of future sea level rise and high water on roads, railways and environmental objects: a GIS analysis of the potential effects of increasing sea levels and highest projected high water in Scania, Sweden (2019).
99. *Syed Muhammad Amir Raza*: Comparison of geospatial support in RDF stores: Evaluation for ICOS Carbon Portal metadata (2019).
100. *Hemin Tofiq*: Investigating the accuracy of Digital Elevation Models from UAV images in areas with low contrast: A sandy beach as a case study (2019).
101. *Evangelos Vafeiadis*: Exploring the distribution of accessibility by public transport using spatial analysis. A case study for retail concentrations and public hospitals in Athens (2019).
102. *Milan Sekulic*: Multi-Criteria GIS modelling for optimal alignment of roadway by-passes in the Tlokweng Planning Area, Botswana (2019).

103. *Ingrid Piirisaar*: A multi-criteria GIS analysis for siting of utility-scale photovoltaic solar plants in county Kilkenny, Ireland (2019).
104. *Nigel Fox*: Plant phenology and climate change: possible effect on the onset of various wild plant species' first flowering day in the UK (2019).
105. *Gunnar Hesch*: Linking conflict events and cropland development in Afghanistan, 2001 to 2011, using MODIS land cover data and Uppsala Conflict Data Programme (2019).
106. *Elijah Njoku*: Analysis of spatial-temporal pattern of Land Surface Temperature (LST) due to NDVI and elevation in Ilorin, Nigeria (2019).
107. *Katalin Bunyevácz*: Development of a GIS methodology to evaluate informal urban green areas for inclusion in a community governance program (2019).
108. *Paul dos Santos*: Automating synthetic trip data generation for an agent-based simulation of urban mobility (2019).
109. *Robert O' Dwyer*: Land cover changes in Southern Sweden from the mid-Holocene to present day: Insights for ecosystem service assessments (2019).
110. *Daniel Klingmyr*: Global scale patterns and trends in tropospheric NO2 concentrations (2019).
111. *Marwa Farouk Elkabbany*: Sea Level Rise Vulnerability Assessment for Abu Dhabi, United Arab Emirates (2019).
112. *Jip Jan van Zoonen*: Aspects of Error Quantification and Evaluation in Digital Elevation Models for Glacier Surfaces (2020).
113. *Georgios Efthymiou*: The use of bicycles in a mid-sized city – benefits and obstacles identified using a questionnaire and GIS (2020).
114. *Haruna Olayiwola Jimoh*: Assessment of Urban Sprawl in MOWE/IBAFO Axis of Ogun State using GIS Capabilities (2020).
115. *Nikolaos Barmpas Zachariadis*: Development of an iOS, Augmented Reality for disaster management (2020).
116. *Ida Storm*: ICOS Atmospheric Stations: Spatial Characterization of CO2 Footprint Areas and Evaluating the Uncertainties of Modelled CO2 Concentrations (2020).
117. *Alon Zuta*: Evaluation of water stress mapping methods in vineyards using airborne thermal imaging (2020).
118. *Marcus Eriksson*: Evaluating structural landscape development in the municipality Upplands-Bro, using landscape metrics indices (2020).
119. *Ane Rahbek Vierø*: Connectivity for Cyclists? A Network Analysis of Copenhagen's Bike Lanes (2020).
120. *Cecilia Baggini*: Changes in habitat suitability for three declining Anatidae species in saltmarshes on the Mersey estuary, North-West England (2020).
121. *Bakrad Balabanian*: Transportation and Its Effect on Student Performance (2020).
122. *Ali Al Farid*: Knowledge and Data Driven Approaches for Hydrocarbon Microseepage Characterizations: An Application of Satellite Remote Sensing (2020).
123. *Bartlomiej Kolodziejczyk*: Distribution Modelling of Gene Drive-Modified Mosquitoes and Their Effects on Wild Populations (2020).
124. *Alexis Cazorla*: Decreasing organic nitrogen concentrations in European water bodies - links to organic carbon trends and land cover (2020).

125. *Kharid Mwakoba*: Remote sensing analysis of land cover/use conditions of community-based wildlife conservation areas in Tanzania (2021).
126. *Chinatsu Endo*: Remote Sensing Based Pre-Season Yellow Rust Early Warning in Oromia, Ethiopia (2021).
127. *Berit Mohr*: Using remote sensing and land abandonment as a proxy for long-term human out-migration. A Case Study: Al-Hassakeh Governorate, Syria (2021).
128. *Kanchana Nirmali Bandaranayake*: Considering future precipitation in delineation locations for water storage systems - Case study Sri Lanka (2021).
129. *Emma Bylund*: Dynamics of net primary production and food availability in the aftermath of the 2004 and 2007 desert locust outbreaks in Niger and Yemen (2021).
130. *Shawn Pace*: Urban infrastructure inundation risk from permanent sea-level rise scenarios in London (UK), Bangkok (Thailand) and Mumbai (India): A comparative analysis (2021).
131. *Oskar Evert Johansson*: The hydrodynamic impacts of Estuarine Oyster reefs, and the application of drone technology to this study (2021).
132. *Pritam Kumarsingh*: A Case Study to develop and test GIS/SDSS methods to assess the production capacity of a Cocoa Site in Trinidad and Tobago (2021).
133. *Muhammad Imran Khan*: Property Tax Mapping and Assessment using GIS (2021).
134. *Domna Kanari*: Mining geosocial data from Flickr to explore tourism patterns: The case study of Athens (2021).
135. *Mona Tykesson Klubien*: Livestock-MRSA in Danish pig farms (2021).
136. *Ove Njøten*: Comparing radar satellites. Use of Sentinel-1 leads to an increase in oil spill alerts in Norwegian waters (2021).
137. *Panagiotis Patrinos*: Change of heating fuel consumption patterns produced by the economic crisis in Greece (2021).
138. *Lukasz Langowski*: Assessing the suitability of using Sentinel-1A SAR multi-temporal imagery to detect fallow periods between rice crops (2021).
139. *Jonas Tillman*: Perception accuracy and user acceptance of legend designs for opacity data mapping in GIS (2022).
140. *Gabriela Olekszyk*: ALS (Airborne LIDAR) accuracy: Can potential low data quality of ground points be modelled/detected? Case study of 2016 LIDAR capture over Auckland, New Zealand (2022).
141. *Luke Aspland*: Weights of Evidence Predictive Modelling in Archaeology (2022).
142. *Luís Fareleira Gomes*: The influence of climate, population density, tree species and land cover on fire pattern in mainland Portugal (2022).
143. *Andreas Eriksson*: Mapping Fire Salamander (Salamandra salamandra) Habitat Suitability in Baden-Württemberg with Multi-Temporal Sentinel-1 and Sentinel-2 Imagery (2022).
144. *Lisbet Hougaard Baklid*: Geographical expansion rate of a brown bear population in Fennoscandia and the factors explaining the directional variations (2022).

145. *Victoria Persson*: Mussels in deep water with climate change: Spatial distribution of mussel (Mytilus galloprovincialis) growth offshore in the French Mediterranean with respect to climate change scenario RCP 8.5 Long Term and Integrated Multi-Trophic Aquaculture (IMTA) using Dynamic Energy Budget (DEB) modelling (2022).
146. *Benjamin Bernard Fabien Gérard Borgeais*: Implementing a multi-criteria GIS analysis and predictive modelling to locate Upper Palaeolithic decorated caves in the Périgord noir, France (2022).
147. *Bernat Dorado-Guerrero*: Assessing the impact of post-fire restoration interventions using spectral vegetation indices: A case study in El Bruc, Spain (2022).
148. *Ignatius Gabriel Aloysius Maria Perera*: The Influence of Natural Radon Occurrence on the Severity of the COVID-19 Pandemic in Germany: A Spatial Analysis (2022).
149. *Mark Overton*: An Analysis of Spatially-enabled Mobile Decision Support Systems in a Collaborative Decision-Making Environment (2022).
150. *Viggo Lunde*: Analysing methods for visualizing time-series datasets in open-source web mapping (2022).
151. *Johan Viscarra Hansson*: Distribution Analysis of Impatiens glandulifera in Kronoberg County and a Pest Risk Map for Alvesta Municipality (2022).
152. *Vincenzo Poppiti*: GIS and Tourism: Developing strategies for new touristic flows after the Covid-19 pandemic (2022).
153. *Henrik Hagelin*: Wildfire growth modelling in Sweden - A suitability assessment of available data (2023).
154. *Gabriel Romeo Ferriols Pavico*: Where there is road, there is fire (influence): An exploratory study on the influence of roads in the spatial patterns of Swedish wildfires of 2018 (2023).
155. *Colin Robert Potter*: Using a GIS to enable an economic, land use and energy output comparison between small wind powered turbines and large-scale wind farms: the case of Oslo, Norway (2023).
156. *Krystyna Muszel*: Impact of Sea Surface Temperature and Salinity on Phytoplankton blooms phenology in the North Sea (2023).
157. *Tobias Rydlinge*: Urban tree canopy mapping - an open source deep learning approach (2023).
158. *Albert Wellendorf*: Multi-scale Bark Beetle Predictions Using Machine Learning (2023).
159. *Manolis Papadakis*: Use of Satellite Remote Sensing for Detecting Archaeological Features: An Example from Ancient Corinth, Greece (2023).
160. *Konstantinos Sourlamtas*: Developing a Geographical Information System for a water and sewer network, for monitoring, identification and leak repair - Case study: Municipal Water Company of Naoussa, Greece (2023).
161. *Xiaoming Wang*: Identification of restoration hotspots in landscape-scale green infrastructure planning based on model-predicted connectivity forest (2023).
162. *Sarah Sienaert*: Usability of Sentinel-1 C-band VV and VH SAR data for the detection of flooded oil palm (2023).
163. *Katarina Ekeroot*: Uncovering the spatial relationships between Covid-19 vaccine coverage and local politics in Sweden (2023).

164. *Nikolaos Kouskoulis*: Exploring patterns in risk factors for bark beetle attack during outbreaks triggered by drought stress with harvester data on attacked trees: A case study in Southeastern Sweden (2023).
165. *Jonas Almén*: Geographic polarization and clustering of partisan voting: A local-level analysis of Stockholm Municipality (2023).
166. *Sara Sharon Jones*: Tree species impact on Forest Fire Spread Susceptibility in Sweden (2023).
167. *Takura Matswetu*: Towards a Geographic Information Systems and Data-Driven Integration Management. Studying holistic integration through spatial accessibility of services in Tampere, Finland. (2023).
168. *Duncan Jones*: Investigating the influence of the tidal regime on harbour porpoise *Phocoena phocoena* distribution in Mount's Bay, Cornwall (2023).
169. *Jason Craig Joubert*: A comparison of remote sensed semi-arid grassland vegetation anomalies detected using MODIS and Sentinel-3, with anomalies in ground-based eddy covariance flux measurements (2023).
170. *Anastasia Sarelli*: Land cover classification using machine-learning techniques applied to fused multi-modal satellite imagery and time series data (2024).
171. *Athanasios Senteles*: Integrating Local Knowledge into the Spatial Analysis of Wind Power: The case study of Northern Tzoumerka, Greece (2024).
172. *Rebecca Borg:* Using GIS and satellite data to assess access of green area for children living in growing cities (2024).
173. *Panagiotis–Dimitrios Tsachageas*: Multicriteria Evaluation in Real Estate Land-use Suitability Analysis: The case of Volos, Greece (2024).
174. *Hugo Nilsson*: Inferring lane-level topology of signalised intersections from aerial imagery and OpenStreetMap using deep learning (2024).
175. *Pavlos Alexantonakis*: Estimating lake water volume fluctuations using Sentinel-2 and ICESat-2 remote sensing data (2024).
176. *Karl-Martin Wigen*: Physical barriers and where to find them (2024).
177. *Martin Storsnes*: Temporal RX-algorithm performance on Sentinel-2 images (2024).
178. *Saulė Gabrielė Petraitytė*: The Relation Between Covid-19 Vaccination and Voting Trends in Lithuania: A Spatial Analysis (2024).
179. *Pedro Martinez Duran*: Olive yield forecasting from remote sensing and climate datasets in the Jaen province (Spain) (2024).
180. *Josefine Kynde Hämberg*: Proximity to Urban Green Spaces for Older Adults in Specific Housings - a Case Study of Malmö, Sweden (2024).
181. *Max Bengtsson*: A Site Selection of An Energy Island in the North Sea: Optimal Location in an Ecological and an Economic Scenario Using a Multicriteria Decision Analysis (MCDA) (2024).
182. *Anna Börmann*: Assessing Great Britain as a relocation site for the threatened Iberian Lynx in a changing climate (2024).
183. *Josephine Roosli*: Flood Risk Assessment for the Kävlinge River for Present and Future Climate Scenarios using HEC-RAS Rain-on-Grid (2024).
184. *Seán Flanagan*: Spatiotemporal dynamics of E-scooter sharing ridership and their associations with the built environment: A Swedish comparative study (2024).

185. *Wouter Vorsters*: Assessing the Impact of Combined Sewer Overflow on the Habitat of Lampetra planeri: A Case Study in Flanders, Belgium (2025).
186. *Kathleen Macdonald*: Cetacean strandings on the Scottish coast: coastal accessibility factors lead to underreporting (2025).
187. *Athanasios Emmanouil Mourampetzis*: Navigating the Shadows: A Comparative Analysis of SAR and Optical Imagery for Detecting (Dark) Vessels (2025).
188. *Nizam-ud-Din*: Spatial Land Records System using Geospatial Techniques: a case study of a Mid-Sized Village in Pakistan (2025).
189. *Nedim Nasic Kjellgren*: Linked Geodata: Improving Rooftop Photovoltaic Production Estimates through BIM-GIS Integration using Semantic Web Technologies (2025).
190. *Vedrana Pretkovic*: Spatio-temporal vegetation changes in the Pacific-Chocó region of Colombia during the conflict and post-conflict periods (2025).
191. *Evelina Bengtsson*: A Socioeconomic Dimension of Crime: A Spatial Study of Firearm-related Violence in Malmö (2025).
192. *Martynas Bielinis*: Application of C-band Radar Interferometry for Dune Monitoring in the Curonian Spit (2025).
193. *Paulina Magdalena Rieke*: Case study of the benefits of BIM and GIS solutions used on a live infrastructure project (2025).
194. *Alina Schärer*: Evaluating the Impact of Urban Green Spaces and Vegetation Characteristics on Land Surface Temperature Across Swiss Cities Using Machine Learning (2025).
195. *Paul Stewart:* Where is wild in Glasgow's Southside? A test of the applicability of relative wildness mapping to suburban Scotland (2025).
196. *Georgios Fylakis:* Spatiotemporal analysis of the integration between shared e-scooters and public transport: Case studies in Oslo and Stockholm (2025).
197. *Andreas Klasson*: Generating 3D building models according to Swedish building specification using footprints and airborne laser scanning (2025).
198. *Agaton Järemo Lawin*: The spread of Japanese knotweed in Scania: Invasion suitability prediction using species distribution modelling (2025).
199. *Jesse Stewart:* Contextualizing the Geographic Influence on Infantry Manoeuvrability in a Historical Battlefield Using GIS: A Case Study of the Canadian Corps in the Second Battle of Passchendaele, First World War (2025).
200. *Oskar Vejkdal Thorsberg*: Automatic geometry extraction in digital building permits: A case study using BIM and NS Building (2025).
201. *Spyridon Gerafentis*: Impact of the COVID-19 "Lockdown" on Air Quality in Athens (2025).
202. *Symeon Andriotis*: Political Violence in Athens, Greece (2008-2024): A Machine Learning Approach for Predictive Modelling of Spatial Risk Patterns (2025).
203. *Simon Westman*: Detecting Structurally Old Scots Pine: A Crown-Metric Approach Using National ALS and LIFT Enrichment (2026).
204. *Freja Randeris Kristoffersen*: Satellite-Derived Bathymetry of Danish Coastal Waters Using Machine Learning with Sentinel-2 and ICESat-2 data (2026).

205. *Markus Honkanen*: Securitas Per Scientiam: GIS-MCDA of Civil Defence Shelter Distribution Efficiency in the Helsinki Capital Region (2026).
206. *Amanda Carolina Santos Motta*: Visualization Tools for Simulation Results Based on 3D City Models: An Urban Planner-Focused Study (2026).
207. *Gintars Krumins*: Mapping forest felling activities in Latvia from Sentinel-2 satellite imagery using machine learning (2026).
208. *Jenny Berntsson*: Using Multi-criteria GIS analysis in nature conservation planning in Lilla Edet municipality (2026).
209. *Sebastian Daland*: Flood impacts on road accessibility and buildings in Gothenburg during a 100-year rainfall event (2026).
210. *Polyxeni Karapanagiotidou*: GIS-based Multi-Criteria Decision Analysis (MCDA) framework for Flood Risk Assessment in the Thermi Basin (2026).